GENETIC AND EPIGENETIC EFFECT OF ESTROGEN ON MESENCHYMAL STEM CELL MAINTENANCE AND DIFFERENTIATION

A THESIS
SUBMITTED TO THE DEPARTMENT
OF MOLECULAR BIOLOGY AND GENETICS AND THE
GRADUATE SCHOOL OF ENGINEERING AND SCIENCE
OF BILKENT UNIVERSITY
IN PARTIAL FULFILLMENT OF THE REQUIREMENTS
FOR THE DEGREE OF
DOCTOR OF PHILOSOPHY

BY

CEYLAN VERDA BİTİRİM

OCTOBER, 2013

I certify that I have read this thesis and that in my opinion it is fully adequate, in scope and in quality, as a thesis for the degree of Doctor of Philosophy.

Assoc. Prof.Dr. Işık YULUĞ (Advisor)

Prof. Dr. K. Can AKÇALI (Co-Advisor)

I certify that I have read this thesis and that in my opinion it is fully adequate, in scope and in quality, as a thesis for the degree of Doctor of Philosophy.

Assist. Prof. Dr.ÖzlenKONU

I certify that I have read this thesis and that in my opinion it is fully adequate, in scope and in quality, as a thesis for the degree of Doctor of Philosophy.

Assoc. Prof. Dr. Rengül Çetin ATALAY

I certify that I have read this thesis and that in my opinion it is fully adequate, in scope and in quality, as a thesis for the degree of Doctor of Philosophy.

Assoc. Prof. Dr. Mayda GÜRSEL

I certify that I have read this thesis and that in my opinion it is fully adequate, in scope and in quality, as a thesis for the degree of Doctor of Philosophy.

.

Prof.Dr.Mehmet Yakup ARICA

Approved for the Graduate School of Engineering and Science

Prof. Dr. Levent Onural
Director of the Graduate School

ABSTRACT

GENETIC AND EPIGENETIC EFFECT OF ESTROGEN ON MESENCHYMAL STEM CELL MAINTENANCE AND DIFFERENTIATION

Ceylan Verda Bitirim
Ph.D. in Molecular Biology and Genetics
Supervisor: Assoc. Prof. Dr. Işık Yuluğ
October 2013, Pages 151

Mesenchymal stem cells (MSCs) have the potential to differentiate into multiple cell types and immune privileged characteristics. These features make MSCs a hope in tissue engineering and cell based treatment applications. Tremendous amount of studies were carried out in order to produce an ideal biomaterial as a scaffold for cell transplantation. In recent studies, carbon nanotubes (CNT) were identified as a novel scaffold array due to their unique physical, chemical and electrical properties among the other biomaterials.The effect of estrogen hormone on the regulation of MSC maintenance, proliferation and differentiation was reported. However, its role in maintenance of MSCs on scaffold materials such as CNTs and the genetic and epigenetic regulation of MSC differentiation have not fully been elucidated. Therefore our aim was to examine the possible role of estrogen in the MSCs' maintenance seeded on CNT surfaces and genetic and epigenetic regulation of the key transcription

factors involved in adipogenic, osteogenic and chondrogenic differentiaton of MSCs. Our results revealed the enhanced effect of estrogen on the viability of MCSs which were seeded and incubated on multiwalled carbon nanotubes (MWCNT). In addition we demonstrated that passaging causes decrease of cell viability and the number of attached cells on CNT materials. We have also shown the effect of estrogen on the epigenetic and genetic regulation of MSC differentiation. Estrogen treatment decreased the expression of major adipogenic transcription factors; C/EBPα, FABP4, PPARγ, Adipsin and increased key osteogenic transcription factor RUNX2 in MSCs from both normal female and ovariectomized rats, suggesting inhibitory and stimulatory effect of estrogen on adipogenesis and osteogenesis respectively. We have also shown that the subcellular localization of PPARγ and ETS1 is changed in response to estrogen deficiency. Among modified histones, we found that H3K27me2, H3K27me3 and H3K36me2 protein levels were reduced after estrogen treatment both in female and ovariectomized animals. In addition, ChIP analysis showed that estrogen treatment caused an increase in H3K27me2, H3K27me3 and ERα levels at the promoters of C/EBPα, FABP4, PPARγ, Adipsin and RUNX2. Bisulfite sequencing analysis revealed that in the absence of estrogen, DNA hypermethylation was established in C/EBPα and PPARγ promoters whereas in ERα promoters CpG hypomethylation was observed after estrogen treatment. In conclusion, estrogen causes epigenetic and genetic changes in maintenace and differentiation of MSCs. Understanding the

effect of estrogen on the genetic and epigenetic regulation of the major transcription factors may lead to clues for new treatment in chronic diseases such as obesity, osteoporosis and ostearthiritis.

ÖZET

ÖSTROJEN HORMONUNUN MEZENKİMAL KÖK HÜCRELERİN MUHAFAZASINDAKİ VE FARKLILAŞMASINDAKİ GENETİK VE EPİGENETİK ETKİSİ

Ceylan Verda Bitirim
Moleküler Biyoloji ve Genetik Doktorası
Tez Yöneticisi: Doç. Dr. Işık Yuluğ
Ekim 2013, Sayfa 151

Mezenkimal kök hücreler (MKH) kemik, yağ, kıkırdak, sinir ve karaciğer hücrelerine dönüşebilme potansiyeli olan, immün reaksiyon oluşturma özelliği olmayan hücrelerdir. Bu özellikler kök hücreleri doku mühendisliği ve hücre tedavisi alanları için yeni bir umut haline getirdi. Hücre transplantasyonunda kullanılmak üzere ideal yüzey üretmek için pek çok çalışma yürütüldü. Son yıllarda farklı fiziksel, kimyasal ve elektriksel özelliklerinden dolayı karbon nanotüpler (KNT) yeni biyomateryal yüzeyler olarak tanımlandı. Östrojen hormonunun mezenkimal kök hücre devamlılığı, çoğalması ve farklılaşması üzerine etkileri rapor edilmiştir. Fakat östrojenin biyomateryal yüzey üzerindeki mezenkimal kök hücrenin devamlılıgındaki ve mezenkimal kök hücre farklılaşmasındaki genetik ve epigenetik rolü tam olarak araştırılmamıştır. Bu nedenle, bu çalışmada östrojenin karbon nantüp üzerine ekilen kök hücrelerin devamlılığındaki ve adipojenik, östeojenik ve kondrojek farklılaşmaya katılan

anahtar transkripsiyon faktörlerinin genetik ve epigenetik regülasyonundaki rolünü araştrmak amaçlanmıştır. Sonuçlarımız östrojenin çok duvarlı karbon nanotüpler üzerindeki MKHlerin canlılıgını arttırıcı etkisini göstermiştir. Ayrıca hücre canlılıgı ve KNT materyalin üzerine yapışan MKH sayısının passajlama ile azaldıgını gösterdik. Bu çalışmada östrojenin MKH farklılaşmasının genetik ve epigenetik regülasyonuna etkisini gösterebildik. Östrojen tedavisi, normal dişi ve overi alınmış dişiden alınan MKH'de temel adipojenik transkripsiyon faktörler olan C/EBPα, FABP4, PPARγ, Adipsinin gen ifadesini azaltırken, anahtar transkripsiyon faktörü olan RUNX2 nin ifadesini arttırır. Bu sonucun östrojenin adipojenik farklılaşma üzerine baskılayıcı etkisini, östeojenik farklılaşma üzerine arttırıcı etkisini gösterdiği söylenebilir. PPARγ ve diğer transkripsiyon faktörü ETS1 proteinlerinin hücresel lokalizasyonunun östrojen yokluguna bağlı değişimi ayrıca gösterilmiştir. Diğer modifiye histonlar arasında, H3K27me2, H3K27me3 ve H3K36me2 protein düzeylerinin östrojen tedavisinden sonra azaldığını bulduk. Ek olarak, kromatin immünopresipitasyon analizleri H3K27me2, H3K27me3 ve ERα düzeylerinin C/EBPα, FABP4, PPARγ, Adipsin ve RUNX2 promotörleri üzerinde östrojen tedavisi sonucu arttıgını gösterdi. Bisülfit sekanslama analizleri östrojen yoklugunda C/EBPα ve PPARγ promotörleri üzerinde DNA hipermetilasyonu görülürken, ERα promotöründe CpG hipometilsayonu görüldü. Sonuç olarak, östrojen MKH devamlılıgı ve farklılaşmasında epigenetik ve genetik değişimlere yol açar. Östrojenin temel transkripsiyon faktölerinin regülasyonundaki etkisinin

anlaşılması obezite, osteoporoz ve osteoartirit gibi kronik hastalıkların tedavisi için yeni ipuçları yaratır.

ACKNOWLEDGEMENT

First and foremost, from my heart, I would like to express my gratitute to my supervisor Prof. Dr. K. Can Akçalı for giving me the opportunity to work in his lab and providing his continuous support, endless patience and knowledge during my PhD study. His valuable guidance opened a door to a new life for me. It has been a big honor for me to work with him.

I want to thank Assoc. Prof. Dr. Özlen Konu, Assoc. Prof. Dr. Rengül Çetin Atalay, Prof. Dr. Yakup Arıca, Assoc. Prof. Dr. Mayda Gürsel and especially Assist. Prof. Dr. Işık Yuluğ for being members of my thesis committee and for their contribution in this thesis through their helpful suggestions.

I would like to express my heartful thanks to the past and present members of Akçalı Group; Merve Aydın, Ece Akhan, Damla Gözen, Şahika Çıngır, Fatma Ayaloğlu-Bütün, Zeynep Tokçaer-Keskin, Sumru Bayın, Sinan Gültekin and to present members of Yuluğ Grup; Nilüfer Sayar and Gurbet Karahan for their patience, tremendous help and understanding during my research. I would also like to thank to the senior students; Fatma Rabia Ürün, Ezgi Kaya and Gizem Gökçe Dinç who helped me and took part in this project with me. Working with

you was great! I also would like to thank Abdullah Ünnü, Füsun Elvan, Bilge Kılıç and Turan Daştandır for being always there for us.

I am very grateful to Assist. Prof. Dr. Erman Bengü for his supervision and to the members of Bengü group, especially Gökçe Küçükayan for her help during the carbon nanotube studies.

I would like to express my sincere appreciation to Assist. Prof. İhsan Gürsel for his support, guidance and encouragement.

I would like to thank The Scientific and Technological Research Council of Turkey (TÜBİTAK) for their financial support throughout my thesis work.

I am truly indebted to all of my beloved friends in MBG family, especially Büşra Yağabasan, Gülşah Dal, Özlem Tufanlı, Dilek Çevik, Pelin Telkoparan-Akıllılar, Füsun Doldur-Ballı, Nilüfer Sayar and Gökhan Yıldız for their support, incredible friendship and help whenever I needed during this long and arduous journey. They were always there to help whenever I had moments of crisis with my PhD. Without them this journey would be very difficult and boring. I would like to dedicate my special thankfulness to my dear friend Gözde Güçlüler for her invaluable friendship and being there for me whenever I needed them the most.

I would like to also dedicate my special thankfulness to my beloved friend Şeyma Demirsoy. Being your friend and sharing the same lab with you was gorgeous.

I would like to express my deepest love and gratitude to Defne Bayık, for everything she has added to my life and to teach me looking the world through different perspectives. She gave more meaning not just to this journey but also to my life with her invaluable friendship, endless patience and encouragement. She will be a part of my family forever.

Once for all, I would also like to extend my sincere gratitude to my family, especially to my dearest mother and father for their unconditional and endless love and support throughout my life; and to my cousin Berk Zafer for his academic guidance and his priceless support. Without his guidance I couldn't be here.

CONTENT

LIST OF FIGURES

LIST OF TABLES

ABBREVIATIONS

ALP	Alkaline Phosphatase
ATF3	Cyclic AMP-dependent Transcription Factor 3
AP-1	Activator Protein 1
ATP	Adenosine Triphosphate
ASC	Adult Stem Cell
BMP4	Bone Morpohogenetic Protein 4
bp	Base pairs
BSA	Bovine Serum Albumin
BSPCR	Bisulfite Specific PCR
CD	Cluster of Differentiation
cDNA	Complementary Deoxyribonucleic Acid
C/EBPα	CCAAT-Enhancer-Binding Protein alpha
CoREST	Co-Repressor repressor Element 1 Silencing Transcription factor
CNT	Carbon Nanotubes
CpG	Unmethylated Cytosine-Guaniosine motifs
CHD1	Chromodomain Helicase DNA-binding 1
Dax-1	Dosage-sensitive sex reversal, adrenal hypoplasia critical region, on chromosome X, gene 1
ddH_2O	Double distilled water
DMEM	Dulbecco's Modified Eagle's Medium

DMEM	Dulbecco's Modified Eagle's Medium Low glucose
DMSO	Dimethyl Sulfoxide
DNA	Deoxyribonucleic acid
DNMT	DNA Methyl transferase
dNTP	Deoxy nucleotide triposphate
ECM	Extra Cellular matrix
EDTA	Ethylenediaminetetraacetic acid
ER	Endoplasmic Reticullum
ERE	Estrogen Receptor Element
ERα/β	Estrogen Receptor alpha/beta
ESC	Embryonic Stem Cells
FABP 4	Fatty Acid Binding Protein 4
FBS	Fetal Bovine Serum
Fgf2	Fibroblast growth factor 2
G	Grams
GVHD	Graft-Versus-Host Disease
H3	Histone 3
HAT	Histone Acetyl Transferease
HDAC	Histone Deacetylase
HKMT	Histone Lysine Methyltransferase
Hsp	Heat shock protein
HSC	Hematopoietic Stem Cell

H3K	Histone-3 lysine
HLA	Human Leukocyte Antigen
HRP	Horse Raddish Peroxidase
IBMX	Isobutyl Methyl Xanthine
ICAM-1	Intercellular Adhesion Molecule 1
ICM	Inner Cell Mass
iPS	Induced Pluripotent Stem
KLF4	Kruppel-Like Factor 4
Jmj	Jumonji
LB	Luria-Bertani Broth
LIF	Leukemia Inhibitory Factor
LSD1	Lysine Specific Demethylase 1
M	Molar
Mg	Mili Gram
ml	Mili liter
mM	Mili molar
mm	Mili meter
MAPK	Mitogen-Activated Kinase
MBD	Methly-CpG Binding Proteins
MSC	Mesenchymal Stem Cell
MWCNT	Multiwalled Carbon Nanotubes
MHC	Major Histocompatibility Complex

NR	Nuclear Receptors
NuRD	Nucleosome Remodeling Deacetylase
Oct	Octamer-binding transcription factor 3
Ovex	Ovariectomized
PAGE	Polyacrylamide Gel Electrophoresis
PBS	Phosphate Buffered Saline
PCR	Polymerase Chain Reaction
PGC	Primordial Germ Cell
PLA	Poly-L-lactide
PLGA	Poly Lactic-co-Glycolic Acid
PPARγ	Peroxisome Proliferator-Activated Receptor gamma
PRC	Polycomb Repressor Complex
PTM	Post-Translational Modifications
PVDF	Polyvinlidenefluoride
RNA	Ribonucleic Acid
RUNX2	Runt-related transcription factor 2
rpm	Revolution per minute
RT-PCR	Reverse Transcriptase PCR
qRT-PCR	Quantitative Real Time PCR
SEM	Scanning Electron Microscope
SDS	Sodium Dodecyl Sulfate
SWCNT	Singlewalled Carbon Nanotubes

TAE	Tris Acetate EDTA
TB	Transformation Buffer
TBS	Tris Buffered Saline
TBS-T	Tris Buffered Saline Tween
TEM	Transmission Electron Microscope
TERT	Telomerase Reverse Transcriptase
TGF-β	Transforming Growth Factor beta
V	Volt
VCAM-1	Vascular Cell Adhesion Molecule 1

CHAPTER 1

INTRODUCTION

In the last several decades researchers have been trying to understand and explain complex processes involved in cellular development and molecular factors which regulate cell differentiation and formation of multi-cellular organisms. However several questions remained unresolved until 1998. Isolation of human pluripotent stem cells in 1998 has provided new opportunities to answer the questions about human development and fundamentals of life.

Stem cells are unspecialized cells that have self-renewal ability and can differentiate into specialized cells of the body (http://stemcells.nih.gov). They can be categorized according to their timing or potency. According to their potency abilities and origin, different types of stem cells were shown in Figure 1.1.

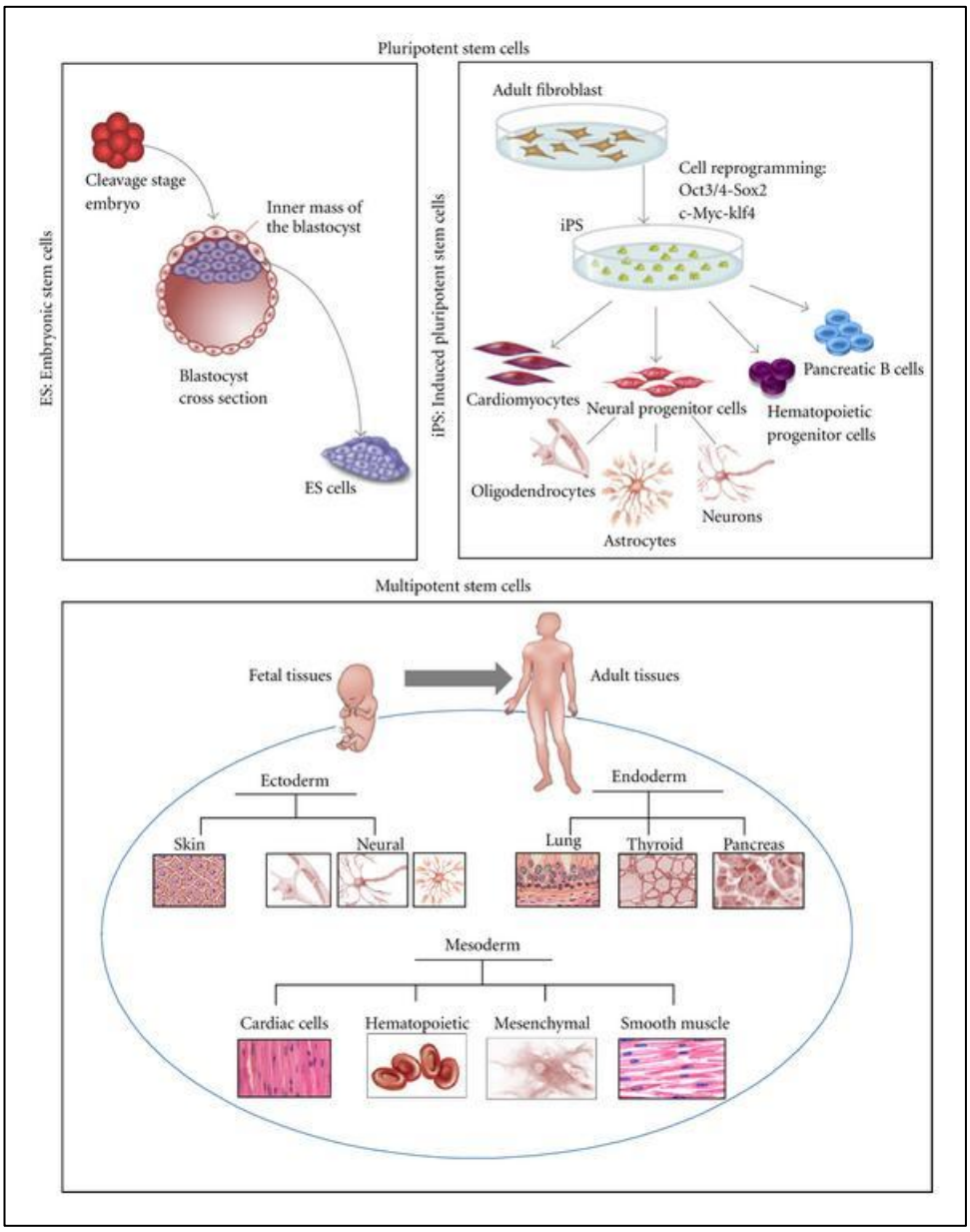

Figure 1.1 Type of stem cells and their origin; pluripotent embryonic stem cells (ES), induced pluripotent stem cells (iPS), and multipotent fetal and adult stem cells (Figure is adopted from [1])

Based on their potency, stem cells can be classified as totipotent, pluripotent, multipotent and unipotent. Totipotent stem cells differentiate into the cells of three embryonic germ layers; ectoderm, endoderm, mesoderm and extra embryonic tissues, whereas pluripotent stem cells differentiate into the cells of three embryonic germ layers, but cannot give rise to the cells of the extra embryonic tissue. Multipotent stem cells can differentiate into the cell types from other different tissues that they originated. Unipotent stem cells can give rise only one specific cell lineage (http://stemcells.nih.gov). Zygote or fertilized egg is a single totipotent cell and generates all the cells in the body, whereas embryonic stem cells (ESC) are pluripotent cells and derived from the inner cell mass of an early mammalian embryo[2,3]. Adult stem cells, are usually multipotent and reside in several specific organs of adults[4,5].

ESCs are undoubtfully key source to understand molecular basis of cellular development as well as cellular threapeutic applications. However due to ethical reasons regarding to the use of human embryo, the scientists focused on the usage of induced pluripotent stem cells (iPSC) and adult stem cells (ASC). iPSCs were first isolated by transfecting four key transcription factors; Oct 4, c-MYC, Sox 2, Klf 4 into mouse fibroblast to differentiate them into embryonic-like stem cells in 2006[6]. This invention seemed to overcome the ethical obstacles against the using of embryo. However the methods of induction with retro viral vectors and their ability to form teratomas are still some of the

factors which may limit their usage.

Among ASCs, mesenchymal stem cells (MSC), also referred to as bone marrow derived stromal cells, have became a potential cell source for regenerative medicine, stem cell-based therapy and tissue engineering applications due to their unique features like differentiation potential, nonimmunogenic characteristics and homing ability[7,8].

In this study, we aimed to investigate the role of estrogen in the maintenance and differentiation of MSCs. In addition to normal culture conditions, we also examined estrogen's effect on MSCs when cultured on carbon nanotube arrays (CNTs). We further investigated the genetic and epigenetic changes during the differentiation of MSCs by estrogen hormone since our previous studies showed that estrogen enhances proliferation and inhibits apoptosis of MSCs.

In the introduction section first I will briefly explain stem cells, ESCs, iPS cells, ASCs. Then the importance of MSCs in tissue engineering applications will be defined. The functions and regulation mechanisms of estrogen hormone and the basic concepts of epigenetics will be explained afterwards. Finally, the introduction chapter will end with the explanation of the epigenetic and genetic regulation of MSCs differentiation upon estrogen treatment.

1.1 EMBRYONIC STEM CELLS AND INDUCED PLURIPOTENT STEM CELLS

Fertilized oocyte undergoes very rapid cellular proliferation which is defined as cleavage stage of early development. ES cells are formed in the inner cell mass (ICM) at this stage. Following cleavage hollow of cells are distributed to the appropriate parts of the developing embryo and this process is called gastrulation. Formation of three germ layers, endoderm, ectoderm and mesoderm, is the final products of gastrulation.

ESCs were first isolated by Evans and Kaufman in 1981 from ICM of mouse embryo and from human embryo by Thomson in 1998[2]. They have indefinite self-renewal capacity and broad differentiation potential to develop cells representative of three germ layers[9].

When they were injected into mouse blastocysts, they fulfill all developmental requirements differentiating into the cells of three embryonic germ layers and transmitting to the germline of chimeric animals[9]. In addition, teratoma and embryoid body formations are evidences of pluripotency properties of these cells *in vivo* and *in vitro* respectively[10]. Maintenance of pluripotency capability of ESCs is provided by expression of key pluripotency genes; Oct4, Sox2, and Nanog[11,12].

Two X chromosomes cytologically or functionally are active in undifferentiated ESCs[13]. During cell cycle, ESCs undergo symmetric division and generates two daughter cells both of which maintain their stem cell identity. The cell cycle structure of ESCs can be characterized by short G1 phase which can account for the rapid rate of cell division[14] . Gı phase activate the cylin dependent kinases (Cdk) in order to begin new round of replication. When ES cells undergo the differentiation, cell cycle structure changes in order to extend significantly G1 phase[15].

Both human and mouse ESCs require a feeder layer from irradiated mouse fibroblasts. It was well established that leukemia inhibitory factor (LIF) is an important mediator which keeps mouse ESCs in undifferentiate state through activation of JAK/Stat3 signaling pathway[16,17]. When LIF is added into the cell culture medium, mouse ESCs can also grow in the absence of feeder layer[17,18]. On the contrary, LIF addition does not support undifferentiated proliferation of human ES cells without feeder layer. On the other hand, self renewal capacity of human ESCs is controlled by different factors like Fgf2, TGF-β, noggin, activin, and Wnt[18,19].

Thanks to their ability to self-renewal and differentiaton potential into the cell types from all germ layers, ESCs have been considered as a promising source

for cell-based therapy in treatment of several degenerative diseases such as diabetes mellitus, Parkinson's disease, Alzheimer, spinal cord injury[20] and osteogenesis imperfecta[21,22].

Despite the advantages of ESCs as a promising tool for cell based therapies, there are also some medical and ethical pitfalls[23]. Since their isolation from blastocyst requires the destruction of the embryo, different political and religious groups are opposed to ESC research. In addition, ESCs cause immune reactions in the host and as mentioned above have ability to form teratomas[22]. Therfore, due to these concerns, researchers sought alternative pluripotent stem cell sources. The reprogramming of fibroblasts to ESC-like cells, which was accomplished by Takahashi and Yamanaka in 2006, was a new hope for stem cell researches[6]. The invention of induced pluripotent stem cells is considered as another major breakthrough in stem cell research field.

Induced pluripotent cells were directly generated from mouse embryonic or adult fibroblast cells by introducing combining of four selected factors; Oct3/4, Sox 2, Klf 4, c-Myc. These transcription factors play key roles in the induction of pluripotency of somatic cells. The factors were chosen among 24 candidate genes. These critical four genes, which are called as Yamanaka factors, were introduced to fibroblasts by retroviral transfection[6, 24].

The iPS cells and ESCs share lots of similarities in many respects. First of all, iPS cells can give rise to cells from three embryonic germ layers; ectoderm, endoderm and mesoderm as exactly similar to ESCs. Moreover, the pluripotency ability of iPS cells was demonstrated by teratoma formation after the subcutaneous injection into nude mice and embryoid body formation in vitro like ESCs. Also the cells are expressing ES cell markers like Nanog, Sox2, Eras, Cripto and Dax1. Furthermore, analyses of genome-wide expression patterns and global histone modifications have shown a high degree of similarity between ESCs and iPSCs. Finally, iPSC clones exhibit similar morphology to ES cells such as round shape, large nucleoli and scant cytoplasm[25,26].

In light of these considerations, iPSCs are seems to be promising tools for cell based therapy, regenerative medicine and drug development overcoming the difficulties regarding the use of human embryos and tissue rejection problem following transplantation in patients. iPSCs enable patient-specific iPS cell based therapy and minimize rejection. In a previous study, it was reported that generation of iPS cells from patients with different genetic diseases including Parkinson disease, adenosine deaminase deficiency-related severe combined immunodeficiency, Huntington disease, Down syndrome and juvenile-onset diabetes mellitus offers opportunity to investigate the causes of these diseases and drug development[27]. Alternatively, if the mutation which causes a disease

was known, it could be repaired in iPS cells by gene targeting. Afterwards, the healthy tissue-specific cells can be transplanted into the patients following differentiation[24,28]. Generation and threapeutic applications of iPS cells was shown in Figure 1.2.

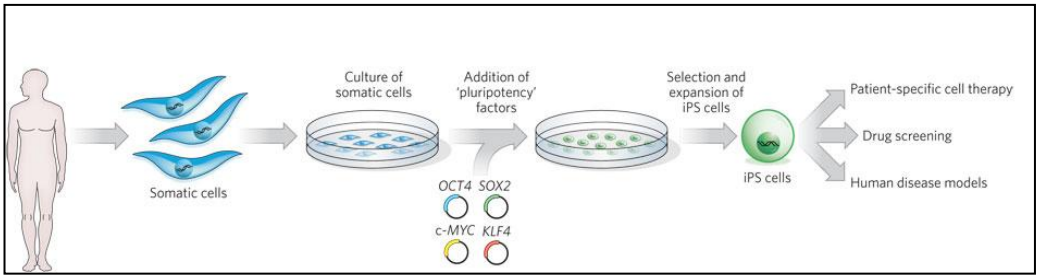

Figure 1.2 Generation and applications of iPS cells (Figure is adopted from[28])

On the other hand, a major limitation of this technology is the use of viruses that integrate into the genome. Using viruses is also associated with the risk of tumor formation due to reactivation of the viral trans-genes. Thereby, after invention of the iPSCs in 2006, transient transfection methods were extensively studied. To improve the efficiency and to overcome the viral transfection issue, different cell sources such as human dermal fibroblasts, foreskin fibroblasts, fetal liver cells and hepatocytes have been used with different delivery techniques such as inducible lentiviral vectors[29], adenovectors[35], plasmids[26] Cre/LoxP system after single plasmid transfection[36]. PiggyBac transposons[31,32], chemical compounds[33], purified recombinant proteins without using any virus or plasmid[40] and synthetic modified mRNA molecules which encode the

Yamanaka Factors and Lin28[41] for reprogramming. However, the efficiency of all these approaches is extremely low. Furthermore, the epigenetic memory problem of iPS cells has not been already solved. Although, somatic cells were reprogrammed to pluripotent cells resembling ESCs, these generated iPS cells keep the epigenetic memory of their tissue of origin [34].

1.2 ADULT STEM CELLS

Adult stem cells (ASC) are undifferentiated cells which reside in a specific organ or tissue. The major role of ASCs is to maintain the homeostasis and to repair the tissue in which they are found. Most types of adult stem cells are multipotent. They have long term, but not unlimited, self-renewal ability and give rise to mature specialized cells[35]. Typically, adult stem cells divide to generate an intermediate cell; progenitor or precursor cell. Progenitor cells develop into terminally differentiated cells[36,37].

ASCs can remain quiescent for a long time in tissue. The specific area in which stem cells reside is called as "niche" (http://stemcells.nih.gov). The ASC reservoir in tissues or organs is protected by asymmetric cell division. Asymmetric cell division is regulated by a niche-derived signals[38]. After the cell division, one of the two daughter cell contacts the niche retaining their stem cell identity, whereas the other daughter cell leaves the niche and committed to

differentiate[38]. Under normal conditions, in case of the tissue injury or when then the maintenance of the tissue is required ASCs are triggered in order to divide and recruit[41]. ASCs show clonal growth. Thanks to the asymmetric cell division, the clones contain many cells that have proliferation potential of progenitor cell[37]. Until now, the existence of ASCs was identified in many tissues and organs and such as blood, bone marrow, liver, skin, testis, ovarian epithelium, muscle, adipose tissue, heart, teeth and brain. Different types of adult stem cells and their location in the body in human was listed in Table 1.1.

Adult bone marrow and peripheral blood contain hematopoietic stem cells (HSC) and MSCs. The first identified ASCs population was HSCs. These cells were first mentioned by Till and McCulloch in 1961[49]. HSCs give rise to all lymphocyte and blood cell types[41,42].

1.2.1 MESENCHYMAL STEM CELLS

MSCs were first identified in stormal part of bone marrow in 1966 by Friedenstein[43] and further characterization was accomplished by Pittenger in 1999[44]. It was demonstrated that human MCSs can give rise to several different cell types including osteocytes, myoctes, adipocytes[45,46], chondrocytes[47], cardiomyocytes[48] and neurons[49]. The types of cells that are derived form MSC

Cell Type	Tissue-Specific Location	Cells or Tissues Produced
Hematopoietic stem cells	Bone marrow, peripheral blood	Bone marrow and blood lymphoid hematopoietic cells
Mesenchymal stem cells	Bone marrow, peripheral blood	Bone, cartilage, tendon, adipose tissue, muscle, marrow stroma, neural cells
Neural stem cells	Ependymal cells, astrocytes, subventricular zone of the central nervous system	Neurons, astrocytes, oligodendrocytes
Hepatic stem cells	In or near the terminal bile ductules (canals of Hering)	Oval cells that subsequently generate hepatocytes and ductular cells
Pancreatic stem cells	Intraislet, nestin-positive cells, oval cells, duct cells	Beta cells
Skeletal-muscle stem cells or satellite cells	Muscle fibers	Skeletal muscle fibers
Stem cells of the skin (keratinocytes)	Basal layer of the epidermis, bulge zone of the hair follicles	Epidermis, hair follicles
Epithelial stem cells of the lung	Tracheal basal and mucussecreting cells, bronchiolar Clara cells, alveolar type II pneumocyte	Mucous and ciliated cells, type I and II pneumocytes
Stem cells of the intestinal epithelium	Epithelial cells located around the base of each crypt	Paneth's cells, brush-border enterocytes, mucussecreting goblet cells, enteroendocrine cells of the villi

Table 1.1 Different types of adult stem cells and their location in the body (Reproduced with permission from Körbling, M et al.[41], Copyright Massachusetts Medical Society)

was shown in Figure 1.3. In addition, MSCs support the long-term hematopoiesis and expansion of embryonic stem cells via expressing cytokines and growth factors[48]. MSCs have been isolated from different tissues other than bone marrow, such as adipose tissue, amniotic fluids, periosteum, fetal tissues, dental pulp, peripheral blood, liver and spleen. Morphologically MSCs show heterogeneity, ranging from narrow spindle shaped to cuboidal, packed cells [51,52].

Phenotypically, adult human MSCs are positive for a number of markers, such as CD90 (Thy-1), CD117 (c-kit), CD71, CD105, CD73, CD44, and adhesion molecules like VCAM-1 (vascular cell adhesion molecule), ICAM-1 (intercellular adhesion molecule), CD166 (activated leukocyte cell adhesion molecule) and CD29 (integrin beta-1). They do not express hematopoietic markers; CD34, CD45, CD14, co-stimulatory molecules CD40, CD86, CD80 [48,51,52,53].

Adult human MSCs express major histocompatibility complex (MHC) class I, whereas human leukocyte antigen (HLA) class II antigens and MHC class II expressions are absent. In addition MSCs have an immunosuppressive function. They inhibit T cell and B cell proliferation and differentiation of B cells into plasma cells. This phenotype shows the non-immunogenic character of the

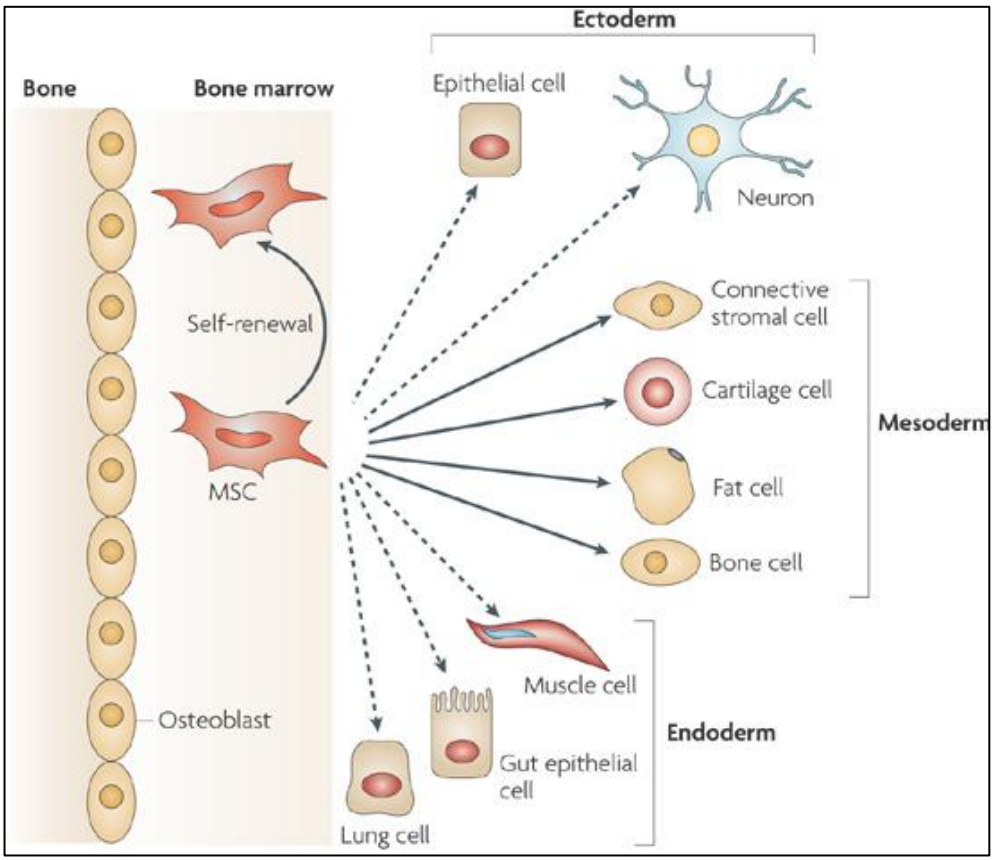

Figure 1.3 Types of cells differentiated from bone marrow derived MSC and their germ layers (Figure is adopted from [54])

MSC[51],[55]. It has been shown by *in vivo* models that MSCs can prevent and treat graft-versus-host disease (GVHD) seen in allogeneic stem cell transplantation[50]. Also MSCs may be used in the treatment of autoimmune disorders[55-57].

While MSCs are differentiating into different cell lineages under appropriate conditions, expression of pluripotency genes such as Oct4, Sox2, TERT (telomerase reverse transcriptase) decrease. The expression of transcription factors, which are involved in MSC differentiation such as RUNX2, ALP,

PPARγ, C/EBPα, are also regulated by epigenetic mechanisms. Histone modifications and CpG methylayion states on these genes are changed upon differentiation induction. Thus, the presence of these epigenetic regulation mechanisms is crucial for MSC differentiation[58,59.]

MSCs may follow different ways during repair of an injured tissue or organ. First, host MSCs can enter into peripheral blood circulation and migrate to target the ischemic tissue. Secondly, MSCs that were injected exogenously can enter the blood circulation and home to injured tissue or inflammation site. As third mechanism, MSCs can be locally injected at the site of injury. The injected MSCs may differentiate into tissue specific stem cells to regenerate. On the other hand, the methods using in MSC homing/trafficking are still inadequate to determine the exact location[7,52,60] .

Due to their differentiation potential and immune-privileged characteristic, MSCs derived from bone marrow is considered as promising cell source for tissue engineering applications in recent years[61]. However, the adhesion of stem cells on ECM is the major concern for particular growth and differentiation. Different types of synthetic and natural biomaterials were demonstrated as scaffold material for MSC transplantation especially for therapeutic applications of cartilage and bone defects[61-63]. Porous ceramics cylinders and biodegradable polymers; poly-L-lactide (PLA) and poly-Llactide-co-glycolide

(PLGA), hydrogel alginate and collagen type gels were demonstrated as alternative scaffolds[60-66]. Adhesion, proliferation and differentiaton of bone marrow derived MSCs on these constructs were demonstrated through *in vivo* and *in vitro* experiments[60,64,66,67]. For instance, repairing of full-thickness articular cartilage defects in knees of rabbits and bone defects in dogs successfully accomplished through the autologous-MSC transplantation on collagen-type-1 gel and porous ceramics cylinders respectively[66,69].

1.3 USE OF CARBON NANOTUBES AS THREE-DIMENSIONAL SCAFFOLD MATERIAL

The fundamental principle of tissue engineering approach is to repair and restore the diseased and damaged tissue with different strategies[70]. Over the past decades, using of biodegradable and biocompatible scaffolds in tissue engineering field have developed.

The major purpose is producing a construct, which can structurally and functionally mimic the extra cellular matrix (ECM) of cells[67,71] , to transplant into diseased or defective tissue after seeding the autologous cells onto these scaffolds. That's why, producing an ideal scaffold protein, which can support different cell types and capable of stimulating cell growth, adhesion and proliferation mimicking the native tissue, is a critical point in tissue

engineering.

In last decade, tremendous amount of attempt have been applied to produce better scaffold construct which can closely mimic the ECM of native tissues[67,72]. For this purpose different kinds of biomaterials were used as scaffold such as porous ceramics cylinders, biodegradable polymers like poly-L-lactide (PLA) and poly-L-lactide-co-glycolide (PLGA), hydrogel alginate and collagen type gels[60-66]. In addition, the importance of topographical pattern on cell viability was also demonstrated in a number of studies. Especially it was shown that dimension and roughness features of surface induce cell growth and support attachment of the cells[72]. Thereby, scaffold proteins are promising tools in tissue engineering due to their patterned surface and nanometer scale dimension[73,74]. It was reported that the rougher surface induced gene expression of fibroblast cells[67]. Moreover, surface properties of scaffolds have potential to develope new environment which is able to stimulate cell proliferation and adhesion[72]. Due to their patterned surface and nanometer scale dimension, scaffold proteins are considered as promising tools in tissue engineering[73-75].

In recent years, carbon nanotubes (CNTs) have became an attractive alternative scaffold material in tissue regeneration field due to their dimension, chemical stability, their high tensile mechanical strength, electrical conductivites, biocompatible feature and chemical properties[74]. Recently, CNT have been

proposed for biomedical applications such as cell tracking and labeling, tissue engineering scaffolds, nanosensors, and vehicles for controlled release of drugs or delivery of bioactive agents[65].

As mentioned, due to their multi-lineage differentiaton potentials and immune-privileged characteristics, MSCs have become a feasible and potential source for tissue engineering applications[76]. It was also reported that CNT–derived patterned surfaces provides an ideal and suitable scaffolds for MSCs and neural stem cells[77, 78].

In addition to topographical features of scaffold material, the growth factors or small molecules which added into cell culture media are also important for tisseue engineering. Because, these factors support the attachment, proliferation and differentiaton of cells seeded onto biomaterial.

1.4 ESTROGEN AND ESTROGEN RECEPTOR PATHWAY

Estrogen, one of the steroid hormones, shows a wide variety of effects on growth, differentiation, sexual behavior, apoptosis, development, reproductive and cardiovascular functions and many physiological processes in female and male[79, 80]. Estrogen shows its effect in a broad range of tissues such as liver,

brain, bone, cardiovascular and reproductive systems[81]. The most dominant estrogen that found in human is 17β estradiol compared to estrone and estriol[82].

Estrogen does not only influence the differentiation, maturation and function of stem cells, but also have a proliferative and antiapoptotic effect by changing the transcriptional activity of related genes[79,83] .

Nuclear receptors (NR) coordinately regulate the expression of genes that have a role in numerous of biological processes such as development, reproduction and homeostasis. NRs activate or repress gene transcription usually by binding to NR-specific ligands such as hormones, vitamins, lipid metabolites and xenobiotics[84].

Steroid hormone receptors are member of nuclear receptor family and act classically as transcription factors. Two major estrogen receptors; estrogen receptor alpha (ERα) and beta (ERβ), convey the regulatory signal of estrogen and control the transcription of target genes. ERs function both as signal transducer and transcriptional factor to regulate the target genes[85].

ERα (NR3A1 in human) was identified by Jensen and Jacobsen in 1962 and ERβ (NR3A2 in human) was identified in 1966 by Gustafsson in human, mouse and rat. Two receptors are encoded by different genes located on different

chomosomes. Moreover, any splice variant was not identified until now[86,87]. ERs share similar structural anatomy and sequence homology. An ER protein consists of six modular domains; N-terminal domain, which is called as A and B domains, is involved in transcriptional activation of target gene; DNA binding domain (C domain) enables the dimerization and binding of receptor to estrogen response element (ERE) on DNA; the hinge (D domain) is involved in receptor dimerization; C-terminal domain (E domain) is E2-binding domain; F domain modulates transcriptional activity of ER[88].

Two major ER pathways were identified so far; genomic or classical pathway and non-genomic pathway. In classical pathway, which is also called as estrogen response element (ERE) dependent pathway, estrogen hormone activates ER in the cytosol resulted in the formation of homodimer. Receptor translocates into to the nucleus after activation and homodimerization respectively and binds to estrogen response element (ERE), which is located at the promoter region of the target gene interacting with specific co-activators and co-repressors subsequently[82,83,89]. ERs localize in cytoplasm associating with heat shock proteins (Hsps) such as Hsp 90, Hsp 70, Hsp 56 in the absence of ligand. The Hsps maintain the estrogen receptors in inactive state. Binding of ligand to ERs trigger them to dissociate from Hsp and to dimerize[90]. The ER activation is generally stimulated in response to binding of 17-estradiol (E2) or other agonists; estrone (E1) and estriol (E3) in humans[82].

In addition to classical ERE-dependent pathway, ERs can also regulate gene expression without direct binding to ERE on DNA. In this alternative pathway, ligand-activated ER associates with another transcription factor such as CRE-like element, which binds to Jun/ATF transcription factors, AP-1 site, which binds to Jun/Fos transcription factor, and CCAAAT site, which binds to SP1 and NF-Y transcription factors[88,90,91], which, in turn regulates the transcription of genes that lack of ERE site.

In the third form of genomic pathway, also referred to as ligand-independent pathway, growth factors are involved in process instead of estrogen. Nuclear ERs are phosphorylated by protein kinases such as ERK 1-2, p38 MAPK, cyclin dependent kinases, protein kinase A and Akt upon growth factor stimulation. Phosphorylated and activated ERs bind to ERE site of target genes [91,92].

In the second major ER pathway, non-genomic pathway, numerous of signaling pathways such as mitogen-activated kinase (MAPK) pathway, PI3K/Akt pathway and JAK/STAT pathway are induced by estrogen-activated membrane bound ER[86]. The estrogen receptor signaling pathways were summarized in Figure 1.4.

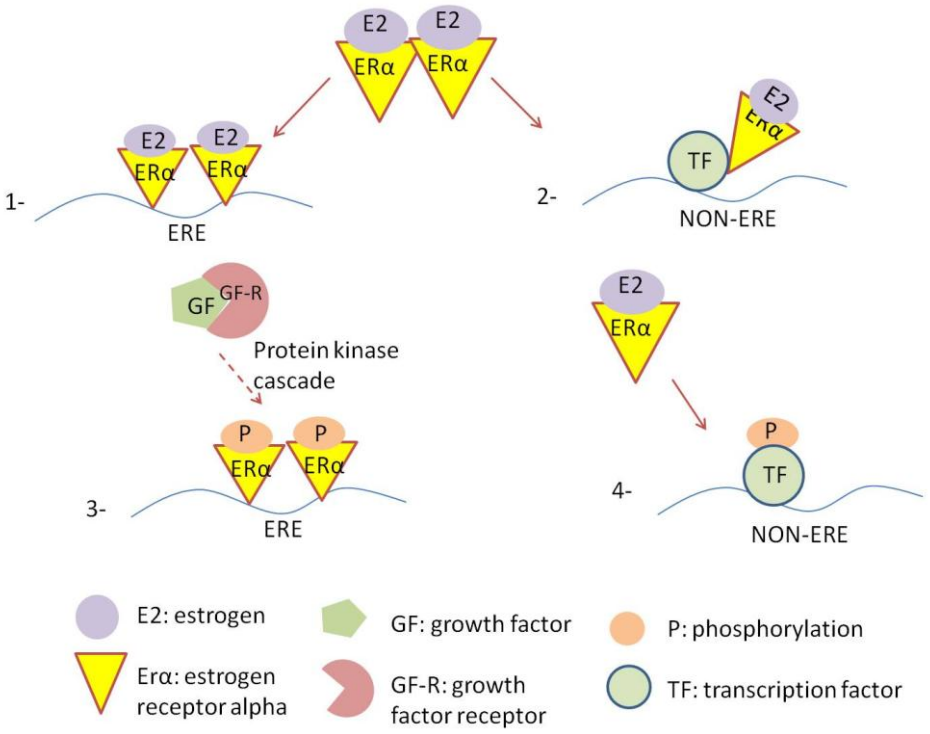

Figure 1.4 Estrogen receptor signaling pathways 1. ERE-dependent classical pathway 2. ERE-independent genomic pathway 3. Ligand-independent genomic pathway 4.Non-genomic pathway

1.5 EPIGENETICS

Conrad Waddington came up with the term "epigenetic" 60 years ago. It is classically defined as stable alterations in gene expression that are mitotically and/or meiotically heritable and occur on DNA or chromatin structure without changing nucleotide sequence[93-95]. Epigenetic modifications include reversible changes on given phenotype, but do not cause any change in genotype. Epigenetic mechanisms are master regulators of transcriptional pathways during major biological processes such as embryonic development, cellular memory,

cell and tissue specific gene expression, differentiation and adult tissue maintenance[96,97]. Gene regulation at the epigenetic level occurs through covalent modifications both on DNA and histones. These modifications regulate the gene transcription by opening chromatin structure (euchromatin), which enables the accessibility of transcription factors to activate gene expression, or facilitating condensed DNA structure (heterochromatin), which does not allow the entering of transcription factors to repress gene expression [97,98]. Loosing of proper chromatin modifications cause lethality during embryonic developmental stage[99,100]. Epigenetic modifications despite of their stability can be reprogrammed using different strategies such as treatment with chemical compounds or hormones, transfection of transcription factors into the cells and nuclear fusion[98]. For instance, generation of iPS cells from somatic parental cells provided insight into epigenetic reprogramming of cells[102].

There are different kinds of epigenetic modifications such as DNA methylation, DNA hydroxymethylation, histone modifications, chromatin remodeling and microRNAs. However, DNA methylation and histone protein modifications are considered as two major epigenetic modifications involved in regulation of stem cell.

1.5.1 DNA METHYLATION

The important role of DNA methylation/demethylation was first suggested by Griffith and Mahler in 1969[103]. DNA methylation is catalyzed by DNA methyltransferases (DNMTs) that add a methyl group (CH3) on 5'position of cytosine (m5C), which is at cytosine-phosphate-guanine (CpG) dinucleotides in some fungal, invertebrates, some bacteria species, flowering plants and in all vertebrates. DNA methyltransferases are conserved proteins and establish methylation at genes during in early development and cell division [109,110]. Regions, which consist of high frequency of CpG residues, are defined as CpG islands[96,104]. CpG islands are located near the promoter regions of genes. According to computational analysis there are almost 29.000 CpG islands in human genome[105].

Epigenetic modifications can be widely reprogrammed in both germ cells and the preimplantated embryo. At two cell stages, the major genome-wide DNA methylation occurs in mammals; in primordial germ cells (PGC) while migrating to genital ridge and after fertilization in embryo. Early PGCs initially possess similar DNA methylation status to somatic cells. Upon fertilization, paternal and maternal genome is passively demethylated before replication and during replication respectively. After implantation, lineage specific de nova methylations which are catalyzed by two different DNMTs; DNMT3a,

DNMT3b. When PGCs enter into the genital ridge, the methylation is erased in response to signal from somatic cells in the gonadal anlagen[106,107]. De novo metylation occurs also in terminally differentiated somatic cells, but slower than embryonic cells and germ cells. Moreover, progressive global hypomethylation pattern on genomic DNA in somatic cells is associated with cancer and age[108,109].

Cytosine methylation is also associated with genomic imprinting and X-inactivation, which is identified as completely silencing one of two identical alleles. Failure in imprinting of specific loci causes several disorders in human [110,111,112]. During X-chromosome inactivation process, one of the two X chromosomes is randomly inactivated in female through dosage compensation mechanism and cytosine methylation [109,110,113].

Methylated DNA associates with methly-CpG binding proteins (MBD) to repress gene expression. The major MBDs identified in mammalian are Mbd1, Mbd2, Mbd3, Mbd4 and MeCP2[114,115]. After binding to methylated CpG, MeCP2 recruits histone deactylases[116], Mbd 1 recruits Suv39H1, which is a histone 3 lysine-9 (H3K9) methylase and HP1, which is a methyl lysine binding protein, respectively[117] and Mbd2 and Mbd3 recruits NuRD, which is a ATP-dependent nucleosome remodeling and histone deactelyase complex[118].

The major question is that how epigenetic modifications can be propagated to daughter cells during cell division. DNA methylation pattern is maintained thanks to semi-conservative replication. DNMT1 enzyme provides the passing of methylation mark on the parental DNA strand to daughter cells during mitosis. On the other hand, de novo methylations both on hemimethylated and unmodified cytosines are catalyzed by DNMT3A and DNMT3B[111,119].

1.5.2 HISTONE MODIFICATIONS

In eucaryotes, double-helix DNA is packaged by tightly wrapping 145-147 base pairs around an octomer. This DNA:protein compact structure is called as chromatin and nucleosome is the basic unit of chromatin. Nucleosome is composed of two copies of four core histone proteins; H2A, H2B, H3 and H4. In addition, histone protein H1 is a linker histone which establishes on DNA between nucleosomes and facilitates condensed nucleosome chain called as chromatin fiber[121]. Core histone protein stucture was shown in Figure 1.5.

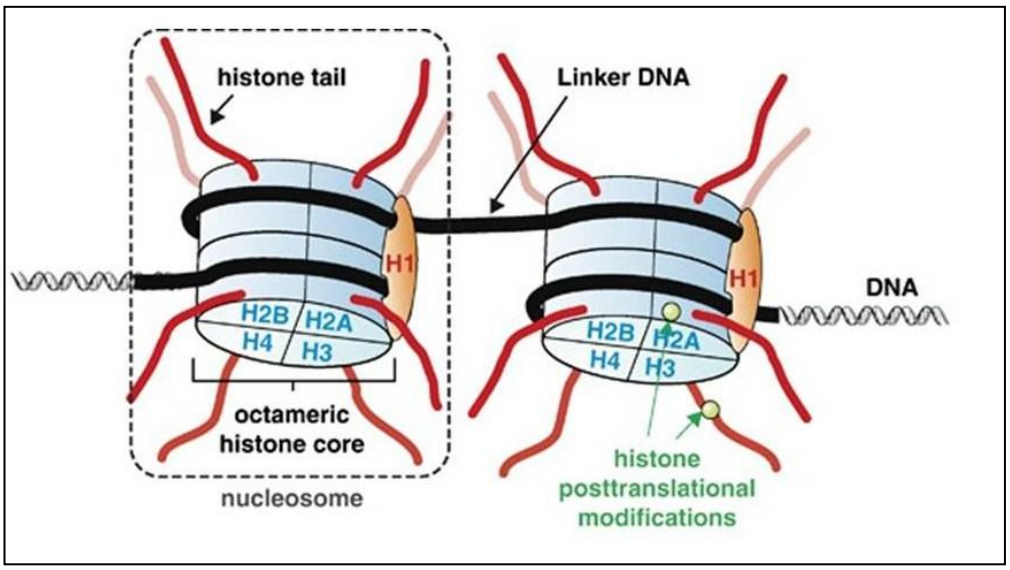

Figure 1.5 Core histone structure (Figure is adopted from[194])

Packaging is required to establish the whole genomic DNA in nucleus. Dynamic N-terminal tails of histones, which protrude out from nucleosome structure, are subjected by post-translational modifications (PTMs). These modifications regulate gene transcription through controlling the accesibilty of transcription factors and co-regulators. There are eight major PTMs; methylation, acetylation, phosphorylation, ubiquitination, sumolaytion, deamination, ADP-ribosylation and proline isomerization. The modifications which occur on histone tails can be propagated to daughter cells during cell division like DNA methylation. Post-translational modifications occur on lysine (K), arginine (R), serine (S) and threonine residues of tails and they are regulated by specific enzymes termed chromatin modifiers. Furthermore, there are different forms of modifications that occur on these residues. For instance,

lysine residues can be mono-, di-, or trimethylated and one or two methyl group can be added to arginine residues [96,118,120,121].

Genes are regulated by different combinations of histone modifications at a specific locus, which is known as histone code. Histone code hypothesis was firstly suggested by Strahl and Allis in 2000 [122,123].

Covalent modifications which take place on specific sites of histone tails associated with both activation and repression of transcription. Methylation of lysine 9 and lysine 27 of histone H3 (H3K9me / H3K27me) correlates with repression state, whereas methylation of lysine 4 or lysine 36 (H3K4me/ H3K36me) and acetylation of lysine 9 (H3K9ac) associates with active genes [124,125]. Post-translational covalent histone modifications on core histone proteins was shown in Figure 1.6.

First identified histone modifier enzyme was a histone acetyltransferase (HAT) Gcn 5[126]. HATs are considered as transcriptional activators because they provide the neuralization of positive charge of lysine via transferring acetyl group to ε amino group of lysine. Thus, they facilitated weakened DNA-histone interaction, which enables the access of transcription factors and co-activators. Histone deacetylases (HDACs) remove the acetyl groups from lysines and considered as repressors[127]. There are three main acetyltransferase families;

GNAT, MYST, and CBP/p300 and four classes of HDAC Classes I, II, IV and III, which is homologous to yeast Sir2[128].

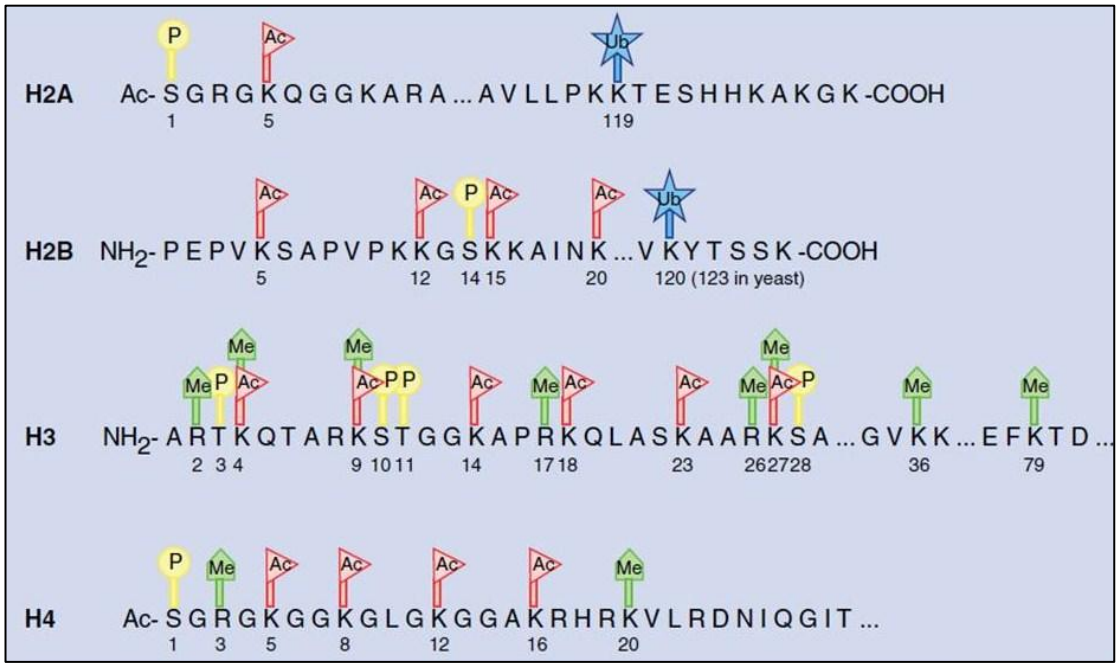

Figure 1.6 Post-translational covalent histone modifications on core histone proteins. P: Phosphorylation, Ac: Acetylation, Ub: Ubiquitinylation, Me: Methylation (Figure is adopted from[118]).

Histone methylation occurs on the lysine and arginine residues of tails. Methylation of lysines implies both active and repressive chromatin states[118]. Methylation of H3K9 and H3K27 associates with silent chromatin state, whereas methylation of H3K4 and H3K36 associates with euchromatin state[129]. In recent studies it was reported that, in mouse embryonic stem cells, bivalent domains are found which contain both H3K27me3 and H3K4me3 marks[130].

SUV39H, which is the first identified histone lysine methyltransferase (HKMT), is responsible for the methylation of H3K9. HKMTs specifically methylate lysine residues at a specific degree; mono-, di-, tri- methylation[132,124]. SET7/9 catalayzes demethylaion of H3K4 and EZH2 targets H3K27. Histone modifier enzymes and modified residues were given in Table 1.2.

Chromatin Modification	Enzyme	Modified Residues
ACETYLATION	HAT1	H4K5, H4K12, H3K14, H3K18
	CBP300/P300	H4K5, H4K8, H2AK5, H2BK12, H2BK15
	PCAF/GCN5	H3K9,H3K14,H3K18
	TIP60	H3K14, H4K5, H4K12, H4K16,
DEACETYLATION	SirT2 (ScSir2)	H4K16
	MLL1/2/3/4/5	H3K4
	SUV39H2	H3K9
	G9a	H3K9
METHYLATION	ESET/SETDB1	H3K9
	EZH2	H3K27
	SET2	H3K36
	SMYD1	H3K36
	DOT1	H3K79
	CARM1	H3R2,H3R17,H3R26
	LSD1	H3K4
DEMETHYLATION	JHDM2a/b	H3K9
	JMJD3	H3K27
	JHDM1a/b	H3K36

Table 1.2 Mammalian histone modification enzymes

1.6 EPIGENETIC ALTERATIONS IN STEM CELLS

In ESCs, lineage specific genes are repressed through both DNA methylation and repressive histone modifications such as Histone-3 lysine-9 (H3K9) and Histone-3 lysine-27 (H3K27), whereas, the expressional regulation of pluripotency assocaited genes such as Oct4, Nanog and Sox2 is correlated with DNA methylation[110,131]. Moreover it was demonstrated that Polycomb group (PcG) protein complexes and HP1 are required for gene repression in ESCs[132]. Regulation of cell lineage speficic genes are mediated by bivalent histone modifications. Bivalent domains are considered as transcription-ready sites. These genes are regulated by both H3K4 and K27 trimethylation and the genes are activated upon differentiation induction[133]. Genome-wide distribution of DNA methylation, histone methylation and chromatin modifications regulates the changes that occur during cell differentiation. Thereby, epigenetic modification patterns including both histone modifications and DNA methylations of ESCs are clearly distinguished from differentiated somatic cells. The genome-scale DNA methylation maps and chromatin-state maps of ESCs revealed that housekeeping genes are highly expressed and enriched with H3K4me3 active mark, whereas lineage specific genes are repressed through both DNA methylation and repressive histone modifications such as H3K9 and H3K27[134]. DNA methylation is under the control of DNA methyltransferase Dnmt3a, Dnmt3b and Dnmt1 during embryogenesis[135]. A failure which changes

the maintenance of DNA methylation results in emryonic lethality in mice[136] and several diseases such as cancer, Alpha-thalassemia, mental retardation and fragile-X syndrome[112]. It was also reported that the passaging also causes change in DNA methylation pattern of ESCs. In a previous study, it was demonstrated that methylation of tumor supressor genes; RASSF1, DCR1 and PTPN6 increase at late passages in human ESCs[138].

Direct reprogramming of somatic cells by transcription-factor transduction yields iPSCs with remarkable similarity to embryonic stem cells. These two pluripotent stem cells share very similar epigenetic profiles[137]. On the other hand large-scale methylation comparisons have identified differences such as CpG methylation which is higher in iPSC than in ESCs[138]. In addition whole-genome screening revelaed the presence of differentially methylated regions (DMRs) within iPSC. These regionas are resistant to reprogramming[139]. Actually, the differences in pluriportent states and differential potential of iPCs and ESCs was not observed, whereas, retaining of the residual epignetic marks after differentiation influences cell fates in iPS cells. This problem manifests the epigenetic memory[140]. For instance, iPSCs derived neural progenitors and fibroblasts demonstrate decreased blood-forming potential in vitro due to the retained residual methylation at loci which is required for haematopoietic cell fate.

In contrast to the promoters of pluripotent stem cells, most of genes specifying

cell types are hypomethylated in MSCs. DNA hypomethylation contributes transcriptionally permissive state. But this hypomethylated state does not predict differentiaton capacity of MSCs. Since these genes are mainly regulated by post-translational histone modifications. H3K4 and H3K27 bivalency on lineage-specific genes was demonstrated. After differentiation induction, H3K27 demethylases activates the transcription of these genes[5, 141]. In MSCs on adipogenic gene promoters including PPARγ2, leptin, fabp4, and lipoprotein lipase (lpl) hypomethylation is established. In addition the adipogenic genes show mosaic CpG methylation patterns[59]. During differentiation demethylation of H3K9, acetylation of H3 and H3K4 trimethylation were also shown on adipogenic gene promoters[142,143]. MSC cultures from bone marrow show stable DNA methylation pattern between early and late passages. Osteocalcin is a ostegeneic linege specific gene and target of RUNX2. In the presence of osteogenic induction, on osteocalcin promoter acetylation of H3 and H4 increases, wheras DNA metyhlation decreases[144]. It was known that osteogenesis has a dominant effect on adipogenesis and osteoblastic inducers; bone morphogenetic protein 2 (BMP2) and Wnt ligands, suppresses transcription of PPARγ recruting repressor histone methyltransferase[145]. It was also reported that JMJD2B and JMJD3B enzymes are the link between the osteogenesis and chondrogenesis. It was shown that overexperssion of these demethylases stimulates the expression of alkaline phospahatase (ALP), which is an osteoblast differentiation marker, whereas depletion of these demethylases

resulted in a significant increase in adipogenic differentiaton in MSCs[146].

1.7 ESTROGEN AND EPIGENETIC REGULATION

Co-activators and co-repressors are directly recruited by nuclear receptors as a consequence of ligand-binding. Until now approximately 285 co-regulators associated with nuclear receptors were identified. Also it was reported that a mutation, which occurs in the expression of these co-regulators, causes diseases such as multiple cancers, Alzheimer, Parkinson and Huntington diseases[84]. Estrogen receptors also regulate gene transcription interacting with co-activators or co-repressors; enzymatic complexes such as HATs, SWI/SNF complexes and HDACs[89].

Effect of estrogen on epigenetic mechanisms has been mostly investigated in breast cancers. In breast cancer, regulation of gene expression is mediated by methylation of DNA and acetylation of histone proteins and estrogen plays an important role in both formation of breast cancer and breast cancer treatment. It was well established that estrogen stimulates development of certain breast cancers and hormonal therapy via anti-estrogen treatment is widely used in treatment of these cancers[147]. H3K9me3 demethylase JMJD2B and H3K4 methyltransferase MLL2 complex directly interacts with ER. This is responsible for the cellular function of ERα in MCF-7 breast cancer cell line[148].

In the ER-negative breast cancer cells, promoter of ER gene is hypermethylated and ER mRNA is absent. Treatment of the ER-negative breast tumors with DNMT and HDAC inhibitors imposes to the reactivation of ERα[149].

In contrast to known stimulator effect of estrogen on gene expression, estrogen occupied ERα may also repress the gene expression by recruiting corepressor/HDAC complexes[150-153] and DNA methyltransferase which enables establishment of hypermethylation on specific CpG loci[152]. On the other hand, high level of acetylation was observed on E2-stimulated genes. The proposed model was demonstrated in Figure 1.7.

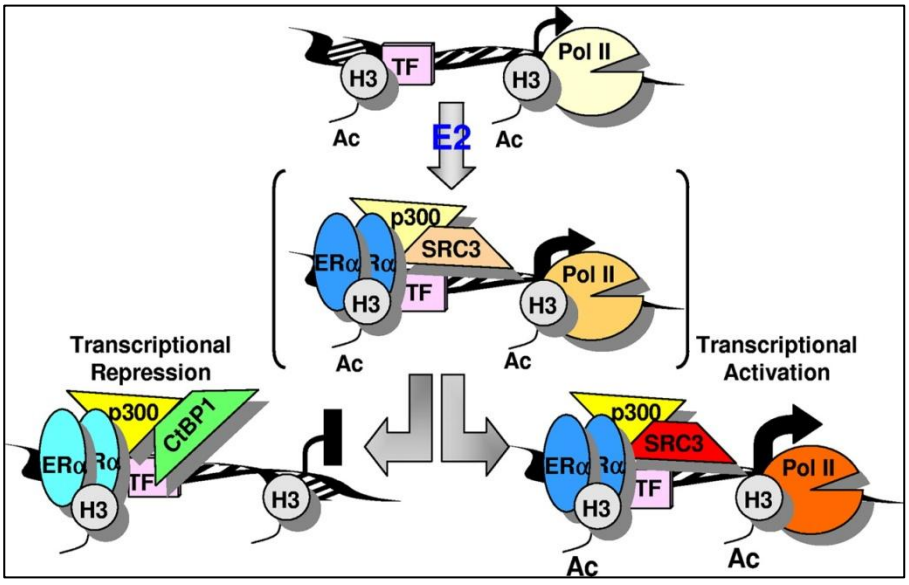

Figure 1.7 Demonstration of repression of early target genes mediated by ERα (Figure is adopted from[153])

CBP/p300, SRC-1 (NCoA-1/p160), SRC-2, SRC-3 are HATs that interact with

ER[154]. Recent studies have shown that in addition to lysine methyltransferases, arginine mehtyltransferases such as CARM1, PRDM1 and PRDM2 are also potential coactivators of ER[154]. Uterine growth in response to estrogen stimulation have demonstrated that PRDM2 directly binds to ER in the presence of estrogen. When ovariectomized mice were treated with estrogen, normal uterine horn growth was observed, whereas in PRDM2-null mutant mice the estrogen response was partially observed suggesting PRDM2 is required for maximal uterine response to estrogen[155].

Hippocampus is necessary for various types of memories such as relational, spatial and contextual information. Studies which focused on the relationship between hippocampus and epigenetic mechanism revealed that exogenous estrogen enhances hippocampus-dependent memory in ovariectomized rodents changing both histone H3 acetylation and DNA methylation[156].

1.7.1 RELATIONSHIP BETWEEN THE ROLE OF ESTROGEN IN EPIGENETIC REGULATION AND MESENCHYMAL STEM CELLS

The effect of estrogen on MSC proliferation and differentiation into adiopocyte, osteocyte and chondrocyte have been shown in several studies[154-166], MSCs are

potential cell source especially for tissue engineering applications due to their differentiaton capacities. The major obstacle was the limited isolated cell number of MSCs. It was reported that 17-β estradiol (E2) enhances effectively MSC proliferation in conventional cell culture media[80]. Moreover estrogen up-regulates HTERT and telomerase activity. By this way, estrogen treatment prevents telomere shortening in MSCs[154-156]. Also, the inhibitory effect of estrogen on apoptosis through the expression of Bcl-2 family genes was demonstrated by our group[79]. Estrogen deficiency is considered as major cause of osteoporosis, osteoarthritis and obesity in postmenopausal women[88,89,156-158]. It was well established that estrogen promotes osteogenesis and chondrogenesis. Throughout life, bone tissue is remodeled by osteoblasts and osteoclasts which play key role in bone formation and bone resorption respectively. It was shown that estrogen treatment prevents the bone loss increasing the osteogenic differentiation activity in MSCs through ER α during postmenapausal stage[157]. In addition, estrogen is crucial for normal longitudinal growth. Further studies demonstrated that, estrogen replacement causes decreasing in vertebral deformation and loss of articular cartilage in postmenopausal women[158,159].

Obesity, which was defined as an excess amount of white adipose tissue accumulation resulted from increased adipocyte cell size, is considered as one of the top ten global health problems by World Health Organization[55, 160,161]. In

previous studies the existence of signal cross-talk between estrogen hormone and adipose tissue was also identified[162]. Both estrogen and phytoestrogen treatment represses adipogenesis inhibiting expression of early and late adipogenic differentiation markers[167,163]. The enhanced fatty acid formation in overieoctimized animals can be reversed by estrogen replacement therapy[162,164]. Studies have shown that, there is an inverse correlation between osteogenesis and adipogenesis. Differentiation of MSC into one lineage represses the differentiaton into another cell lineage[165]. Estrogen promotes osteogenesis and chondrogenesis in MSCs while inhibiting adipogenic differentitation through recruitment of co-repressors on the PPARγ and other adipose specific-genes [166]. It was known that osteogenesis dominates the adipogenesis and bone morphogenetic protein 2 (BMP2) and Wnt ligands, which are osteoblastogenesis inducers, suppresses transcription of PPARγ through the activation of H3K9 methyl transferase SETDB1 and G9a[145,146].

CHAPTER 2

AIM OF THE STUDY

Mesenchymal stem cells (MSCs) are considered as potential cell source for tissue engineering and regenerative medicine applications due to their multi-lineage differentiation capacity, non-immunogenic characteristics, homing ability and easy isolation techniques. Moreover, until now different types of biomaterials were reported as scaffold material for MSC transplantation. In recent years, CNT was demonstrated as a new alternative scaffold material due to their unique physical properties such as injectable, cytocompatible features and nanoscale sizes.

The key role of estrogen in the regulation of MSC proliferation, maintenance and differentiation is known. However, the effect of estrogen on the genetic and epigenetic regulation of MSC differentiation into specific cell types and on the maintenance of MSCs seeded on scaffold materials have not been fully elucidated.

There is an inverse correlation between osteogenesis, chondrogenesis and

adipogenesis processes. Estrogen treatment stimulates osteogenesis and chondrogenesis while leads to the inhibition of adipogenesis in bone marrow stromal cells. Therefore, understanding the epigenetic and genetic mechanisms underlying MSC differentiation upon estrogen treatment and examination of cell viability and maintenance of MSCs on CNT biomaterial in the presence of estrogen may provide insight into the regulation of MSC-fate determination and increase our ability to use MSCs therapeutically.

In this thesis, we aimed to study the genetic and epigenetic changes in transcription factors that regulate MSC differentiation with an emphasis on adipogenesis and osteogenesis upon estrogen treatment and the effect of estrogen hormone on the maintenance of MSCs on carbon nonatube arrays.

The maintenance/viability of MSCs on CNT arrays at different passages were assessed in the presence and absence of estrogen. In addition we also tested whether CNTs could replace the presence of extracellular matrix by culturing them without collagen.

The effect of estrogen on the expression and differential localization of transcription factors involved in adipogenesis, osteogenesis and chondrogenesis differentiation of MSCs were examined. In addition, estrogen's effect on the histone modifications and histone modifier enzymes were investigated.

Promoter regions of adipogenic and osteogenic transcription factors were examined for possible binding of Erα. CpG methylation status of adipogenic transcription factors and ERα were also investigated upon estrogen treatment.

CHAPTER 3

MATERIALS AND METHODS

3.1 ANIMALS

For the experiments, normal female and ovariectomized Sprague Dawley rats were used. The animals were kept in the animal holding facility of the Department of Molecular Biology and Genetics at the Bilkent University permitting unlimited access to food and water at all times .The animals were housed under controlled environmental conditions with 12 hour light and 12 hour dark cycles and at 22˚C. The experimental protocols were performed according to Bilkent University's guidelines on humane care and use of laboratory animals.

3.1.1 OVARIECTOMIZATION

The ovariectomization procedure was performed under full anesthesia using Ketamine (Park Davis, Michigan, USA) at a concentration of 30 mg/kg. On the vertebrate two incisions were made. Ovaries which are at the tip of each uteri

horn were tied with silk and removed. The incisions were sutured and kept under control until animals recovered from the anesthesia. Ovariectomized animals were used for experiments almost after 2 months after the operation to ensure the total deficiency of estrogen.

3.2 SYNTHESIS, PATERNING CHARACTERIZATION OF CARBON NANOTUBES

Carbon nanotubes (CNT) were prepared by Assist. Prof. Dr. Erman Bengü and Gökçe Küçükayan in Bilkent University, Department of Chemistry. In this study multi-walled type carbon nanotube (CNT) samples were used. The vertically aligned carbon nanotubes arrays were synthesized performing chemical vapor deposition (ACCVD) method on Si substrates. The catalyst layers were formed on the Si surface using sandwich catalyst design; Al:Co:Al as reported in previous study[167]. The aforementioned layers were introduced into the ACCVD furnace for growth of carbon nanotube. Asperities were created on vanta surfaces in patterning step. For this purpose, deinozied water was dropped on the vanta surfaces to form cavities resulting of water contact. After the synthesis and patterning steps, characterization of syhtnesized CNTs was done using scanning electron microscope (SEM) analysis was performed by Assist. Prof. Dr. Erman Bengü and Gökçe Küçükayan in Bilkent University, Department of Chemistry.

To examine the effect of collagen on the attachment and cell viability, patterned CNTs were also treated with 2.5 μl of 1 μg/μl sterilized collagen solution. Collagen coated and non-coated CNT layers were sterilized under UV for 45 minutes before using in cell culture.

3.3 ISOLATION AND CULTURING OF MSC FROM RAT BONE MARROW

Bone marrow heterogeneous cell population was collected from the tibia and femur of the normal female and ovariectomized nine-week old, 280-300 g Sprague-Dawley rats. After cervical dislocation, tibia and femur bones were removed and bone marrow cells were flushed with a 5 mL syringe in DMEM (HyClone, Logan, USA) containing 10% fetal bovine serum (FBS) (HyClone, Logan, USA) and 1% penicllin-streptomycin antibiotic (HyClone, Logan, USA). The cell suspension was centrifuged at 1500 rpm for 5 minutes and the supernatant was removed. Cell pellet was resuspended in 10 ml of 1X phosphate buffered saline (PBS) and then centrifuged again at 1500 rpm for 5 minutes. The washing step was performed two more times with the same conditions. The bone marrow cells were cultured in MesenCult medium (StemCell Technologies, Vancouver, Canada) including 20% supplement (StemCell Technologies, Vancouver, Canada) and a 1% penicillin–

streptomycin solution (HyClone, Logan, USA) for fourteen days to obtain mesenchymal stem cell. The equal number of cells was plated onto the cell culture flasks. The cells were counted with hematocytometer and calculation was done according to formula given below:

Total number of cells = number of cells in mm^3 X 10^4 X dilution factor

The media were changed every 4 days, after washing with sterile 1XPBS. In addition to untreated group, for treatment either 10^{-7} M estrogen (17 ß-estradiol, Sigma, Germany) or 10^{-6} M tamoxifen (Sigma, Germany) was added to the culture plates from the first day of culture and until the last day to obtain the estrogen or tamoxifen treated counterparts. Tamoxifen treated groups were used for chromatin immunoprecipitation experiments.

To investigate the role of estrogen in the maintence of MSCs on CNTs, at the end of the 14th day, 10^4 cells which were incubated in the absence and presence of the estrogen were seeded on non-coated CNT surfaces. The cells were incubated cultured on CNTs for 3 days.

In addition, to examine the changes of cell viability and growth of MSCs on the collagen coated and non-coated CNTs, cells were passaged when they reach confluency. The groups were stated as passage zero (P0), passage 1 (P1) and passage 2 (P2). After each passage, 10^4 cells were seeded on patterned CNT

placed in 96-well plates to measuere cell viability and 3 $x10^5$ cells were seeded on patterned CNT placed in 6-well plates to count the number of cells. MSCs, which were seeded on to 96-well culture plates without CNT arrays, were used as control group.

3.4 IMAGING OF MSCS ON CARBON NANOTUBES

The CNTs were placed in 6-well plates. $3x10^5$ MSCs from P0, P1 and P2 were cultured in Mesencult media on the CNTs. The cells were washed with 1XPBS at the end of the 3rd day of culture and their image was taken by SEM at low vacuum mode.

3.4.1 CALCULATION OF THE NUMBER OF ATTACHED MSCS ON CNT SURFACES

$3x10^5$ MSCs from P0, P1 and P2 were seeded onto non-coated and collagen coated patterned CNT surfaces. At the end of the 3rd day of incubation, SEM analysis was performed. The number of attached cells were counted from the SEM images and average areal density was calculated by dividing this number to the total surface area.

3.4.2 CELL PROLIFERATION ASSAY FOR THE MSCS ON CNT SURFACES

The viability of MSCs on the coated and non-coated CNTs were examined by cell proliferation assay (3-(4,5-dimethyl-2-thiazolyl)-2,5-diphenyl-tetrazolium bromide- MTT) using Cell Proliferation Kit I (Roche). 10^4 cells were seeded onto patterned CNTs in 96-well culture plates. At the end of the 3rd day of incubation, MTT assay was performed according to the manufacturer's instructions. Control group was obtained from cells seeded onto 96-well culture plates without CNT arrays and their viability was accepted as 100%. Spectrophotometrical absorbance of the samples was measured by ELISA reader with the wavelength between 550 and 600 nm.

3.5 ADIPOGENIC AND OSTEOGENIC DIFFERENTIATION

MSCs were trypsinized (Hyclone, Logan, USA) and plated onto new cell culture flasks at day 14 of their culture and incubated with Mesencult media until they reached 85-95% confluency. After that, the media was replaced with adipogenic induction media containing 100 μM indomethacine (Sigma,Germany), 1 μM dexamethasone (Sigma,Germany), 0.5mM IBMX (Sigma,Germany), 10 μg/mL insulin (Sigma,Germany), 1% penicillin/streptomycin (HyClone,Logan, USA), 10% FBS (HyClone, Logan,

USA) in DMEM-LG (HyClone Logan, USA) and osteogenic induction media containing 0.1 μM dexamethasone, 10 mM glycerol phosphate salt hydrate (Sigma,Germany), 0.2 mM ascorbic acid γ-irradiated (Sigma,Germany), 10 % FBS (Hyclone, Logan, USA) and 1% penicillin/streptomycin (Hyclone Logan, USA) in DMEM low glucose (Hyclone, Logan, USA). The media was changed three times a week. Adipogenic and osteogenic induction media were prepared freshly before every medium change. As negative control, the cells were incubated only with DMEM low glucose (Hyclone, Logan, USA) for 24 days in the presence and absence of estrogen.

3.6 DETECTION OF ADIPOGENIC AND OSTEOGENIC INDUCTION

3.6.1 OIL RED O STAINING

At the end of the 13^{th} day and 24^{th} day of the adipogenic differentiation, the medium was removed and cells were washed with 1XPBS. They were incubated in 10% formaldehyde for 10 minutes at room temperature (RT) and washed once with 1XPBS and then with water. Cells were incubated with Oil red O (Sigma, Germany) solution for 50 minutes at room temperature.

Afterwards, Oil red O solution was aspirated and the cells were washed with tap water. The photos were taken under the light microscope.

3.6.2 ALIZARIN RED STAINING

At the end of the 13th day and 24th day of the osteogenic differentiation, the media was aspirated and cells were washed with 1XPBS. Then they were fixed with 70% ethanol at room temperature for 1 hour. After that the cells were washed with distilled water and stained with 40 mM Alizarin Red S (Sigma, Germany) (pH:4.1) at room temperature for 30 minutes. The cells were washed with tap water. Photos were taken under light microscope.

3.7 TOTAL RNA ISOLATION FROM MSCs AND DIFFERENTIATED CELLS

Total RNA was isolated from MSCs at the end of the 14th day of the cell culture and from adipogenic and osteogenic differentiated cells at the end of the 13th day, 17th day and 24th day of the differentiation. The cells were washed with 1XPBS twice and trypsinized (Hyclone, Logan, USA) at 37˚C for 3 minutes. The cells were collected from cell culture flasks adding DMEM (Hyclone , Logan, USA) containing 10 % FBS (Hyclone Logan, USA) and 1% penicilin-

streptomycin (Hyclone, Logan, USA). The cell suspension was centrifuged at 1500 rpm for 5 minutes. After centrifugation supernatant was sucked and pellet was resuspended in 10 ml 1XPBS to wash and centrifuged again at 1500 rpm for 5 minutes. The supernatant was removed. The cell pellet was used for RNA isolation using Nucleospin RNA II kit isolation kit (Macherey-Nagel, Germany) according to instructions of the manufacturer. At the end of the protocol RNA was eluted with RNase free water and the concentration was determined with NanoDrop ND1000 spectrophotometer (Nanodrop technology, USA).

3.8 cDNA SYNTHESIS

For each cDNA synthesis reaction 2 µg of RNA was used by using DyNAmo cDNA synthesis kit (Finnzymes, Finland). 2 µg RNA was mixed with DEPC treated ddH2O to a total volume of 12 µl. 2 µl of Oligo (dT) primer was added to the mixture. The mixture was incubated at 65˚C for 5 minutes and then chilled on ice for 3 minutes. 20 µl of 2X RT buffer including dNTP mix and $MgCl_2$, and 4 µl of M-MuLV RT RNase H+ enzyme was added to the mixture and then incubated at 25˚C for 10 minutes, 45˚C for 45 minutes and 85˚C for 5 minutes. The cDNA samples were kept at -20˚C.

3.9 PRIMER DESIGN FOR QUANTITATIVE REAL TIME PCR AND REVERSE TRANSCRIPTASE PCR

Primers which were used for quantitave real time PCR (qRT-PCR) and reverse transcriptase PCR (RT-PCR) were designed by using Primer exe, Primer3 and Primer Blast (NCBI) programs. The amplified fragment size of the PCR products of each primer and the specificity of the primers were controlled with NCBI and ENSEMBLE databases which are publicly available. The primer sequences were listed in the Table 3.1

3.10 QUANTITATIVE REAL TIME PCR

The real time PCR reactions were performed using SYBR green real time PCR kit (Finnzymes, Finland) at a reaction volume 12.5 µl containing 6.25 µl of SYBR green master mix, 1µl 10 pmol forward, 1µl of 10 pmol reverse primers, 3.25 µl of ddH_2O, 1 µl of cDNA. Cyclophilin was used as a housekeeping gene and expression results for all transcription factors were normalized according to Cyclophillin expression level. Before performing qRT-PCR reactions using experimental samples, amplification efficiencies for all primers were calculated by using 1:2 dilution series according to the below formula:

Efficiency = 2^ (-1/slope)

Fold changes in the expression of the genes were analyzed based on the comparative ($2^{-\Delta\Delta Ct}$) method. Normal female MSCs were used as calibrator. The qRT-PCR reaction conditions for all investigated genes were given in the Table 3.2. Each protocol was followed by melt curving to control purity of the amplification. Efficiencies of primers were stated in Table 3.3.

3.11 REVERSE TRANSCRIPTASE PCR

DNA amplification for adipogenic transcription factors; C/EBPα, FABP4, PPARγ and osteogenic transcription factor; RUNX2 were performed using Phire Hotstart Taq Polymerase (Finnzymes, Finland). Taq DNA Polymerase was used for β-actin amplification. The MSCs seeded onto CNTs were characterized by using CD90, CD70, CD45, CD34 and CD29 markers. For characterization experiment, RT-PCR was performed using Taq Polymerase (Finnzymes, Finland). RT-PCR conditions were given in the Table 3.4.

Name of the Genes	Sequences of Forward and Reverse Primers	Size (bp)
CEBP α	forward 5'-AGTCGGTGGATAAGAACAGC-3' reverse 5'-CATTGTCACTGGTCAACTCC-3'	118
PPAR γ	forward 5’-TTTTCAAGGGTGCCAGTTTC -3’ reverse 5’-AATCCTTGGCCCTCTGAGAT-3’	178
FABP4	forward 5'-CACCGAGATTTCCTTCAAAC-3' reverse 5'-TCACCATCTCGTCTCCTCTT-3'	136
Adipsin	forward 5’-TGGTGGATGAGCAGTGGGT -3’ reverse 5’-AGGGTTCAGGACTGGACAGG- 3’	110
RUNX2	forward 5'-TAACGGTCTTCACAAATCCTC -3' reverse 5-'GGCGGTCAGAGAACAAACTA -3'	115
SOX9	forward 5'-GTGGATGTCAAAGCAACAGG-3' reverse 5'-TCTTGATGTGCGTTCTCTGG-3'	168
ATF3	forward 5'-ACAACAGACCTCTGGAGATG-3' reverse 5'-CAGGCACTCTGTCTTCTCTT-3'	120
MEF2C	forward 5'-TTGAGTAGAAGGCAGGGAGA-3' reverse 5'-CAGCAGCAGCACCTACATAA-3'	107
ETS1	forward 5’-CCCTGGTAACGTGCAGAAGT-3 reverse 5’-CTTCCAGATGTCCAGGTGAG-3	158
Cyclophilin	forward 5’-GGGAAGGTGAAAGAAGGCAT-3’ reverse 5’-GAGAGCAGAGATTACAGGGT-3’	211
CD90	forward 5’- CCAGTCATCAGCATCACTCT-3’ reverse 5’- AGCTTGTCTCTGATCACATT- 3’	374
CD34	forward 5’- TGTCTGCTCCTTGAATCT -3’ reverse 5’- CCTGTGGGACTCCAACT- 3’	281
CD29	forward 5’-ACTTCAGACTTCCGCATTGG -3’ reverse 5’- GCTGCTGACCAACAAGTTCA-3’	190
CD45	forward 5’- ATGTTATTGGGAGGGTGCAA-3’ reverse 5’- AAAATGTAACGCGCTTCAGG-3’	175
CD71	forward 5’- ATGGTTCGTACAGCAGCAGA-3’ reverse 5’- CGAGCAGAATACAGCCATTG-3’	182
BETA ACTIN	forward 5’-CTGGCCTCACTGTCCACCTT-3’ reverse 5’-GGGCCGGACTCATCGTACT-3’	65

Table 3.1 The product size and sequences of primers used for qRT-PCR

Name of the Genes	First Denaturation	Denaturation	Annealing	Extension	Cycle	Final Extension
CEBPα	95°C, 15 min	94°C, 30 sec	60°C, 60 sec	72°C, 40 sec	30	72°C, 50sec
FABP4	95°C, 15 min	94°C, 30sec	60°C, 60 sec	72°C, 40 sec	30	72°C, 50sec
PPARγ	95°C, 15 min	94°C, 30sec	60°C, 45 sec	72°C, 45 sec	30	72°C, 50sec
RUNX2	95°C, 10 min	94°C, 30 sec	60°C, 45 sec	72°C, 40 sec	30	72°C, 50sec
SOX9	95°C, 10 min	94°C, 30 sec	63º C,60sec	72°C, 20 sec	30	72°C, 50sec
ATF3	95°C, 10 min	94°C, 30 sec	64º C,45sec	72°C, 20 sec	30	72°C, 50sec
MEF2C	95°C, 10 min	94°C, 30 sec	64º C,45sec	72°C, 20 sec	30	72°C, 50sec
ETS	95°C, 10 min	94°C, 30 sec	64º C,45sec	72˚C, 20sec	30	72°C, 50sec
Adipsin	95°C, 15 min	94°C, 30 sec	60º C,45sec	72°C, 20 sec	30	72°C, 50sec
Cyclophillin	95°C, 15 min	94°C, 30 sec	55º C,45sec	72°C, 20 sec	30	72°C, 50sec

Table 3.2 qRT-PCR conditions

Name of the Genes	Efficiency
CEBP α	2.1
PPAR γ	2.2
FABP4	1.7
Adipsin	2.08
RUNX2	2.1
SOX9	2.2
ATF3	1.9
MEF2C	2
ETS1	2.2
Cyclophillin	1.9

Table 3.3 Efficiencies of primers used for qRT-PCR

Name of the Genes	First Denaturation	Denaturation	Annealing	Extension	Cycle	Final Extension
CEBPα	98°C, 30 sec	98°C, 5 sec	63°C, 60 sec	72°C, 40 sec	35	72°C, 50sec
FABP4	98°C, 30 sec	98°C, 5 sec	63°C, 60 sec	72°C, 40 sec	35	72°C, 50sec
PPARγ	98°C, 30 sec	98°C, 5 sec	60°C, 45 sec	72°C, 40 sec	35	72°C, 50sec
RUNX2	98°C, 30 sec	98°C, 5 sec	60°C, 45 sec	72°C, 40 sec	35	72°C, 50sec
β actin	95°C, 30 sec	95°C, 30 sec	60°C, 35 sec	72°C, 40 sec	25	72°C, 50sec
CD90	95°C, 5 min	94°C, 30 sec	55°C, 30 sec	72°C, 30 sec	30	72°C, 5 min
CD34	95°C, 5 min	94°C, 30 sec	55°C, 30 sec	72°C, 30 sec	30	72°C, 5 min
CD71	95°C, 5 min	94°C, 30 sec	66°C, 60 sec	72°C, 45 sec	35	72°C, 5 min
CD29	95°C, 5 min	94°C, 30 sec	60°C, 30 sec	72°C, 30 sec	26	72°C, 5 min
CD45	95°C, 5 min	94°C, 30 sec	60°C, 30 sec	72°C, 30 sec	45	72°C, 5 min

Table 3.4 RT-PCR conditions

3.12 AGAROSE GEL ELECTROPHORESIS

1XTAE was used to prepare 1% agarose gel and 1 mg/ml ethidium bromide was added to agarose-TAE mixture prior to polymerization. Before loading the samples onto the gel, 6X agarose gel loading dye was added to the PCR products at a final concentration of 1X. Gene ruler DNA ladder mix (Fermentas, Canada) and 100 bp DNA Ladder (New England, Biolabs, MA, USA) was used as markers and 5 µl was loaded to gel. The gel was run at 85 Volt for 25-40 minutes and visualized under transluminator (Gel-Doc Biorad Vilber Lourmat, France). ChemiCapt (Vilber Lourmat) software was used to take the photographs of the gel.

3.13 SEMI QUANTITATIVE ANALYSIS

After the gel photos were taken, semi quantitative analysis for RT-PCR results was performed using Bio1D (Vilber Lourmat) to calculate the band intensities.

3.14 IMMUNOFLUORESCENCE STAINING FOR TRANSCRIPTION FACTORS

At the end of the 14^{th} day of culture MSCs were trypsinized and $1.5x10^5$ cells were seeded onto cover slips (Deckglaser 100 No.1 12mm) in the 6-well cell plates. They were fixed with ice-cold methanol for 10 minutes. The cells were

washed with 1X PBS-Tween solution twice and left in blocking solution for 1 hour at room temperature. After that, blocking solution was removed and the cells were incubated with primary antibodies for 1 hour at room temperature. All primary antibodies were purchased from Santa Cruz (Santa Cruz, USA). After primary antibody incubation, cells were washed twice with 1XPBS-Tween and incubated with FITC-labeled secondary antibodies for 1 hour at room temperature. All secondary antibodies were purchased from Santa Cruz (Santa Cruz, USA). Finally, after the secondary antibody incubation, cover slips were washed twice with 1XPBS-Tween solution and mounted with mounting medium containing DAPI (Santa Cruz). The images were captured by fluorescent microscope with 490 nm and 359 nm wavelengths for FITC and DAPI respectively. Primary and secondary antibodies used in immunofluorescence staining and their dilution concentrations were stated in Table 3.5.

Antibody	**Dilution**
PPAR g	1:200
Ets1	1:200
FITC-Anti Rabbit	1:200
FITC-Anti Mouse	1:200

Table 3.5 Dilution rates of antibodies used for immunofluorescence staining

3.15 PROTEIN ISOLATION AND QUANTIFICATION

3.15.1 TOTAL PROTEIN ISOLATION AND QUANTIFICATION

MSCs were scraped from cell culture flasks in 10ml 1XPBS with a scraper. Cell suspension was centrifuged at 1500 rpm for 5 minutes at 4˚C. The pellet was dissolved in lysis buffer and incubated on ice for 30 minutes by finger tipping every 5 minutes. Then, the lystes were centrifuged at 13000 rpm for 20 minutes at 4˚C. Supernatant containing total proteins was taken and stored at -80˚C. The protein concentration was determined performing Bradford assay[168].

3.15.2 HISTONE PROTEIN EXTRACTION FROM MSCs

At the end of the 14th day, MSCs were scraped and cell pellet was dissolved in 400 µl TEB buffer containing 1XPBS, 0.5% Triton X-100 (Sigma, St. Louis, Germany), 0.02% NaN_3 (Merck, Darmstadt, Germany), 1X Protease inhibitor. Samples were centrifuged at 2000 rpm for 10 minutes at 4°C and supernatant was removed. Cell pellet was resuspended in 200 µl the TEB buffer and centrifuged again at 2000 rpm for 10 minutes at 4°C. The pellet was dissolved in 150 µl 0.2N HCL and incubated at 4°C with rotating for over-night. Samples were centrifuged at 2000 rpm at 4°C for 10 minutes and supernatant containing histone proteins was collected. Samples were kept -80˚C.

3.15.3 CYTOPLASMIC AND NUCLEAR PROTEIN EXTRACTION FROM MSCs

Nuclear and cytoplasmic protein isolation was performed using NE-PER Nuclear and Cytoplasmic Extraction Reagents according to manufacturer's protocol (Thermo Scientific, USA). MSCs were trypsinized (Hyclone, Logan, USA) and collected in 1.5 ml microcentrifuge tube. After centrifugation at 500 g for 3 minutes, the pellet was mixed with 200 µl of CER 1 and 11 µl of CER 2 solutions respectively. By centrifugation at 16000 g for 5 minutes, supernatant including cytoplasmic extract was removed and kept. The pellet was dissolved in 100 µl of NER solution and after centrifugation at 16000 g for 10 minutes, supernatant including nuclear extract was removed. Extracted proteins were kept at -80 °C. Primary and secondary antibodies used for western blotting after and their dilution concentrations were listed in Table 3.6.

Antibody	Blocking Solution	Dilution
PPAR gamma	5% milk powder in 0.3% TBS-T	1:250
Ets1	5% milk powder in 0.3% TBS-T	1:250
Atf3	5% milk powder in 0.3% TBS-T	1:250
Calnexin	5% milk powder in 0.3% TBS-T	1:1000
Cyclin E1	5% milk powder in 0.3% TBS-T	1:200
H3K27me2	5% BSA in 0.1% TBS-T	1:500
H3K27me3	5% BSA in 0.1% TBS-T	1:500
H3K9me2	5% BSA in 0.1% TBS-T	1:750
H3K9me3	5% BSA in 0.1% TBS-T	1:750
H3K36me3	5% BSA in 0.1% TBS-T	1:750
EZH2	5% BSA in 0.1% TBS-T	1:750
LSD1	5% BSA in 0.1% TBS-T	1:750
SET 7/9	5% BSA in 0.1% TBS-T	1:750
H3	5% BSA in 0.1% TBS-T	1:750
CD29	5% milk powder in 0.3% TBS-T	1:250
CD34	5% milk powder in 0.3% TBS-T	1:500
Actin	5% milk powder in 0.3% TBS-T	1:1000
HRP-Anti Rabbit	5% milk powder in 0.3% TBS-T	1:2500
HRP-Anti Mouse	5% milk powder in 0.3% TBS-T	1:2000
HRP-Anti Goat	5% milk powder in 0.3% TBS-T	1:5000

Table 3.6 Primary and secondary antibodies used in western blotting and their dilution rates in blocking solutions.

3.17 WESTERN BLOTTING

3.17.1 SDS- POLYACRYLAMIDE GEL ELECTROPHORESIS

The protein samples were resolved by SDS-PAGE gel with 15% (for histone proteins) and 10% (for cytoplasmic and nuclear proteins) separating gel and 5% stacking gel. 30 μg protein sample for the cytoplasmic-nuclear extracted proteins and 5-10 μg samples for the histone proteins were used. The protein samples were mixed with 2% cracking buffer including 10% β-mercapthoethanol (Sigma, St. Louis, USA) and boiled at 95˚C for 10 minutes for denaturation. 24 μl of the denaturated protein samples and 7 μl of the prestained protein marker (Fermentas, Canada) were loaded on the gel and run at 85 V. The running was terminated when the marker was seperated enough to detect the required range of weight.

3.17.2 TRANSFER OF THE PROTEINS TO PVDF MEMBRANE

3.17.2.1 SEMI-DRY TRANSFER

Proteins in the range of 20-75 kDa were transferred by semi dry transfer method to a polyvinylidene fluoride membrane (PVDF) (0,45 μm, Thermo

Scientific, MA, USA). Beforehand, PVDF membrane was put in methanol for 20 seconds for activation and then washed in ddH_2O for 2 minutes to remove the excess methanol. 4 whatmann papers which were cut according to the size of the gel and membrane were put into semi-dry transfer buffer. The gel was washed with ddH_2O and the stacking part was cut and removed. Seperating part of the gel was soaked in semi dry transfer buffer almost 3 minutes. Gel, 4 whatmann papers and PVDF membrane were placed onto the semidry transfer apparatus (Bio-Rad, CA, USA) at a specific order of; 2 whatmann papers, PVDF membrane, gel and 2 whatmann papers. Transfer was performed with a current of 3,5 mA/cm^2 membrane for 45 minutes. The gel was stained with comassie brilliant blue for 30 minutes and destained with destaining solution for over night to control the transfer of the proteins from the gel to the membrane.

3.17.2.2 WET TRANSFER

The histone proteins are smaller than 20 kDa. Therefore wet transfer method was performed. Firstly, PVDF membrane was put in methanol for 20 seconds for activation and then washed in ddH_2O for 2 minutes to remove the excess methanol. 4 whatmann papers and 2 sponges were soaked into the 1X wet-transfer buffer prepared for small proteins. The gel was washed with ddH2O and the stacking part was cut. Seperating part of the gel was soaked in wet

transfer buffer almost 3 minutes. The proteins were transfered at 40V and for 2,5 hours at +4˚C within BioRad gel tank (Bio-Rad, CA, USA). The gel was stained with comassie brilliant blue for 15 minutes and destained with destaining solution for over night to control.

3.17.2.3 IMMUNOLOGICAL DETECTION OF THE PROTEINS

After the transfer of the proteins to membrane, membrane was blocked with the blocking solution as indicated in Table 3.5 for different antibodies for 2 hours. After the blocking, the membrane was left in primary antibodies for incubation at 4˚C for over-night on shaker (RotaMix, Thermolyne, IA, USA). The primary antibodies were diluted in block solution at various concentrations as given in Table 3.6 H3 was used as loading control of histone modification protein. Cyclin E1 and Calnexin were used to check cytoplasmic-nuclear seperation of proteins in MSCs. The following day, the membrane was washed 3 times for 10 minutes with 1XTBS-(0.3%) Tween solution and incubated on shaker for 1 hour at RT with the related horseradish peroxidase (HRP) secondary antibodies listed in the Table 3.5. Subsequently the membrane was washed for 3 times for 10 minutes with 1XTBS-(0.3%) Tween. Chemiluminescence was detected using the Super Signal West Femto Maximum Sensitivity Substrate (Thermo Scientific, IL, USA) for 1.5 min and developed.

Histone antibodies were purchased from Cell Signaling (Danvers, MA, USA), HRP conjugated secondary antibodies and PPARγ, ETS1, RUNX2, SOX9, MEF2C, ATF3, Actin, Calnexin, CD29 and CD34 antibodies were purchased from Santa Cruz (Santa Cruz, CA, USA). The band intesties of histone modifications proteins were calculated. The photographs of X-ray films were taken under transluminator (Gel-Doc Biorad Vilber Lourmat, France). ChemiCapt (Vilber Lourmat, France) software was used to take the photographs of the developed films. After the photos were taken, the band intensities were calculated using Bio1D (Vilber Lourmat, France). Protein expression results for all modified histone proteins were normalized to H3 expression.

3.18 CHROMATIN IMMUNOPRECIPITATION (ChIP) ASSAY

3.18.1 IN VIVO CROSSLINKING AND DIGESTION OF CHROMATIN

The assay was performed using SimpleChIP Enzymatic Chromatin IP Kit Agarose Beads (Cell Signaling Technology, USA) according to manufacturer's protocol. Without sucking the media, 40% fresh formaldehyde was added in

cell culture plates at the end of the 14th day of the cell culture to crosslink proteins to DNA. Final formaldehyde concentration was 1% in media. Culture plates were swirled briefly and incubated at room temperature for 10 minutes. 2 ml of 10X glycine was directly added to each plate and mixed by swirling the plate briefly. Cells were incubated for 5 minutes at room temperature. After that media containing formaldehyde and glycine was completely removed and cells were washed two times with 20 ml ice-cold 1X PBS. 2ml ice-cold 1X PBS + PMSF solution was added into each culture plate and cells were scraped into this cold buffer. Cells in 3 plates were combined into one 15 ml canonical tube and centrifuged at 1.500 rpm for 5 minutes at 4˚C. Supernatant was removed. Cells were resuspended in 4 ml ice-cold Buffer A+DTT+Protease inhibitor cocktail (PIC) + PMSF solution and incubated on ice for 10 minutes by inverting tube every 3 minutes. After centrifugation at 4°C for 10 minutes at 3000 rpm supernatant was removed and pellet was resuspended in 4 ml ice-cold buffer B+DTT. Centrifugation was repeated and sample was solved in 1 ml buffer B +DTT. 0.125ul Miccrococcal Nuclease was added into sample and incubated for 10 minutes at 37˚C by inverting every 3 minutes. To stop digestion 100 ul of 0.54 M EDTA was added into tube placed on ice. After the centrifugation at 13000 rpm for 1 minute at 4 °C supernatant was removed and nuclear pellet was resuspended in 1 ml of 1X ChIP buffer + PIC + PMSF. Sample was splitted into two tubes of 500 µl and then incubated on ice for 10 minutes. Each tube of lysates was sonicated with 8 sets of 15-second pulses

with Sonics Sonicator (Sonics& Materials, USA). Between pulses samples were incubated on wet ice for 30 seconds. To clarify, lysates were centrifuged at 10000 rpm for 10 minutes at 4°C. Supernatant containing the cross-linked chromatin preparation was transferred into a new tube.

3.18.2 ANALYSIS OF CHROMATIN DIGESTION AND CONCENTRATION

25 µl of chromatin samples were mixed with 50 µl nuclease-free water, 6 µl 5 M NaCl and 2 µl Proteinase K and incubated at 65˚C for 2 hours. DNA was purified as recommended in the protocol and eluted in 15 µl elution buffer. DNA concentration was determind with NanoDrop ND1000 spectrophotometer (Nanodrop technology, USA). Samples were loaded onto 1% agarose gel mixing with 5 µl loading dye to control DNA fragmentation. DNA should be digested to 1 to 5 nucleosomes (150-900 bp).

3.18.3 CHROMATIN IMMUNOPRECIPITATION AND DNA PURIFICATION

9 µg of chromatin DNA was mixed with 100 µl of 1X ChIP buffer. 10% of sample from each DNA+ ChIP buffer mixture was removed and kept at -20˚C

as input sample. H3K27me2, H3K27me3 and EZH2 antibodies were used for immunoprecipitations (IP) and all antibodies were used with 1:50 dilution rate. Primary antibodies were added into DNA + ChIP buffer mixture, samples were incubated for overnight at 4°C with rotation. Following day, immunoprecipiated samples were incubated with 30 µl of ChIP-Grade Protein G Agarose Beads for 2 hours at 4 °C with rotation. Washing procedures were followed as recommended in protocol. For reverse cross-linking of proteins, immunoprecipitated and input samples were mixed with 6 ul 5 M NaCl and 2 µl Proteinase K and incubated at 65 ˚C for 2 hours. DNA purification was performed using spin columns following instructions of manufacturer. Purification was done in 25 µl elution buffer.

3.18.4 QUANTIFICATION OF IMMUNOPRECIPITATED DNA BY qPCR

ChIP assay were analyzed with quantitative PCR using Real Q-PCR 2X Master mix (Ampliqon, Denmark) and results were expressed using the percent input method and formula was shown below:

Percent input= (primer efficiency) $^{\wedge (\text{CT input} - \text{CT IP sample})}$ x percentage of input

The average of "percent input" values of H3K27me2 and H3K27me3 accumulation on adipogenic genes were calculated.

PCR conditions were 95˚C for 15 minutes, 95˚C for 30 seconds, 60˚C for 1 minute, 72 ˚C for 1 minute and 30 cycles, 72 ˚C for 10 min. Each protocol was followed by melt curving to control purity of the amplification. Primers used for quanitification of immnuprecipitation were given in Table 3.1.

3.19 BISULFITE SEQUENCING ANALYSIS

3.19.1 BISULFITE CONVERSION

DNA methylation of ERα, PPARγ and C/EBPα genes was analyzed by bisulfite sequencing. DNA was purified from MSCs using either DNeasy Blood&Tissue Kit (Qiagen) or NucleoSpin Tissue kit (Machery-Nagel, Germany) following the manufacturer's instructions. Bisulifte conversion was performed using EpiTech Bisulfite Kit (Qiagen, USA) and 350 ng of DNA was used for each reaction.

3.19.2 PREPARING OF DH5α COMPETENT CELLS

10 µl of bacteria samples from DH5α glycerol stock was streaked on Luria-Bertani broth LB) agar plate and incubated for over-night at 37˚C. Following

day, single colony was picked up and incubated in 15 ml LB without selective antibiotic for over-night at 37˚C. Afterwards, some from 15 ml over-night culture was mixed with 100 ml LB in 1000 ml flask until OD_{600} reaches 0.2 at preparation mix. This mixture was incubated at 25˚C for almost 6 hours on shaker until OD_{600} reaches 0.5-0.6. Then, bacteria culture was separated into two 50 ml falcons and centrifuged at 2500 g for 15 minutes at 4˚C following incubation on ice for 10 minutes. Supernatant was removed and cell pellet was resuspended in 64 ml ice-cold transformation buffer (TB) separating into two 50 ml falcons and incubated on ice for 10 minutes. Bacteria-TB mixture was centrifuged at 2500 g for 15 minutes at 4˚C. Supernatant was removed and cell pellets were resuspended in 8 ml ice-cold TB containing 7% DMSO. Bacteria competent cells were aliquoted into cold 1.5 ml eppendorfs and tubes were immediately put into liquid nitrogen. Competent cells were stored at -80˚C.

3.19.3 TA CLONING AND PLASMID DNA ISOLATION

Converted DNA was used as template for bisulfite specific PCR (BSPCR) using HotstarTaq Polymerase (Qiagen). Bisulfite specific primers were designed using Methprimer software (http://www.urogene.org/methprimer/) for PPARγ, C/EBPα. ERα primers were designed as given in a previous study[169]. Distrubition of CpG residues in promoter regions which were examined in this

project were given in Figure 3.2. Primers used in BSPCR and PCR conditions were stated in the table 3.7 and 3.8 respectively.

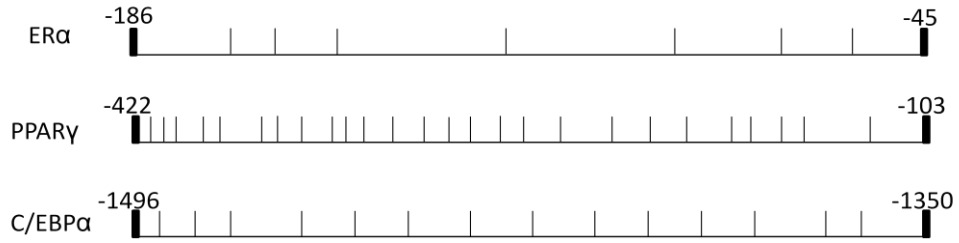

Figure 3.1 Distrubition of CpGs in promoter region Each vertical line represents a single CpG residue.

Genes	Sequences of Forward and Reverse Primers	Size (bp)
ER α	forward 5'-TTAGGAATGTTGATTTTAGTGGTGT-3' reverse 5'-TAAACAAAACACTTAACAACCCCTC-3'	141
CEBP α	forward 5'-TGGGTGTTTATTAGGTTTTTTTTGT-3' reverse 5'-AACCCCCTATCCAATCCTTAAA-3'	167
PPAR γ	forward 5'-TTTTAGGTTTTTTTAGAAGGTGTTT-3' reverse 5'-TCCAATTAACCCTACCCTATACTC-3'	368

Table 3.7 List of primers used for Bisulfite Specific PCR and amplicon size

Genes	First Denaturation	Denaturation	Annealing	Extension	Cycle	Final Extension
CEBPα	95°C, 15 min	94°C, 60 sec	54.5°C, 60 sec	72°C, 60 sec	30	72°C, 10 min
PPARγ	95°C, 15 min	94°C, 60sec	54.5°C, 60 sec	72°C, 60 sec	30	72°C, 10 min
ERα	95°C, 15 min	94°C, 60 sec	55.5°C, 60 sec	72°C, 60 sec	30	72°C, 10 min

Table 3.8 Bisulfite Specific PCR conditions

PCR products were extracted from 1% agarose gel using QIAquick Gel Extraction kit (Qiagen) and purified DNA concentration was measured by nanodrop. Amlified and purified DNA fragment was inserted into vector with 1:3 ratio of vector to insert. Amounts of reaction components were given in Table 3.9. For transformation into DH5α bacteria cells TA Cloning (pGEM -T Easy Vector system, Promega) was used. The Biomath calculator (www.promega.com/biomath) used to determine the amount of insert DNA needed. 10 µl of ligated product was mixed with 100 µl competent cells and incubated on ice for 20 minutes. Afterwards, the mixture were put into water-bath at exactly 42˚C for 50 seconds and put on the ice for 2 minutes respectively. 950 µl LB without antibiotic was added into tube and cells were incubated shaking at 37˚C for 1.5 hours. Tube was centrifuged at 13000 rpm for 30 seconds and supernatant was removed. Cell pellet was solved in 100 µl fresh LB and seeded onto LB agar plate containing amphicillin antibiotic. Plate was incubated for over-night at 37˚C. Following day, 5 single colonies were picked up and cultured in 5 ml LB with amphicillin for over-night. Plasmid DNA was isolated by using Plasmid Mini Kit (Qiagen, USA). 5 clones were sequenced by commercial services (İONTEK, Turkey and DONE Genetics, Turkey).

Reaction Component	Volume
2X Rapid Ligation Buffer	5 µl
Easy Vector (50ng)	1 µl
PCR product	variable
T4 DNA Ligase	1 µl
Nuclease-free water	variable
Final volume	10 µl

Table 3.9 Amounts of Reaction Components for ligation

3.20 STATISTICAL ANALYSIS

All data from CNT experiments were analyzed with ANOVA and expressed as mean ± standard deviation (SD) (n=3) . Multiple comparisons of control to other groups were performed using Fisher's test using Minitab 15 Statistical Software. The statistical difference between groups in qRT-PCR and RT-PCR experiments were analyzed by the unpaired, Student's t test using GraphPad Software and Microsoft Office Excel. The values from qRT-PCR were expressed as the means ± standard error (SEM) (N=3) and the values from RT-PCR were expressed as the means ± SD (N=6). Significant difference between two groups was declared if $p<0.05$.

CHAPTER 4

RESULTS

In this thesis, the effect of estrogen on the maintenance and differentiation of MSCs was examined. First, we tested estrogen's role during the maintenance of MSCs in normal culture conditions as well as using CNTs as scaffold. In addition, we also tested estrogen's genetic and epigenetic effect on the differentiation of MSCs into adipocyte and osteocytes. In order to accomplish our aim, we focused on the role of estrogen in the expression and differential localization of transcription factors, which are involved in adipogenesis, osteogenesis and chondrogenesis from MSCs. Furthermore, we examined histone modifications and histone modifier enzymes as well as CpG methylation status during differentiation.

Throughout this thesis MSCs were isolated from; normal female (hereafter stated as female) and ovariectomized female (hereafter stated as ovex) rats. To investigate the role of estrogen in regulation of transcription factors involved in MSC differentiation in the presence of 10^{-7} M estrogen or 10^{-6} M tamoxifen in the cell culture media. Our experimental groups were as follows; MSCs from

normal female rat (hereafter stated female), estrogen treated MSCs from normal female rat (hereafter stated as female+est), tamoxifen treated MSCs from normal female rat (hereafter stated as female+tam), MSCs from ovariectomized rat (hereafter stated as ovex), estrogen treated MSCs from ovariectomizd female rat (hereafter stated as ovex+est), and tamoxifen treated MSCs from ovariectomized female rat (hereafter stated as ovex+tam). MSCs were cultured in Mesencult media for 14 days.

Furthermore, at the end of the 14^{th} day of cell culture, MSCs were incubated with adipogenic and osteogenic induction media for differentiation. The differentiated cells were collected on 13^{th} day (female 13. day, female+est 13. day), 17^{th} day (female 17. day, female+est 17. day) and 24^{th} day (female 24. day, female+est 24. day) of the adipogenic and osteogenic differentiation.

Finally, to investigate the effect of estrogen on the maintenance/viability of MSCs on CNT arrays, the cells were seeded onto multiwalled CNT (MWCNT) arrays in the absence and presence of estrogen. In addition, changes in the number and viability of attached MSCs on collagen-coated and non-coated CNT through passages were examined.

4.1 CHARACTERIZATION AND EXPERIMENTAL DESIGN OF CNT ARRAYS

Scanning Electron Microscope (SEM) analysis was performed for characterization of the vertically aligned CNT arrays. Characterization was performed by Assist. Prof. Dr. Erman Bengü and Gökçe Küçükayan from Bilkent University, Department of Chemistry. SEM images of the vertically aligned CNT arrays revealed that CNTs were approximately 10 μm in height (Figure 4.1 A-B) and multi-walled with an average diameter of 10 nm. Experimental design of patterned CNTs was shown in Figure 4.1C.

4.2 CHARACTERIZATION OF MSC

MSCs were characterized both at mRNA and protein level for P0, P1 and P2 passages. RT-PCR results demonstrated that cells from all passages express MSC markers, CD90, CD71 and CD29, but not hematopoietic stem cell markers; CD45 and CD34 (Figure 4.2A). Moreover, we confirmed this result at the protein level by performing western blot analysis. MSCs for all passages were positive for CD29, but negative for CD34 (Figure 4.2B). We also characterized MSCs that were used to test the effect of estrogen on their maintenance (Figure 4.2C). No change in the expression of the markers was

observed after estrogen treatment suggesting that there was no effect of estrogen on the characteristics of MSCs.

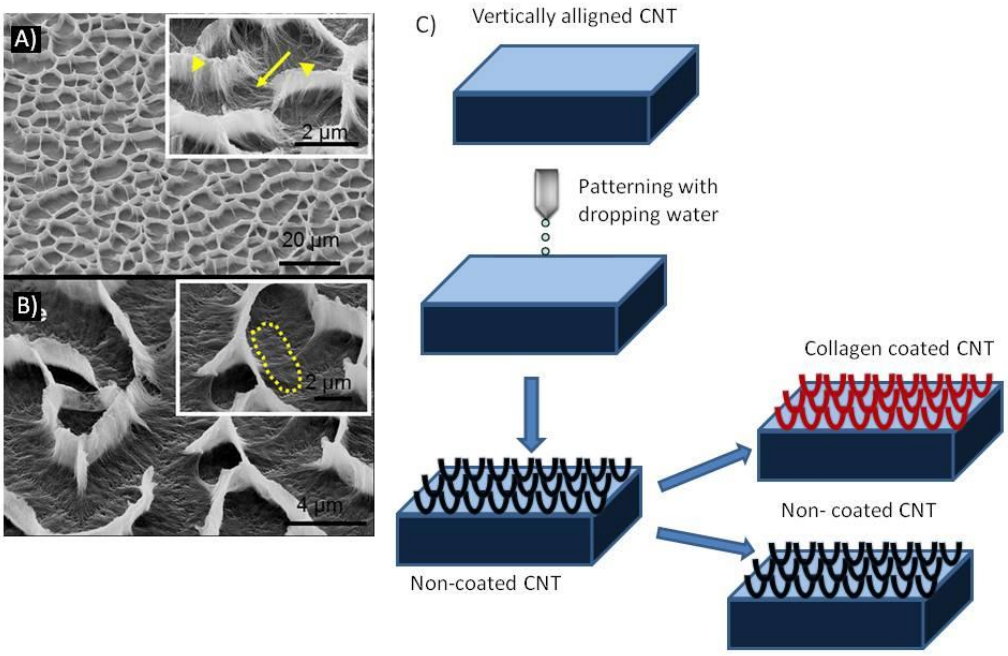

Figure 4.1 Preparation of CNTs. A) 45° tilted SEM image of patterned CNT surfaces with the inset showing a high magnification image of the collapsed CNT arrays (arrow heads: collapsed and laid CNTs, arrows: CNTs that were shrunk to form the razor-sharp peaks) B) 45° tilted SEM image of the collagen coated patterned CNT surface with the inset showing the smoothing/leveling effect of collagen coating (dotted lines). C) Schematic representation of experimental design of patterned vertically alligned CNTs before cell culturing

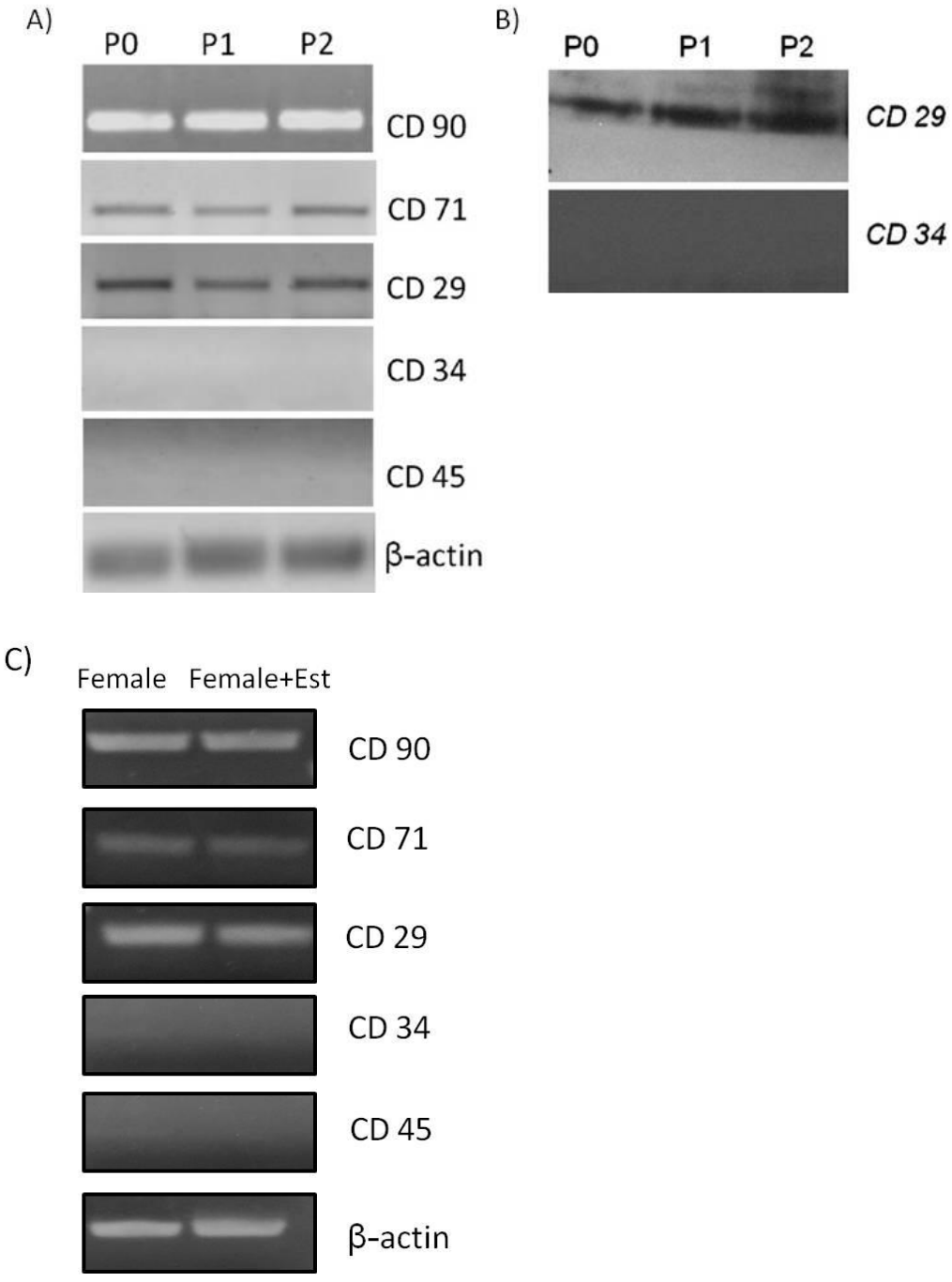

Figure 4.2 Characterization of MSCs, A) Expression of MSC and HSC markers from P0, P1 and P2 passages of the cells at mRNA level, B) Expression of MSC and HSC marker from P0, P1 and P2 passages of the cells at protein level, C) Expression of MSC and HSC markers after the cells were treated with estrogen at P0.

4.3 SEEDING OF MSC ON THE CNT ARRAYS

4.3.1 CELL VIABILITY OF MSCs ON NON-COATED CNTs IN THE PRESENCE AND ABSENCE OF ESTROGEN

It was well established that estrogen promotes MSC proliferation and maintenance. To examine whether estrogen hormone has a positive effect on the cell viability of MSC seeded onto non-coated patterned CNT arrays in the absence and presence of estrogen, we performed MTT assay. Our results revealed that estrogen treatment tends to increase the viability percentage of MSCs on CNTs at P0 (Figure 4.3.1).

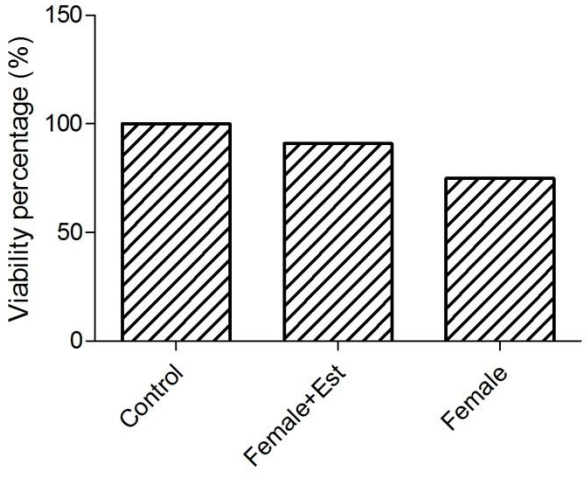

Figure 4.3.1 Evaluation of the percent of viable MSCs isolated and seeded onto non-coated patterned CNT arrays by MTT assay at P0. Control group was

obtained from MSCs seeded on 96-well culture plates containing no CNT layers.

4.3.2 CALCULATION OF THE NUMBER OF ATTACHED MSCs ON COLLAGEN COATED AND NON-COATED CNTs

SEM analysis was performed to calculate the number of attached MSCs from P0, P1 and P2 passages (Figure 4.3.2 A-B). $3x10^5$ cells were seeded onto non-coated and collagen coated patterned CNT surfaces and incubated for 3 days. The number of attached cells was counted and average areal density was calculated (Figure 4.3.2C). Our plot showed that the number of the attached MSCs both on collagen coated and non-coated CNT surfaces decreased through the passages P0, P1 and P2. The decrease in the number was significant at P1 and P2 compared to P0, however no significant change was observed between P1 and P2.

In addition, our result clearly showed that the number of the MSCs was significantly higher on non-coated CNT arrays compared to collagen coated CNT arrays at P0, but not at P1 and P2 groups. These data suggest that early passages of MSCs have higher attachment potential on CNT array. Moreover collagen coating of CNT surfaces have a negative effect on attachment of cells from P0, whereas no change was observed at P1 and P2.

4.3.3 CELL VIABILITY OF PASSAGED MSCs ON COLLAGEN-COATED AND NON-COATED CNTs

To understand whether the patterned CNT arrays have any cytotoxic effect on cell viabilty, we examined the effect of collagen coated and non-coated CNTs on MSCs from subsequent three passages performing MTT assay. MSCs which were cultured on cell culture plate containg no CTN layers were used as control group. Our results clearly demonstrated that MSCs viability was significantly higher at P0 compared to P1, P2 and control group (Figure 4.3.3).

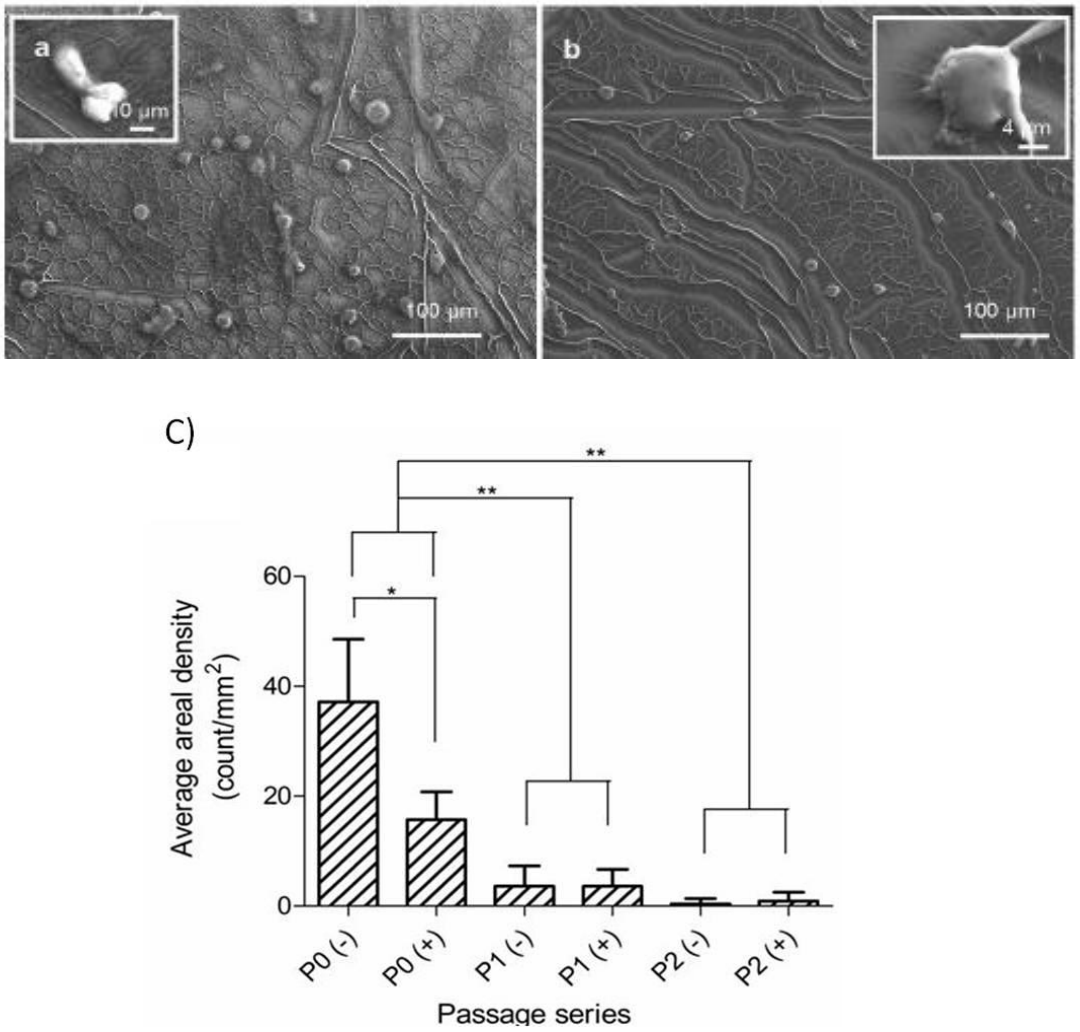

Figure 4.3.2 Scanning Electron Microscope images of MSCs at P0 after seeding and culturing for 3 days on the a) non-coated patterned CNTs and b) collagen coated patterned CNTs , c) Average area density of MSCs on non-coated (represented by -) and collagen coated (represented by +) patterned CNT arrays at P0, P1 and P2. ANOVA was significant at $p<0.001$. Multiple comparisons of control to other groups were performed using Fisher's test (Minitab 15 Statistical Software). * indicates $p<0.05$ and ** indicates $p<0.001$, Mean ± Standard Deviation

Therefore, we can state that patterned CNT arrays have no cytotoxic effect on viability of MSCs from P0. Also, we suggest that either collagen coated or non-coated patterned CNT arrays may provide a suitable environment for MSCs to survive.

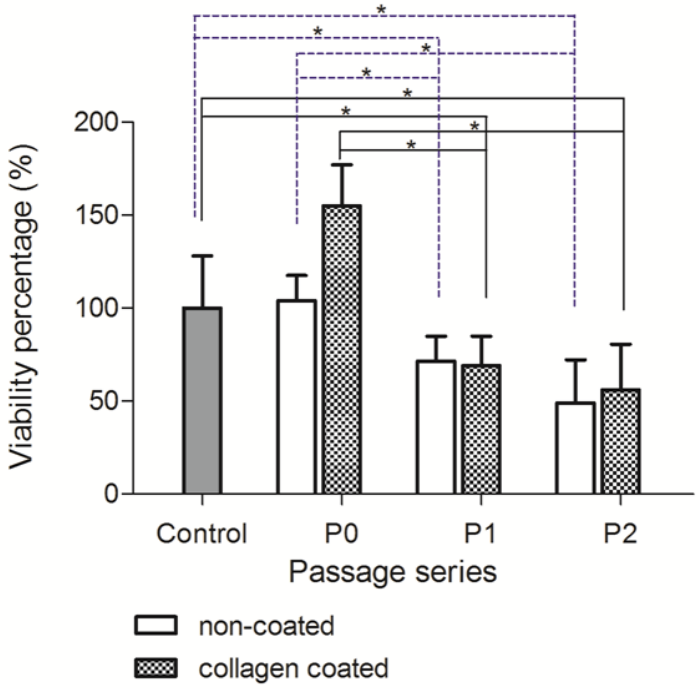

Figure 4.3.3 The percent of viable MSCs on non-coated patterned (empty bars) and collagen coated patterned CNT arrays (solid bars) at P0, P1 and P2 by MTT assay. Control group was obtained from cells seeded on 96-well culture plates without CNT arrays. ANOVA was significant at $p = 0.041$ and $p<0.001$ for non-coated and collagen coated CNT arrays, respectively. Multiple comparisons of control to other groups were performed using Fisher's test (Minitab 15 Statistical Software). * indicates $p<0.05$, Mean ± Standard Deviation

4.4 EXPRESSION OF TRANSCRIPTION FACTORS INVOLVED IN ADIPOGENIC, OSTEOGENIC AND CHONDROGENIC DIFFERENTIATION IN MSCs

To investigate the effect of estrogen treatment in the genetic regulation of transcription factors, which are required for adipogenic, osteogenic and chondrogenic differentiation of MSC, we first examined their mRNA levels in MSCs obtained from normal female and ovex rats and cultured in the absence and presence of estrogen. By performing qRT-PCR, we evaluated the effect of estrogen on adipogenic transcription factors; PPARγ, C/EBPα, FABP4, Adipsin, osteogenic transcription factors; RUNX2, ETS1 and chondrogenic transcription factors; SOX9, ATF3 and MEF2C. Cyclophilin was used as a housekeeping gene and expression results of transcription factors were normalized according to Cyclophilin expression. Female samples were used as calibrator.

We found a decrease in the expression level of adipogenic genes in both female and ovex animals when MSCs were incubated in the presence of estrogen. This finding suggested that estrogen might have an inhibitory effect on the expression of adipogenic transcription factors (Figure 4.4 A-D).

It was well established that estrogen has a stimulatory effect on bone and cartilage formation. In this study, we observed a significant increase in mRNA level of RUNX2, osteogenic transcription factor, upon estrogen treatment in MSCs isolated from both female and ovex rats as expected (Figure 4.4E). On the contrary, we demonstrated that estrogen has an opposite effect on the transcriptional regulation of another osteogenic gene, ETS1. Estrogen treatment caused a significant reduction in ETS1 gene expression both in female and ovex animals (Figure 4.4F).

Furthermore, estrogen treatment enhanced expression rates of chondrogenic transcription factors in female animals. But we could not detect an expected and consisted expression pattern in chondrogenic genes in ovex samples (Figure 4.4 G-I). Estrogen treatment resulted a significant decrease in SOX9 and ATF3 expression, whereas MEF2C level increased as expected upon estrogen treatment in ovex samples. Fold changes and P values of each gene for all groups were provided in Table 4.1.

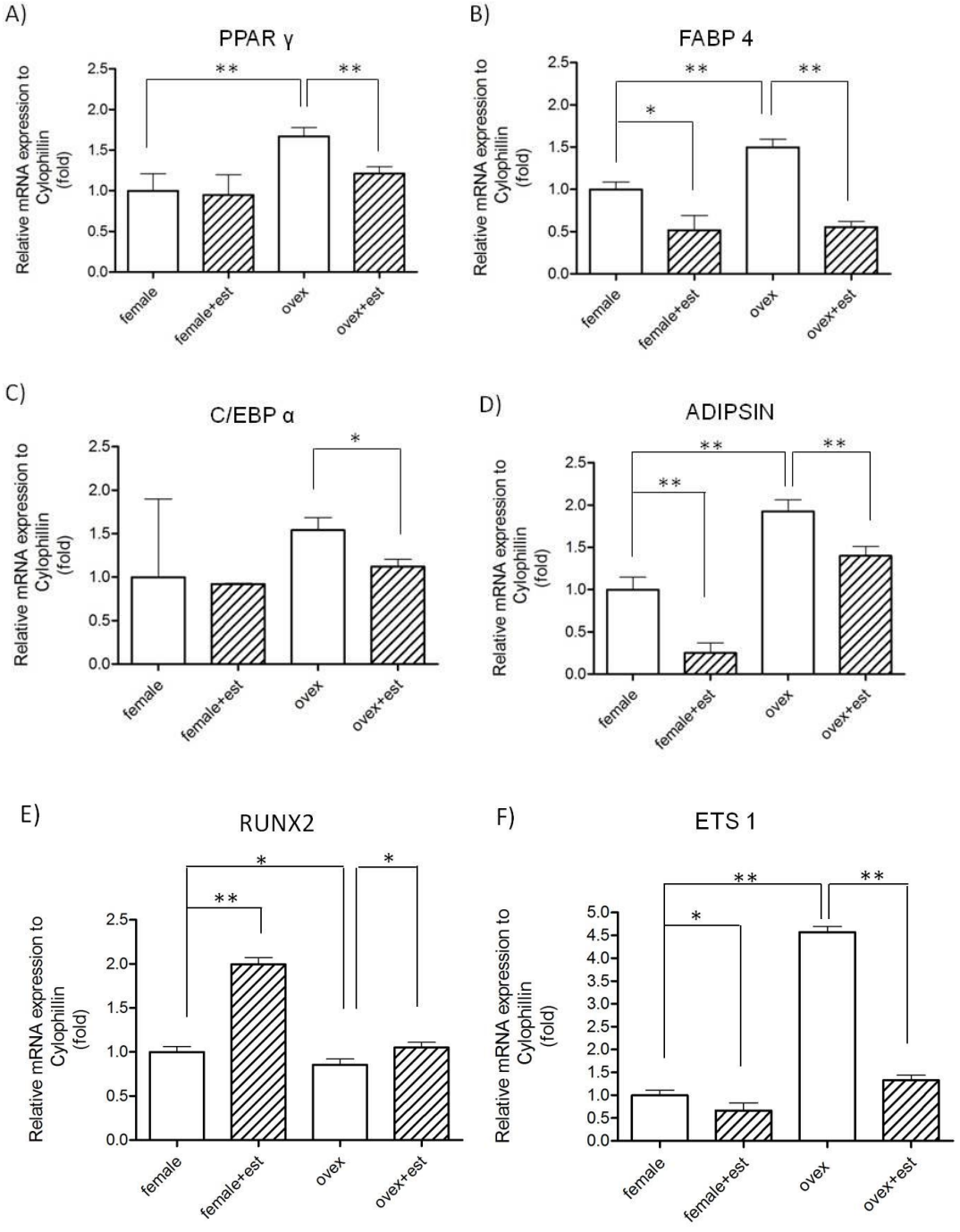
A)
PPAR γ
Relative mRNA expression to Cylophillin (fold)
female
female+est
ovex
ovex+est
B)
FABP 4
C)
C/EBP α
D)
ADIPSIN
E)
RUNX2
F)
ETS 1

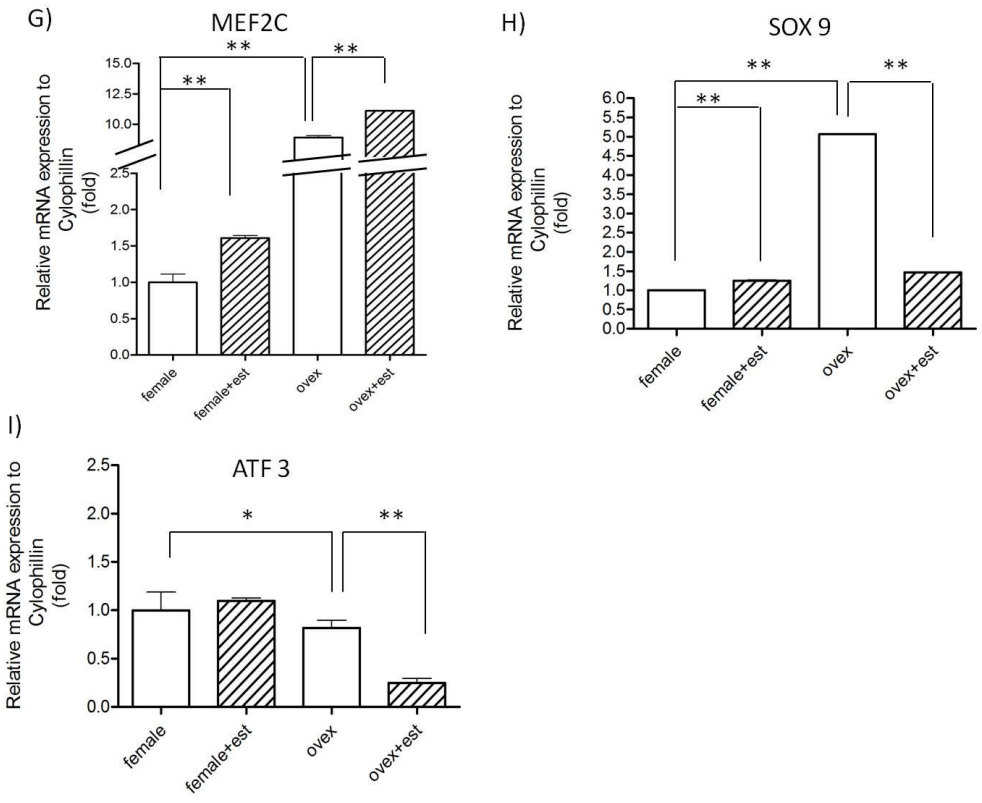

Figure 4.4 Effect of estrogen on the expression profile of the (A-D) adipogenic (E, F) osteogenic and (G-I) chondrogenic transcription factors in MSCs by qRT-PCR at P0. Relative expression to cyclophillin was calculated. N=6, * indicates $p<0.05$, ** indicates $p<0.0001$, Mean ± Standard Deviation

GENES	FEMALE +EST vs FEMALE	P VALUE	OVEX vs FEMALE	P VALUE	OVEX+EST vs OVEX	P VALUE
PPAR	0.95	0.6772	1.67	<0.0001	0.72	<0.0001
C/EBP	0.92	0.832	1.54	0.172	0.71	0.0001
FABP4	0.517	0.0001	1.497	<0.0001	0.369	<0.0001
ADIPSIN	0.25	<0.0001	1.92	<0.0001	0.729	<0.0001
RUNX2	1.99	<0.0001	0.855	0.0022	1.22	0.0002
ETS1	0.66	0.0007	4.56	<0.0001	0.288	<0.0001
MEF2C	1.6	<0.0001	8.9	<0.0001	1.434	<0.0001
SOX9	1.25	<0.0001	5.064	<0.0001	0.29	<0.0001
ATF3	1.098	0.25	0.8169	0.0466	0.302	<0.0001

Table 4.1 Fold changes and P values were calculated using Unpaired Student t test for each gene. Estrogen treated MSCs were compared to untreated MSCs. Ovex MSCs were compared to female MSCs.

4.5 EXPRESSION OF ADIPOGENIC AND OSTEOGENIC TRANSCRIPTION FACTORS IN DIFFERENTIATED MSC

We investigated changes in the expression level of the adipogenic transcription factors during differentiation of MSCs to adipocytes at different time points**.** At first, cells were stained with Oil Red O on the 13^{th} and 24^{th} day of adipogenic induction to check differentiation (Figure 4.5A). As a negative control, the cells were incubated in DMEM with no differentiaton induction factors for 24 days in the presence and absence of estrogen. The non-induced cells were also stained with Oil Red O on the 13^{th} and 24^{th} days of differentiation(Figure 4.5B). Lipid vacuole formation increased at the end of the 24^{th} days of induction. No droplets were seen at negative controls.

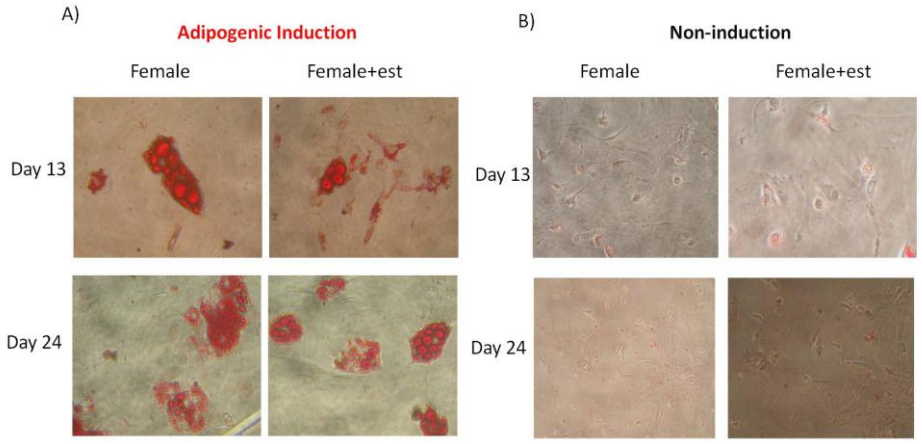

Figure 4.5 Detection of adipogenic differentiation of MSCs isolated from female rats and cultured in the absence and presence of estrogen. A) Cells were stained with Oil Red O on the 13th day and 24th day of the induction. B) Cells were incubated only in DMEM in the absence/presence of estrogen and stained with Oil Red O on the 13th day and 24th day of the culture and used as negative control.

To see whether estrogen treatment alters the mRNA expression of adipogenic transcription factors during differentiation, we performed RT-PCR for PPARγ, FABP4 and C/EBPα genes. MSCs which were isolated from normal female rats and cultured in the absence and presence of estrogen, were collected on the 13th day, 17th day and 24th day of the adipogenic differentiation. Our RT-PCR results revealed that estrogen has an opposite effect on the expression of PPARγ, FABP4 and C/EBPα genes in adipocytes compared to that of MSCs.We found that expression of the adipogenic transcription factors tends to increase after estrogen treatment in adipocytes differentiated from MSCs both on the 13th day and 24th day of the differentiation (Figure 4.6)

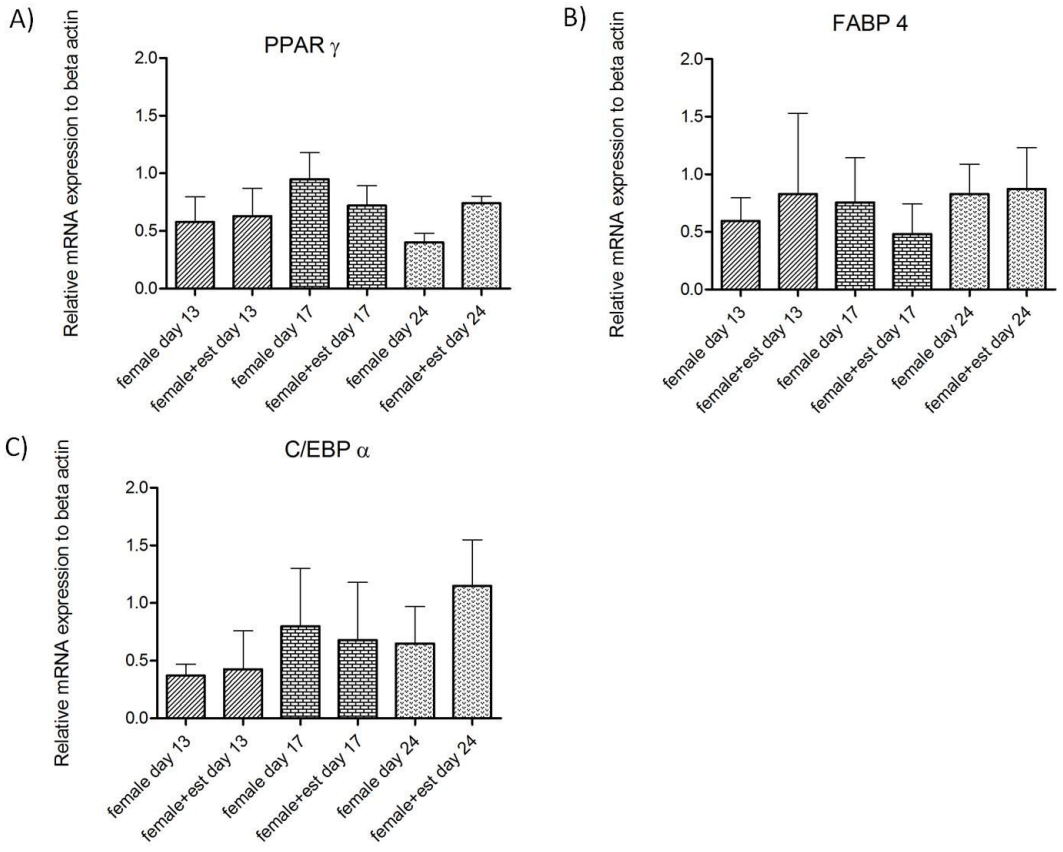

Figure 4.6 Effect of estrogen on the expression profile of the adipogenic transcription factors in adipocytes differentiated from MSCs by RT-PCR. The cells were isolated at the end of the 13th, 17th and 24th day of adipogenic differentiation. Semi quantitative analysis was done relative to β-actin expression. N=3, Mean ± Standart Error

According to our qRT-PCR results, estrogen treatment resulted a significant increase of RUNX2 osteogenic transcription factor in MSCs. To see how estrogen treatment influences the mRNA level of RUNX2 during osteogenic differentiation, MSCs were induced in osteogenic induction medium for 24 days. The cells were stained with alizarin red on the 13th and 24th days of

induction to determine osteogenic differentiation (Figure 4.7A). As negative control, cells were incubated in DMEM without differentiaton induction factors for 24 days in the presence and absence of estrogen. The non-induced cells were also stained with Alizarin Red on the 13th and 24th days of differentiation (Figure 4.7B). Calcium deposits were detected at the end of the 13th and 24th days of induction. No staining was seen at negative control samples.

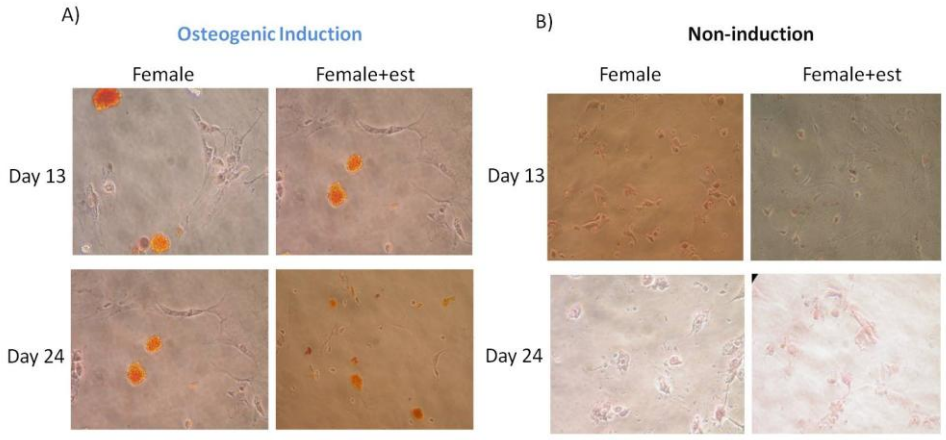

Figure 4.7 Detection of osteogenic differentiation of MSCs isolated from female rats and cultured in the absence and presence of estrogen. A) MSCs were stained with Alizarin Red on the 13th day and 24th day of the differentiation culture. B) As negative control, the cells were incubated only in DMEM in the absence/presence of estrogen and stained with Alizarin Red on the 13th day and 24th day of the differentiation culture

The cells were collected on the 13th day, 17th day and 24th day of the osteogenic differentiation to investigate the alteration in the expression of RUNX2 gene during differentiation. It was observed that expression of the RUNX2 gene

tends to increase upon estrogen treatment in osteocytes differentiated from MSCs both on the 17th day and 24th day of osteogenic induction (Figure 4.8).

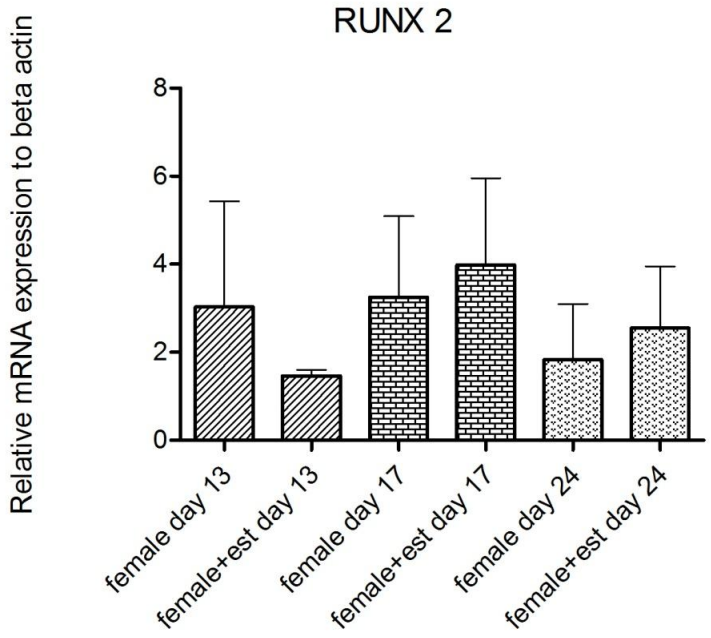

Figure 4.8 Effect of estrogen on the expression profile of RUNX2 in osteocytes differentiated from MSCs by RT-PCR. Cells were isolated at the 13th, 17th and 24th day of osteogenic differentiation.Semi quantitative analysis was done relative to β actin expression. N=3, Mean ± Standart Error

4.6 TRANSCRIPTION FACTOR LOCALIZATION

Our qRT-PCR and RT-PCR results revealed that the presence of estrogen caused a change in the expression of transcription factors involved in MSC differentiation. To detect whether estrogen deficiency influences transcription

factor localization in MSCs, we performed western blotting and immunofluorescence labeling.

We first controlled whether cytoplasmic and nuclear fraction of cells can be separated properly. For this purpose, we examined Calnexin expression, which localizes in cytoplasm, and Cyclin E1expression, which localizes nucleus, in two different fractions (Figure 4.9.)

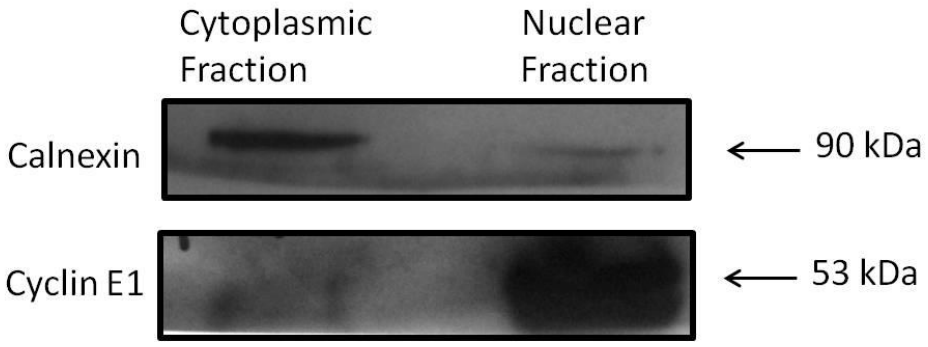

Figure 4.9 Confirmation of procedure performed to seperate nuclear and cytoplasmic fraction in MSCs isolated from normal female animal by western blotting at P0 using Calnexin and cylin E1 antibodies which localize cytoplasm and nucleus, respectively.

Immunofluorescence results revealed that estrogen deficiency cause a dramatic alteration in the subcellular localization of two transcription factors; PPARγ and ETS1. PPARγ localized in cytoplasm and especially in endoplasmic reticulum in female, while it was in nucleus in ovex (Figure 4.10). Thus, the presence or absence of estrogen seems to have effect on the succellular localization of

PPARγ. On the other hand, estrogen treatment did not interfere with the accumulation pattern of PPARγ protein in MSCs isolated from either female or ovex as shown by western blot (Figure 4.11).

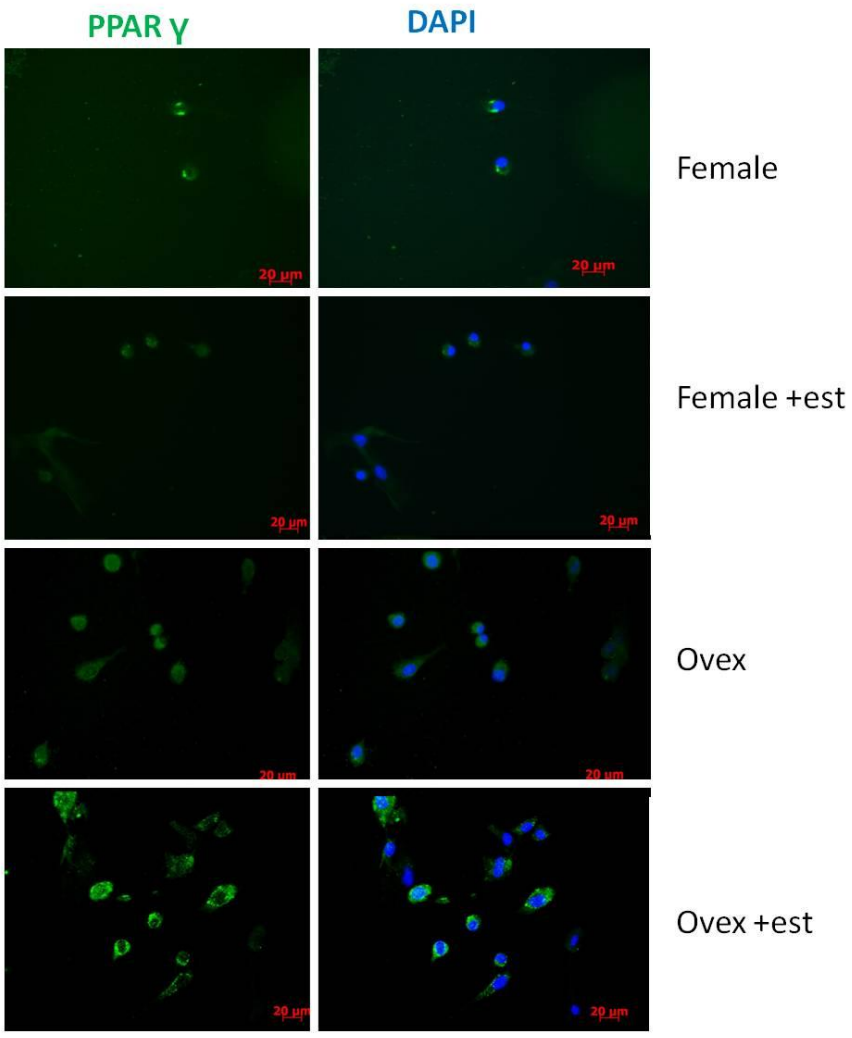

Figure 4.10 Subcellular localization of PPARγ protein in MSCs isolated from female and ovex rat and cultured in the absence and presence of estrogen by immunofluorescence staining at P0 (Magnification 20X).

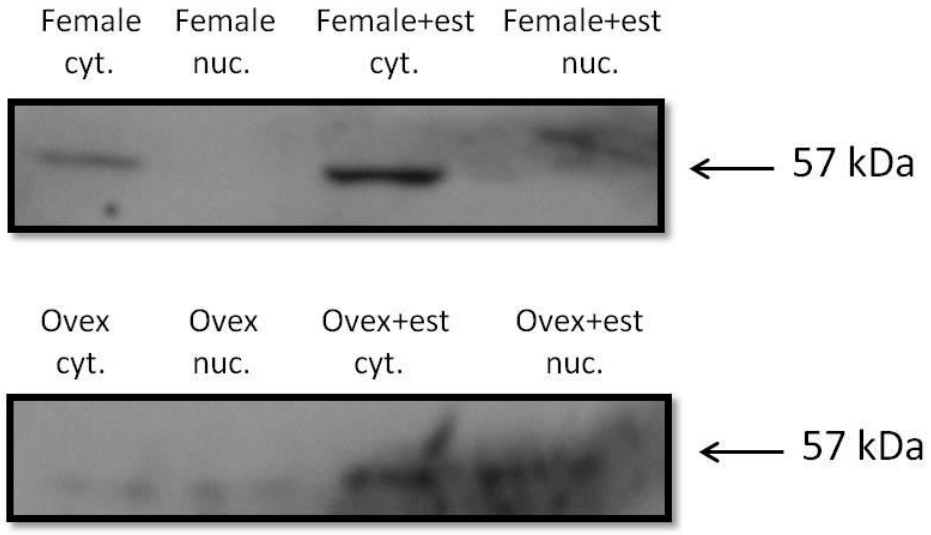

Figure 4.11 Subcellular localization of PPARγ protein in MSCs isolated from female and ovex rat and cultured in the absence and presence of estrogen by western blotting at P0.

We also tested the effect of estrogen in the subcelluar localization of osteogenic transcription factor ETS1both in MSCs isolated from female and ovex animals. Our results showed that ETS1 protein was mainly in cytoplasm in female, whereas it localized in both cytoplasm and nucleus in ovex by immunofluorescein (Figure 4.12) and western blotting (Figure 4.13).

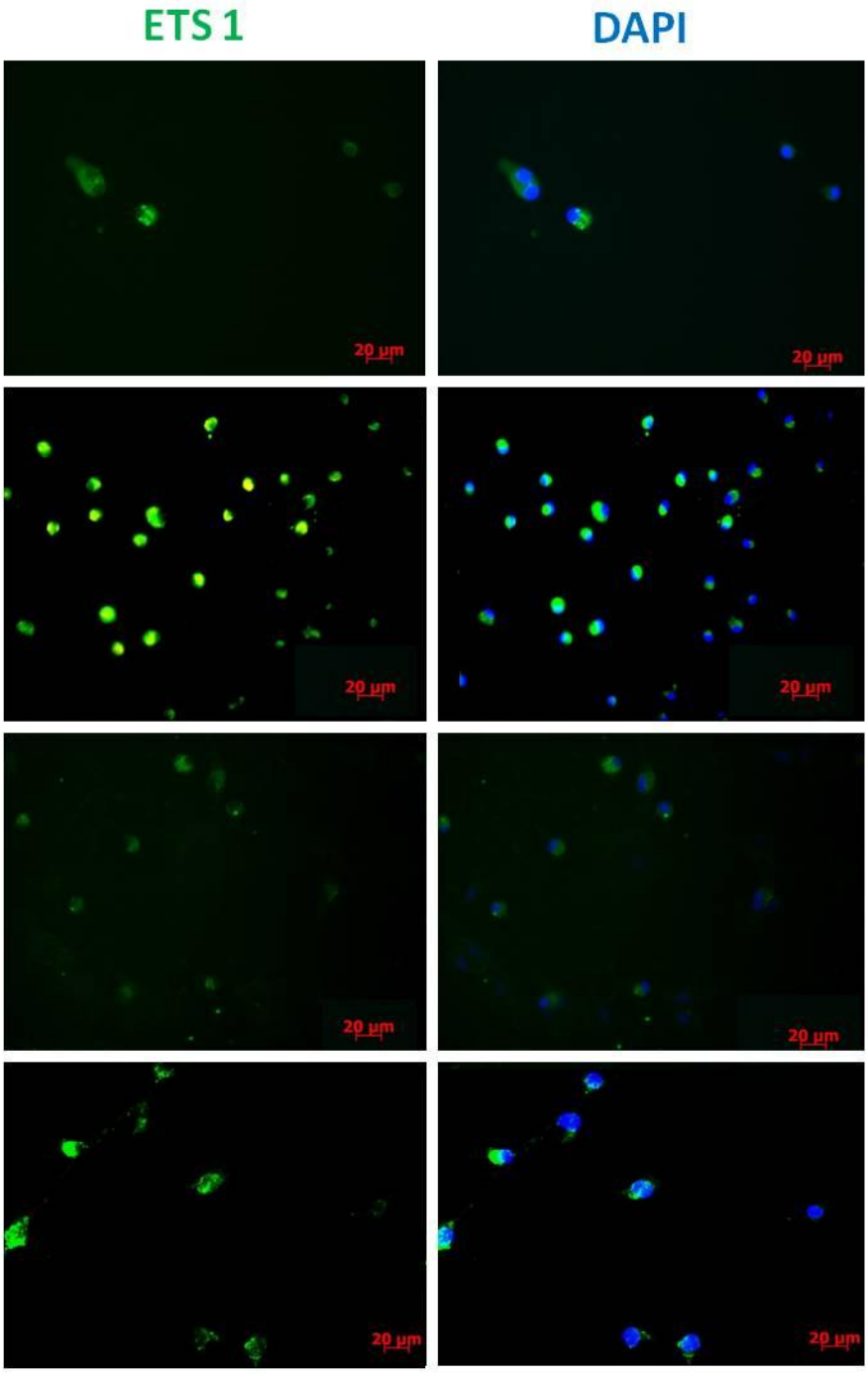

Figure 4.12 Subcellular localization of ETS1 protein in MSCs isolated from female and ovex rat and cultured in the absence and presence of estrogen by immunofluorescence staining at P0 (Magnification 20X).

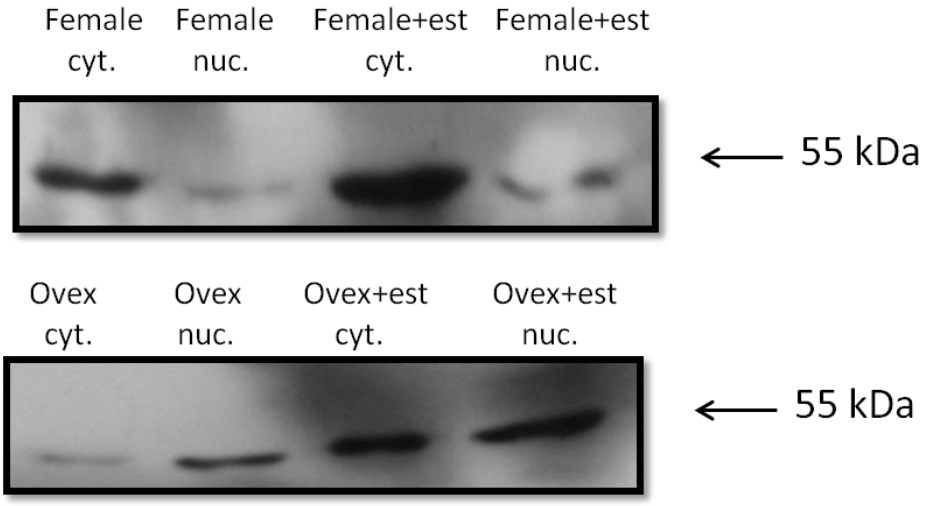

Figure 4.13 Subcellular localization of ETS1 protein in MSCs isolated from female and ovex rat and cultured in the absence and presence of estrogen by western blotting at P0 (Magnification 20X).

4.7 EFFECT OF ESTROGEN ON THE EXPRESSION OF HISTONE MODIFICATION PROTEINS AND ENZYMES IN MSCs

Previously, by our group it was demonstrated that estrogen treatment protects MSCs from apoptosis. It is possible that estrogen can regulate the expression of target genes changing the modifications on the histone protein. To test this possibility, we evaluated expression level of histone modifications; H3K27me2, H3K27me3, H3K9me2, H3K9me3 and H3K36me2 (Figure 4.14) and modifier enzymes; H3K27 methyltransferase EZH2, H3K9 demetyhlase LSD1 and

H4K9 methyltransferase SET 7/9 (Figure 4.15) upon estrogen treatment. We performed western blotting using acid extracted histone proteins and found that H3K27me2, H3K27me3 and H3K36me2 protein levels tend to decrease after estrogen treatment both in female and ovex animals (Figure 4.14A, 4.14B, 4.14E). For H3K9Me2 and H3K9Me3, estrogen tends to have a positive effect in MSCs isolated from ovex but not from female animals (Figure 4.14C, 4.14D).

Our results also showed that the level of histone modifier enzymes; EZH2, LSD1 and SET 7/9 were also affected from estrogen. However fluctuations in the level of enzymes were not consistent. Additionally, any correlation was not observed between protein level of modifed histones; H3K27me2/me3, H3K9me2/me3 and modifier enzymes; EZH2 and LSD1. (Figure 4.15A, 4.15B). On the other hand, SET 7/9 showed a consistent expression pattern between treated and untreated samples. It was observed that SET 7/9 expression tends to decrease upon estrogen treament both in ovex and normal female MSCs (Figure 4.15C).

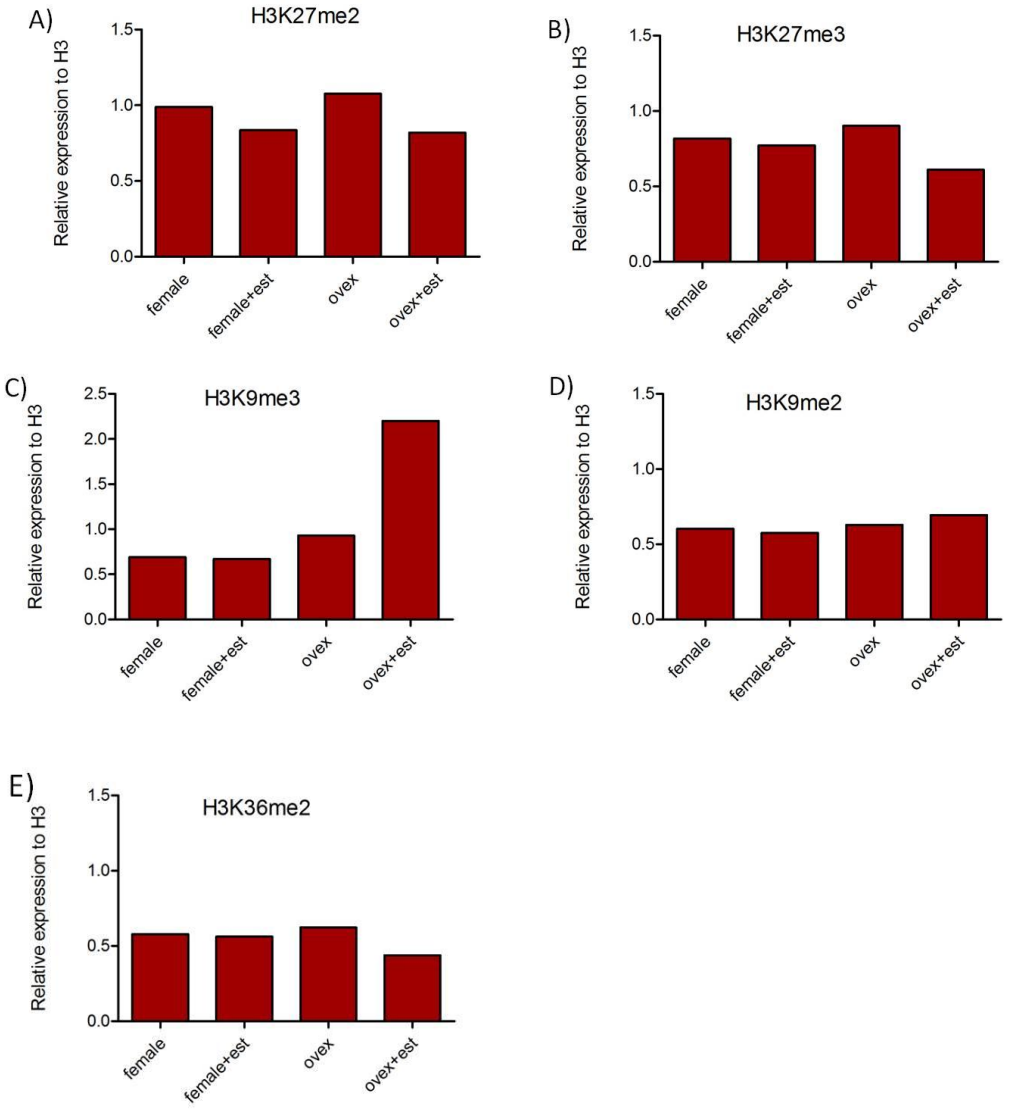

Figure 4.14 Evaluation of total protein level of histone modification proteins in MSCs by western blotting at P0. H3 was used as loading control and protein levels were normalized according to H3 expression.

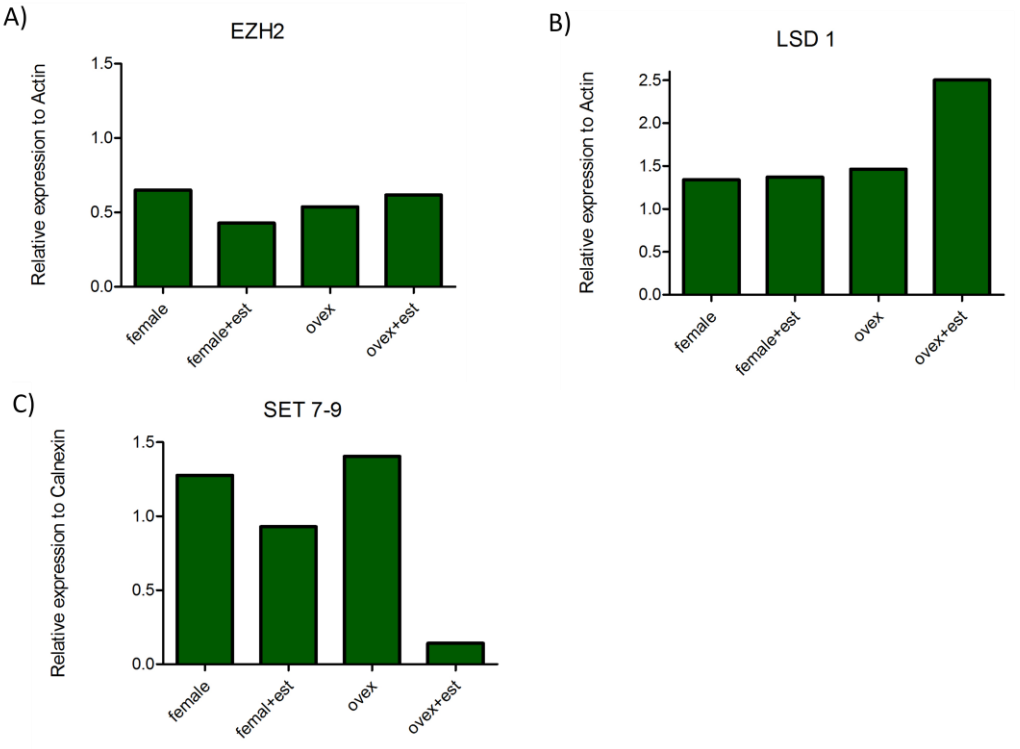

Figure 4.15 Evaluation of total protein level of histone modifier enzymes proteins in MSCs by western blotting at P0. Actin and Calnexin was used as loading control and protein expression results were normalized according to Actin and Calnexin expression.

4.8 ChIP ASSAY

4.8.1 EZH2, H3K27me2 AND H3K27me3 BINDING STATUS ON ADIPOGENIC GENES

Identification of binding status of histone modifications on key adipogenic transcription factors is critical to understand epigenetic regulation mechanism

of estrogen. qRT-PCR results showed that estrogen has an inbitory effect on adipogenic transcription factors examined in this thesis. In order to test whether estrogen treatment changes the accumulation of inactive histone marks; H3K27me2, H3K27me3 and EZH2 enzyme on adipogenic genes, we performed ChIP analysis in estrogen treated, tamoxifen treated and untreated MSCs obtained from both female and ovex rats.

After the chromatin digestion, 25 µl of digested chromatin samples were mixed with Proteinase K and incubated at 65 ˚C for 2 hours for reverse-crosslinking. DNA was purified as recommended in protocol. DNA concentration was determined and samples were loaded onto agarose gel to check DNA fragmentation. We clearly observed fragments, which 150 bp in length, in all samples (Figure 4.16).

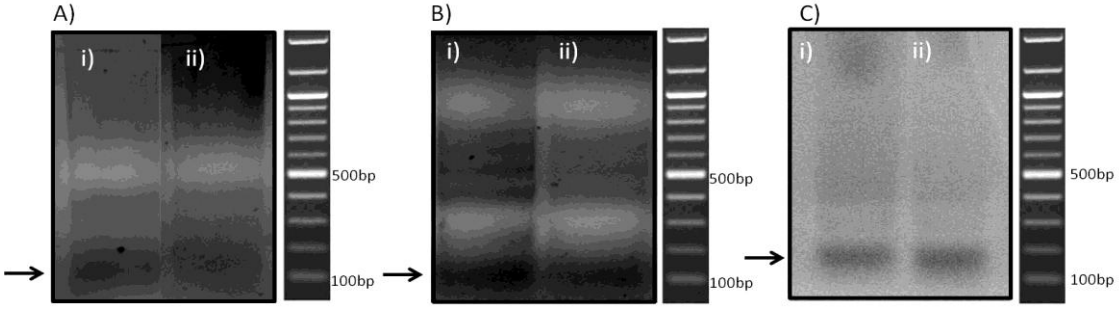

Figure 4.16 Confirmation of the digestion of chromatin samples in MSCs at P0 from A) Female (i), Female+est (ii), B) Ovex (i), Ovex+est (ii), C) Female+tam (i), Ovex+tam (ii), by agarose gel electrophoresis . Arrow indicates 150 bp.

After estrogen treatment, the occupancy of inactive marks; H3K27me2 and H3K27me3 tend to increase on the PPARγ, C/EBPα, FABP4 and Adipsin promoter regions in MSCs isolated from both female (Figure 4.17A) and ovex (Figure 4.17B). Moreover, when we treated MSCs with tamoxifen, which is an estrogen receptor antagonist, H3K27me2 and H3K27me3 accumulation on these genes promoters tend to reduce. EZH2 level on the adipogenic genes also tend to increase following estrogen treatment, especially in female rats (Figure 4.18A-D).

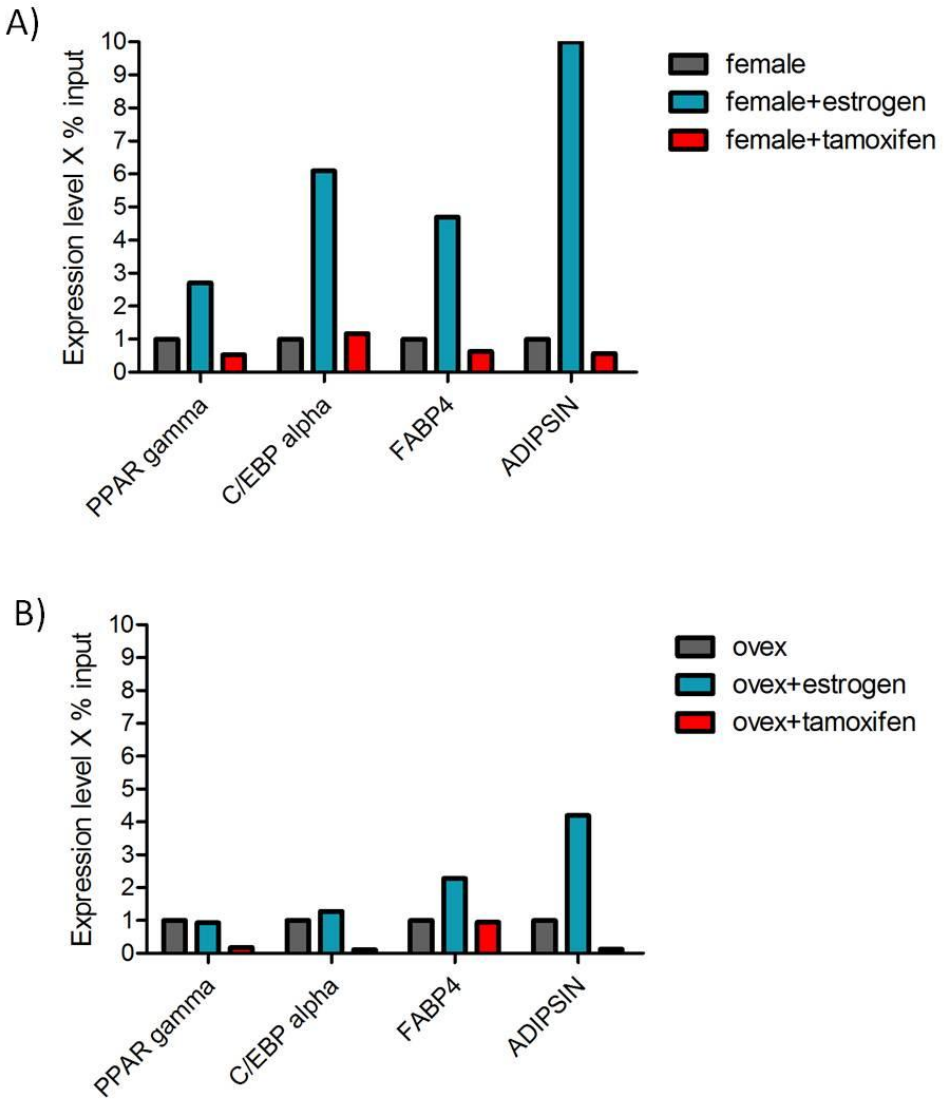

Figure 4.17 Histone modifications at the adipogenic genes: ChIP analysis of H3K27me2 and H3K27me3 in MSCs from normal (A) and ovariectomized (B) female animals and cultured in the absence and presence of either estrogen or tamoxifen. Quantitative PCR was performed on immunoprecipiated DNA fragments using primers for the PPARγ, C/EBPα, FABP4 and Adipsin. The average of "percent input" values of H3K27me2 and H3K27me3 accumulation on adipogenic genes were calculated.

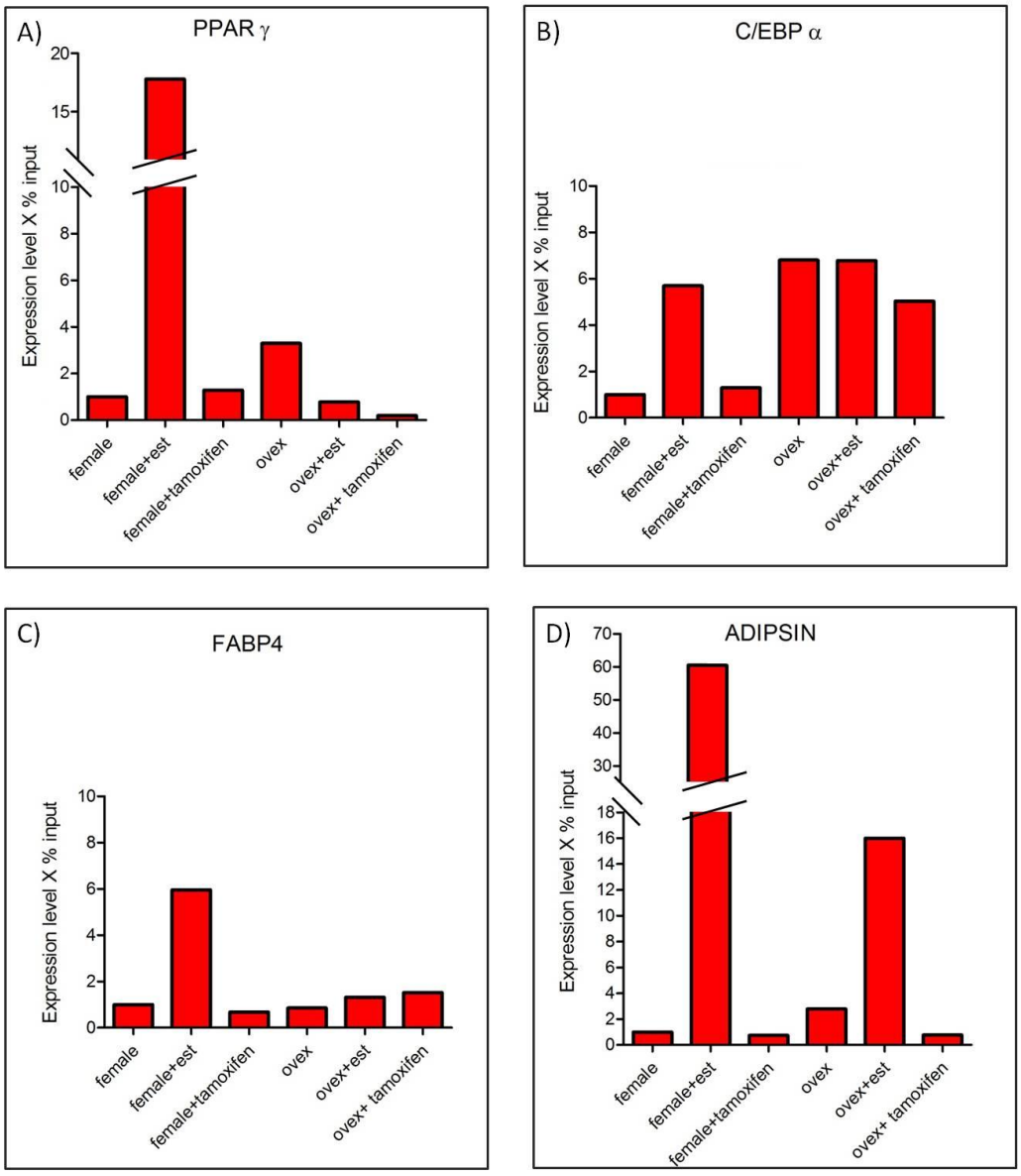

Figure 4.18 EZH2 occupancy at the adipogenic genes: ChIP analysis of EZH2 in MSCs from normal and ovariectomized female animals and cultured in the absence and presence of either estrogen or tamoxifen. Quantitative PCR was performed on immunoprecipiated DNA fragments using primers for the PPARγ, C/EBPα, FABP4 and Adipsin.

4.8.2 H3K27me2 AND H3K27me3 BINDING STATUS ON RUNX2 GENE

According to qRT-PCR results, estrogen hormone acts as a transcriptional activator of RUNX2 gene. To understand whether RUNX2 gene is regulated by estrogen through methylation of H3K27, we investigated the accumulation status of this type of histone modifications on RUNX2 gene promoter. Interestingly, after the estrogen treatment, H3K27me2 and H3K27me3 (Figure 4.19A-B) occupancy tend to increase on the RUNX2 promoter region.

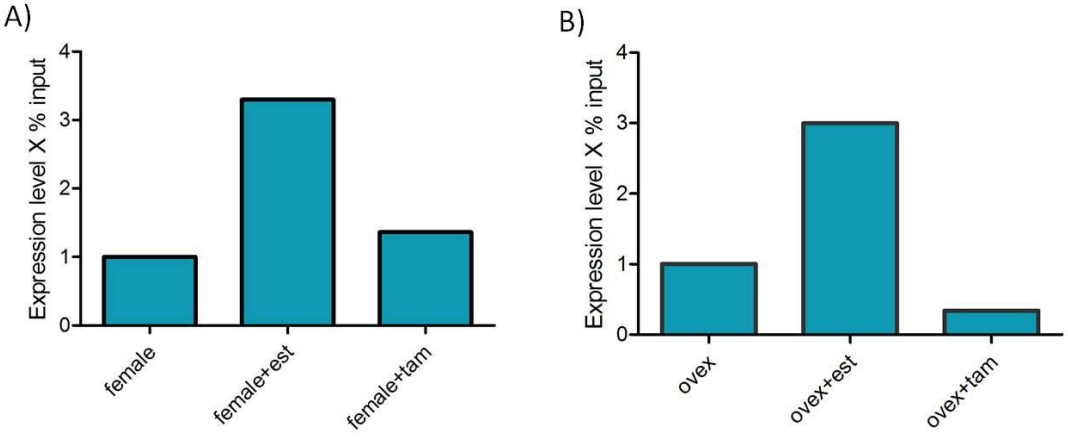

Figure 4.19 Histone modifications at RUNX2 gene: ChIP analysis of H3K27me2 and H3K27me3 in MSCs isolated from A) female and B) ovex animals and cultured in the absence and presence of either estrogen or tamoxifen. Q-PCR was performed on immunoprecipiated DNA fragments using primers for RUNX2. The average of "percent input" values of H3K27me2 and H3K27me3 accumulation on adipogenic genes were calculated.

Consistent with this data, when MSCs were treated with an estrogen receptor antagonist, tamoxifen, H3K27me2 and H3K27me3 levels at RUNX2 promoters tend to reduce.

4.8.3 ERα BINDING STATUS ON ADIPOGENIC AND OSTEOGENIC GENES

As we have shown, estrogen treatment resulted in an increase of H3K27me2 and H3K27me3 occupancies on PPARγ, C/EBPα, FABP4, Adipsin and RUNX2 promoter regions. Estrogen receptors convey the regulatory signal of estrogen interacting with coactivators, corepressors, HATs and histone deacetylases HDACs to control the transcription of target genes. We have performed ChIP assay to understand how binding of ERα changes on transcription factors upon estrogen treatment. We demonstrated that accumulation of ERα tend to increase on promoter regions after estrogen treatment in female (Figure 4.20).

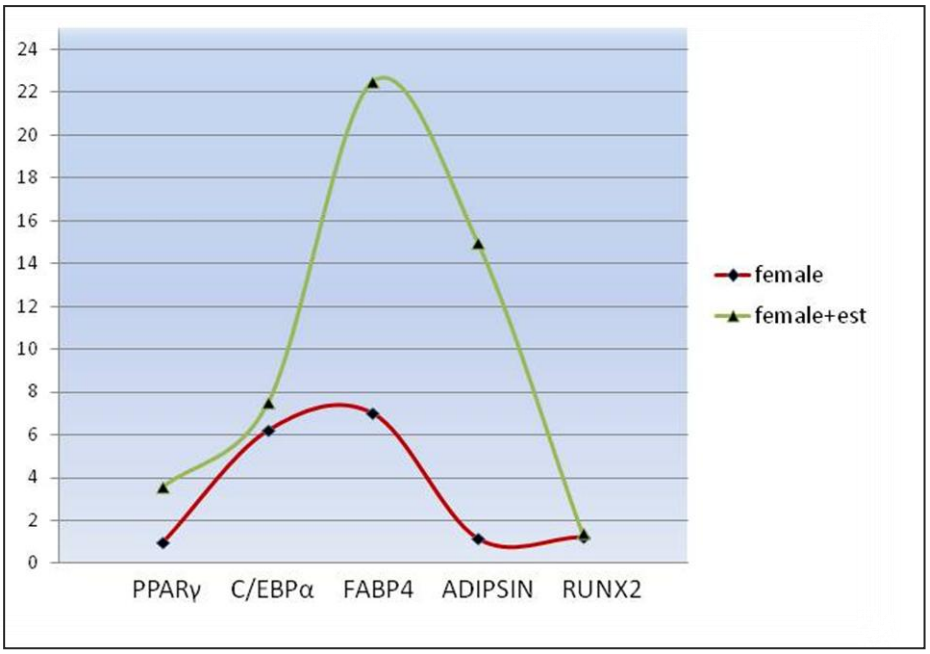

Figure 4.20 ERα occupancy at the adipogenic genes and RUNX2 gene: ChIP analysis of ERα in MSCs from normal female animals and cultured in the absence and presence of either estrogen.Quantitative PCR was performed on immunoprecipiated DNA fragments using primers for the PPARγ, C/EBPα, FABP4, Adipsin and RUNX2.

4.9 CpG METHYLATION STATUS OF ADIPOGENIC GENE PROMOTERS

In addition, we examined the DNA metyhlation status of adipogenic genes. For this purpose, CpG methylation analysis of ERα and two major transcription factors PPARγ, and C/EBPα promoters was performed in polyclonal cultures of MSCs. We determined the level of CpG methylation at each gene by taking the average percentage of CpG methylation from three colonies to create a CpG

methylation pattern table for ERα PPARγ, and C/EBPα genes. Bisulfite sequencing analyses revealed DNA hypermethylation in C/EBPα and PPARγ promoters after estrogen treatment in MSCs from female animals as expected (Figure 4.21A). On the other hand, in ovex rats estrogen treatment caused a decrease in percentage of DNA methylation (Figure 4.21B). Furthermore, it was also observed that ERα shows an opposite CpG methylation pattern compared to C/EBPα and PPARγ both in female and ovex animals. Mosaicism in the methylation status of CpGs between colonies was also seen on promoters of adipogenic genes and ERα. Methylation variation between clones was also demonstrated in Figure 4.22

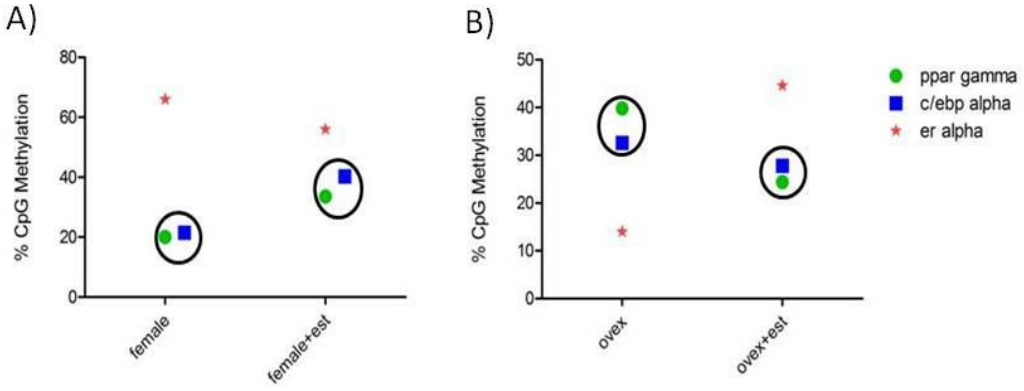

Figure 4.21 Determination of the level of CpG methylations at PPARγ, C/EBPα, and ERα promoters in MSCs by bisulfite sequencing analysis at P0. Bisulfite converted DNA was amplified with bisulfite specific primers for PPARγ, C/EBPα and ERα. Average percentage of CpG methylation from three colonies in female and ovex animals was taken.

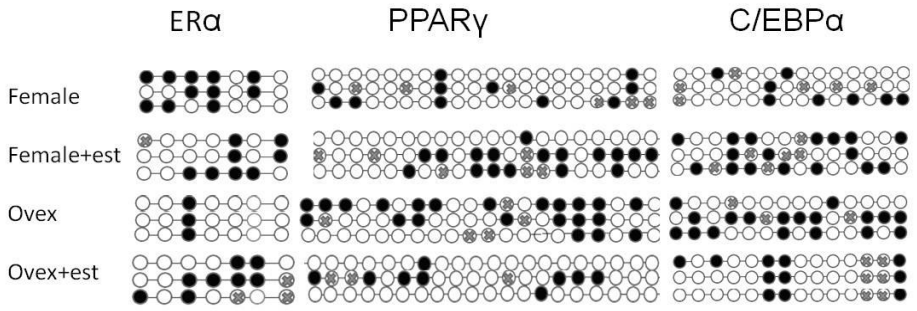

Figure 4.22 Bisulfite analysis of ERα, PPARγ and C/EBPα in 3 MSC clones from one normal and ovariectomized rat. Methylated CpG is indicated by ● at each locus for each clone. X indicates the CpG residues which could not be sequenced.

CHAPTER 5

DISCUSSION

Identification and characterization of stem cells provide opportunities to develop treatment options for several diseases. Because of this reason, the improvement in isolation, identification and therapeutic applications of stem cells has generated great excitement. The ethical problems related the use of ESC and the issues associated with effective using of iPS cells such as possible viral integration site increased the therapeutical value of ASCs. Among the other ASCs, MSCs have a distinguished place due to their unique features. First of all MSCs can be isolated from different parts of the body like bone marrow, adipose tissue, liver, dental pulp, umblical cord and blood. These cells have immune-privileged feature which permits the allogeneic transplantation and have homing ability which enables the migration to injured tissue easily. Due to these reasons, MSCs are suitable cell source for stem-cell based applications and tissue engineering.

In last decade, there have been numerous advances in tissue engineering to repair and replace injured organ and tissue by using stem cells. For this

purpose, many attempts have been applied to generate suitable scaffold material. Carbon nanotubes have become attractive scaffold materials due to their remarkable properties chemical stability, nano-scale size and electrical comductivity. On the other hand maintenance of attachment, growth, proliferation differentiaton of the cells on the scaffold surfaces is critical point in biomaterial applications. Estrogen hormone plays a key role in regulation of proliferation, differentiation and maintenance of cells and it has been shown by us and others that estrogen has also very important regulatory functions on MSCs 17-β estradiol (E2) enhances effectively MSC proliferation and up-regulates HTERT and telomerase activity preventing telomere shortening in MSCs[154,170,171]. In previous study, our group reported the inhibitory effect of estrogen on apoptosis through modulating the expression of Bcl-2 family genes[79]. Therefore, in this thesis we aimed to investigate effects of estrogen on MSC viability both on normal cell culture conditions and on CNT surfaces and investigated estrogen's genetic and epigenetic effects on MSC.

We first tested whether CNT surfaces have any effect on the characteristics of MSCs. Our results showed that MSCs were positive for the expression of MSC markers (CD90, CD71 and CD29) but negative for hematopoietic stem cell markers (CD45 and CD34) for all passages (Figure 4.2). These data suggest that exposure to CNT does not affect the features of MSCs. In order to understand the effect of estrogen on the viability and maintenance of MSCs on CNT

surfaces, the cells were incubated in the presence and absence of estrogen for 14 days. Moreover, the effect of non-coated and collagen coated CNTs on three passages (P0-P3) were also investigated. The passaged cells were incubated on non-coated and collagen coated CNT surfaces. Our plot revealed that the number of the MSCs decreased through the passage of the cells. The decrease was statistically significant when the number of the cells were compared between P0 and P1 and P2 (Figure 4.3.2c). Thus, these data suggest that very early passages of MSCs should be used for seeding purposes. The number of the cells both on coated and non-coated patterned CNTs continued to decrease at P2 compared to P1 but we did not observe a statistical significance between them. Interestingly, the number of the MSCs was significantly higher when they were cultured on non-coated compared to that of collagen coated CNT arrays at P0 but not at P1 and P2. Especially in bone tissue engineering, the scaffold material is the key component. An ideal scaffold should support growth of bone tissue having high porosity and unique physical properties[175]. It was demonstrated that, single-walled carbon nanotubes (SWNTs) are potential promising scaffold material for bone tissue engineering. They have also injectable and cytocompatible features and can mechanically improve the bone tissue formation[65,175,176]. Furthermore, a few investigations were done focusing on potential applications of SWNTs in drug delivery and cancer therapy[177]. Due to the smilar sizes with protein fibers that are used in cell growth media, CNTs can be considered as an alternative 3D collagen scaffold surface. Rat primary

osteoblasts were implanted on the CNT-coated sponge and succesfull bone formation was detected[78]. CNTs were also used as carrier materials for bone morphogenetic protein[178]. On the other hand, in some studies the biocompatibility and cytotoxicity of CNTs were discussed. It was demonstrated that powdered multi-walled carbon nanotubes (MWCNT) have a cytotoxic effect on mouse embryonic stem cells inducing DNA damage[179]. On the contrary, it was also shown that the patterned surface of CNTs support adhesion and growth of fibroblasts without any toxic effects promoting firmly attachment of cells to the surface[180,181]. Since there are concerns about the cytotoxic effect of CNT, we examined the viability of MSCs using MTT assay for estrogen treated and untreated samples. Contrary to previous concerns about the deleterious effect of CNT array on cells, we did not detect a toxic effect on the viability of MSCs (Figure 4.3.3). Furthermore, estrogen treatment enhanced the viability of cells comparing to untreated cells (Figure 4.3.1). As a conclusion we suggested that scaffolds comprised of CNTs can be used for seeding MSCs due to their non toxic properties and estrogen treatment enhances the maintenance of MSCs on CNT scaffold arrays.

Our results also showed that MSCs from early passages (P0) not only had the highest capacity of viability both on non-coated and collagen coated patterned CNT surfaces, but also higher than the control groups, whereas this level increased through the passages. Our MTT result was also parallel to the result

of calculation of the number of attached MSCs on collagen coated and non-coated CNTs. The cells were calculated under SEM and it was detected that number of attached cells significantly decreases through the passages. This result can be explained by the aging of MSCs[8]. According to these results we concluded that CNT has no cytotoxic effect on MSCs at P0 both on collagen coated and non-coated surfaces. On the other hand, the negative effect of CNTs on the metabolic activity of MSCs can be seen on later passages. Thus, our data demonstrated that either non-coated or collagen coated patterned CNT arrays provide an ideal native environment for cells from early passages to maintanece the differentiation potential. Overall, this study demonstrated that patterned CNT arrays can serve as a permissive scaffold for MSC growth and adhesion. CNT has no adverse effects on cell biocompatibility, proliferation and they are not biodegradable and as such that they can be used as scaffolds where long-term substrates are needed for tissue engineering such as in regeneration after spinal cord or brain injury.

After observing the similar response of estrogen on the maintenance and proliferation of MSCs when cultured either on CNTs or normal culture conditions, we focused on the role of estrogen on genetic and epigenetic regulation of MSCs by using normal culrure conditions. For this purpose, first, we investigated the effect of estrogen in regulation of transcription factors involved in MSC differentiation.

We examined the mRNA expression levels of transcription factors which are necessary for MSC differentiation and demonstrated that estrogen treatment causes decrease in expression level of four major adipogenic transcription factors; PPARγ, C/EBPα, FABP4 and Adipsin (Figure 4.4A-D) both in normal female and ovex animals. Significant increase in mRNA levels of osteogenic transcription factor RUNX2, upon estrogen treatment was also shown (Figure 4.4E). In previous studies it was demonstrated that estrogen represses adipogenesis through inhibiting expression of early and late adipogenic differentiation markers while promoting osteogenesis in MSCs[145,146,182]. We showed this inhibitory and stimulatory effect of estrogen hormone on adipogenic and osteogenic transcription factors respectively, especially in ovex samples which were treated with 10^{-7} M estrogen in cell culture. Estrogen deficiency is considered as major cause of osteoporosis, osteoarthritis and obesity in postmenopausal women[162-166, 183]. It was well established that there is a balance between adipogenesis, osteogenesis and chondrogenesis. Estrogen has a stimulator effect on bone and cartilage formation while inbiting adipogenic differentiaton[183]. The inverse relationship between adipogenesis, osteogenesis and chondrogenesis requires to be further elucidated. Our results suggested that estrogen inhibits adipogenesis decreasing expression of PPARγ, C/EBPα, FABP4 and Adipsin transcription factors, whereas it stimulates osteogenesis increasing RUNX2 expression in MSCs isolated from both female and ovex

rats. This result would attribute the key role to estrogen in MSC differentiation and can improve the usage of MSCs in treatment of obesity, osteoporosis and estrogen deficiency related diseases.

ETS1 plays pivotal role in osteogenesis interacting with RUNX2 to control osteogenic differentiation especially in preosteoblasts. We have observed that estrogen has an opposite effect on the expression of ETS1 (Figure 4.4F). Interestingly, the highest ETS1 level was demonstrated in ovex animals. Therefore we proposed that estrogen deficiency may inhibit ETS1 expression in MSCs and osteogenesis may be controlled through the regulation of RUNX2 gene by estrogen addition.

On the other hand, estrogen treatment caused reduced expression level of chondrogenic transcription factors; MEF2C, SOX9 and ATF3 in female animals as expected. But we could not observe similar and consisted expression pattern in ovex samples (Figure 4.4G-I). In a previos study it was reported that estrodial treament may inhibit the condrogenesis in a dose dependent manner in spite of the fact that estrogen is crucial for normal longutinal growth and its deficiency causes osteoarthiritis in postmenopausal women[161]. We suggest that the differences in response pattern of chondrogenic genes may be the result of the concentration of estrogen used in treatment of MSCs in ovex rats. Another possibility could be that estrogen treatment alone is not responsible in the

regulation of chondrogenesis in MSCs due to the absence of the other regulatory factors or pathways that are involved in this process.

Interestingly, significant reduction after estrogen treatment both in female and ovex animals was observed in the expression of FABP4 and Adipsin genes. Adipocyte differentiation is regulated by a network including numerous of transcription factors. These transcription factors are required for establisment of the mature fat cell phenotype[182, 183, 184]. PPARγ and C/EBPα are at the center of this network and responsible for the regulation of adipocyte specific genes such as FABP4 and Adipsin[185-187]. In the light of this knowledge and according our results, we proposed that since the FABP4 and Adipsin are downstream adipogenic genes, the significant change in expression level is only observed in these genes.

In contrast to known stimulatory effect of estrogen, estrogen receptor, liganded ERα also represses the gene expression recruiting corepressors/histone deactylases (HDAC) containing complexes enables establishment of hypermethylation on specific CpG loci[153,154,190]. Stossi reported that histone acetyltransferase p300 binds to both E2 (estradiol)-repressed and E2-stimulated genes with other co-activator SRC-3. This accumulation causes transient gene activation. After formation of early transient complex of p300:SRC3 with pioneer transcription factors, histone deacetylas CtBP1, is recruited with p300

on E2-repressd genes. We demonstrated that estrogen has an opposite effect on adipogenic genes in adipocytes derived from MSCs in normal female (Figure 4.6). While estrogen treatment causing decreases in expression of PPARγ, C/EBPα, FABP4 and Adipsin, it stimulates adipogenic gene expression in adipose cells differentiated from MSCs. Our results suggested that estrogen can show either its stimulator or repressor function on the same genes depending on the cell type. In addition, estrogen maintains to stimulate expression of RUNX2 gene in osteocytes differentiated from MSCs in normal female (Figure 4.8).

Furthermore, among the other transcription factors, we detected the localization change only in PPARγ (Figure 4.10, Figure 4.11) and ETS1 (Figure 4.12, Figure 4.13) proteins upon estrogen deficiency. PPARγ localization shifted from endoplamic reticulum to nucleus in response to estrogen deficiency. ETS1 protein was mainly in cytoplasm in female whereas it localized both in cytoplasm and nucleus in ovex animals. These results were consistent with our mRNA expression level data.

To support our genetic results, we aimed to examine the epigenetic regulation mechanisms which control transcription factors in MSCs with emphasis on adipogenic and osteogenic genes. Our western blotting results revealed a higher protein level of H3K27me2, H3K27me3 and H3K36me2 in untreated MSCs obtained both normal and ovex animals comparing to estrogen treated samples

(Figure 4.14). With this result we could also confirm a previous study in which it was reported that H3K27me3 and H3K9me3 are significantly higher in MSCs from ovex mice comparing to sham-operated mice[146].

The opposite relationship between osteogenesis and chondrogenesis was also tried to explain at epigenetic level in a previous study by Ye et.al in 2012[146]. In this study it was shown that JMJD2B and JMJD3B enzymes are involved in osteogenic differentiation of MSCs by removing H3K9me3 and H3K27me3. Upon osteogenic induction, overexperssion of these demethylases enhances the expression of alkaline phospahatase (ALP), which is an osteoblast differentiation marker. On the other hand, depletion of JMJD2B and JMJD3B causes a significant increase in adipogenic differentiaton in MSCs.

On the other hand, histone modifier enzymes; EZH2, LSD1 and SET 7/9 were also affected by estrogen, but there is no correlation between the global protein expression rates of modifier enzymes and modified histone proteins after estrogen treatment (Figure 4.15). Although the inhibitory effect of estrogen on total H3K27me2 and H3K27me3 protein levels in MSCs, enhanced occupancy of H3K27me2 and H3K27me3 on the promoters of adipogenic genes; PPARγ, C/EBPα, FABP4 and Adipsin, upon estrogen treatment was demonstrated by ChIP analysis. Furthermore, the addition of tamoxifen, which is an estrogen receptor antagonist, caused a decrease in the accumulation of H3K27me2 and

H3K27me3 (Figure 4.17). In conclusion we could demonstrate that however estrogen treatment reduces total protein level of H3K27me2, H3K27me3, it causes the enhanced accumulation of of inactive marks; H3K27me2 and H3K27me3, on adipogenic gene promoters in order to repress transcription.

In addition, we demonstrated that estrogen treatment also regulate the occupancy of methylated H3K27 proteins on RUNX2 gene (Figure 4.19). The reduced EZH2 phosphorylation increases H3K27 trimethylation and causes repression of RUNX2 and osteopontin genes, which are osteogenic markers[191]. As contradiction to this finding and in contrast to our qRT-PCR results, H3K27me2 and H3K27me3 binding is also enhanced upon estrogen treatment on RUNX2 promoter as well as on PPARγ, C/EBPα, FABP4 and Adipsin promoters. It was known that genes which have bivalanet promoters are regulated by a combination of histone marks[191,193,194]. These domains consist of regions for both inactive and active histone modifications such as H3K27 and H3K4. From this result we concluded that RUNX2 gene may be regulated by another active histone marks such as H3K4 or H3K36, which are stimulated to bind to RUNX2 upon estrogen induction.

Furthermore, the important role of H3K27 methyltransferase EZH2 in the inhibition of MSCs differentiation was reported. We showed that estrogen induced the accumulation of EZH2 on adipogenic genes, especially in female

animals (Figure 4.18). Our results suggested that estrogen regulates the expression of key adipogenic transcription factors altering the binding of H3K27me2, H3K27me3 and their methyltransferase enzyme EZH2. By this mechanism, estrogen influences the adipogenesis commitment of MSCs.

Another important finding is the ehnanced binding of ERα to PPARγ, C/EBPα, FABP4, Adipsin and RUNX2 after estrogen treatment in normal female animals (Figure 4.20). As mentioned, ERα have both stimulator and repressor function in the regulation of expression of target genes. ERα recruits corepressors/HDAC and costimulators/HAC enzyme complexes[150-154]. On the RUNX2 promoter region we could not detect any accumulation. This may suggests that RUNX2 may be regulated by ERβ binding to its promoter. However, on the adipogenic gene promoters, especially on FABP4 and Adipsin genes estrogen increases the accumulation of ERα receptor. We proposed that estrogen induction causes increase in the accumulation of ERα on PPARγ, C/EBPα, FABP4 and Adipsin genes recruiting corepressors/HDAC complexes to repress expression. In addition, the reason of the highest accumulation of ERα on FABP4 and Adipsin may be that these two genes are the downstream targets of adipogenic process.

In order to investigate DNA methylation status of adipogenic genes upon estrogen administration, we focused on the master adipogenic genes; PPARγ,

C/EBPα and ERα promoters. Similar to a previous study[59] in our experiment we have also observed mosaic CpG methylation profile on adipogenic gene promoters and variations in the percentage of CpG methylations between colonies (Figure 4.22). Our bisulfite sequencing analyses revealed DNA hypomethylation in C/EBPα and PPARγ promoters without estrogen (Figure 4.21). On the contrary, estrogen treatment caused establishment of hypomethylation on the same genes in ovex cells. In both normal female and ovex colonies, DNA methylation pattern of ERα showed opposite profile. According to these results we concluded that epigenetic modifications do not regulate the adipogenesis process in the same way in MSCs isolated from female and ovex animals.

In conclusion, in this thesis we have shown CNTs are ideal scaffold biomaterials to be used for seeding MSCs especially at P0 and estrogen enhances viability of cells on CNT arrays. Estrogen genetically and epigenetically regulates the expression of key transcription factors involved in MSC differentiation by not just changing the gene expression, protein localization of transcription factors involved in differentiation of MSCs, but also influencing binding of histone modification proteins and modifier enzymes to the promoter of these genes. Epigenetic mechanisms are reversible. That's why, identification of genetic and epigenetic reprogramming of MSCs by estrogen treatment may provide an important insight for clinical applications in

both treatments of obesity, osteoarthiridis, osteosclerosis and tissue engineering applications.

CHAPTER 6

FUTURE PERSPECTIVES

In this thesis the effect of estrogen on maintenance and differentiation of MSCs was examined. We have found that estrogen treatment increases the maintenance of MSCs seeded on CNTs. Furthermore we have also shown that cell viability and the number of attached cells decreases through the passages. In order to better understand whether estrogen treatment can enhance the cell viability on CNTs even if in the later passages, detection of MSC viability on CNT arrays not only at P0, but also at later passages could be critical as to document the importance of positive effect of estrogen in tissue engineering field. Moreover, MSCs may undergo osteogenic or chondrogenic differentiation on CNTs arrays. The differentiation can be detected by using gold-label antibodies for osteogenic and chondrogenic markers and cell viability can be evaluated by MTT assay.

In this study, we have mainly focused on the genetic and epigenetic alterations in regulation of adipogenic and osteogenic transcription factors. To explain the role of estrogen in the regulation of chondrogenesis, should be examined in a

dose dependent manner. To detect the optimum estrogen concentration, at which the expression of chondrogenic differentiation factors is stimulated, could be useful for further analysis. Similar estrogen gradient pattern may be applied to invesitagate the transcriptional change of ETS1 gene.

To investigate the total protein level of histone modifications and modifier enzymes, we unfortunately could use the protein samples isolated from one female and ovex animal. To confirm our results, the number of animal samples should be increase and the experiments should be repeated. Similarly, to confirm the results and to calculate the fold change in the expression of the PPARγ, C/EBPα, FABP4, Adipsin and RUNX2 genes after the immunoprecipitation with histone modifications proteins, ChIP assay should be repeated using chromatin from MSCs obtained from more than one normal and ovariectomized female animal. ChIP experiment should be also performed for other histone modifications such as H3K9me2, H3K9me3 and H3K36me2 in MSCs. Also, knock-down of modifier enzymes such as LSD1, SET 7/9 and EZH2 using siRNA or shRNA both before and after differentiation, could provide the evalution of their contribution to control of differentitation.

We also suggest that RUNX2 gene may have bivalent domain on promoter region and can be regulated by other active histone marks such as H3K4 and H3K36 in addition to H3K27. To test this possibility, ChIP should be

performed for H3K4, H3K36 and SET 7/9, which is a H3K4 methyltransferase. in MSCs. Accumulation of the active histone marks and SET 7/9 enzyme on RUNX2 gene can be quantified by qRT-PCR.

Finally, in this thesis we suggest that estrogen induction causes increase in the accumulation of ERα on PPARγ, C/EBPα, FABP4 and Adipsin and ERα recruits EZH2 enzyme on these to repress expression. We do not know whether there is direct interaction between ERα and EZH2 protein or not. Understanding of how ERα represses the activation of adipogenic gene upon estrogen treatment is important while explaining the epigenetic effect of estrogen. Therefore, the interaction of ERs not just with EZH2 protein, but also other HMTs, should be investigated by ChIP and co-immunoprecipitation analysis.

REFERENCES

1. Wislet-Gendebien, S., Laudet, E., Neirinckx, V. & Rogister, B. Adult bone marrow: which stem cells for cellular therapy protocols in neurodegenerative disorders? *Journal of biomedicine & biotechnology* **2012,** 601560 (2012).

2. Thomson, J. a. Embryonic Stem Cell Lines Derived from Human Blastocysts. *Science* **282,** 1145–1147 (1998).

3. Yamanaka, S. Strategies and new developments in the generation of patient-specific pluripotent stem cells. *Cell stem cell* **1,** 39–49 (2007).

4. Mezey, E. The therapeutic potential of bone marrow derived stromal cells. *Journal of cellular biochemistry* 1–14 (2011). doi:10.1002/jcb.23216

5. Collas, P. Programming differentiation potential in mesenchymal stem cells. *Epigenetics : official journal of the DNA Methylation Society* **5,** 476–82 (2010).

6. Takahashi, K. & Yamanaka, S. Induction of pluripotent stem cells from mouse embryonic and adult fibroblast cultures by defined factors. *Cell* **126,** 663–76 (2006).

7. Karp, J. M. & Leng Teo, G. S. Mesenchymal stem cell homing: the devil is in the details. *Cell stem cell* **4,** 206–16 (2009).

8. Tokcaer-keskin, Z. *et al.* Timing of induction of cardiomyocyte differentiation for in vitro cultured mesenchymal stem cells : a perspective for emergencies 1. **150,** 143–150 (2009).

9. Nebigil, C. G. *et al.* Overexpression of the serotonin 5-HT2B receptor in heart leads to abnormal mitochondrial function and cardiac hypertrophy. *Circulation* **107,** 3223–9 (2003).

10. Pera, M. F., Reubinoff, B. & Trounson, a. Human embryonic stem cells. *Journal of cell science* **113 (Pt 1,** 5–10 (2000).

11. Nichols, J. & Smith, A. Naive and primed pluripotent states. *Cell stem cell* **4,** 487–92 (2009).

12. Hanna, J. H., Saha, K. & Jaenisch, R. Pluripotency and cellular reprogramming: facts, hypotheses, unresolved issues. *Cell* **143,** 508–25 (2010).

13. Gartler, S. M. X-Chromosome Inactivation. 1–6 (2001).

14. Stead, E. *et al.* Pluripotent cell division cycles are driven by ectopic Cdk2 , cyclin A / E and E2F activities. **4,** 8320–8333 (2002).

15. White, J. & Dalton, S. Cell cycle control of embryonic stem cells. *Stem cell reviews* **1,** 131–8 (2005).

16. Matsuda, T. *et al.* STAT3 activation is sufficient to maintain an undifferentiated state of mouse embryonic stem cells. *The EMBO journal* **18,** 4261–9 (1999).

17. Ying, Q. L., Nichols, J., Chambers, I. & Smith, A. BMP induction of Id proteins suppresses differentiation and sustains embryonic stem cell self-renewal in collaboration with STAT3. *Cell* **115,** 281–92 (2003).

18. Levenstein, M. E. *et al.* Basic fibroblast growth factor support of human embryonic stem cell self-renewal. *Stem cells (Dayton, Ohio)* **24,** 568–74 (2006).

19. Vallier, L., Alexander, M. & Pedersen, R. a. Activin/Nodal and FGF pathways cooperate to maintain pluripotency of human embryonic stem cells. *Journal of cell science* **118,** 4495–509 (2005).

20. Barnabé-Heider, F. & Frisén, J. Stem cells for spinal cord repair. *Cell stem cell* **3,** 16–24 (2008).

21. Horwitz, E. M. *et al.* Isolated allogeneic bone marrow-derived mesenchymal cells engraft and stimulate growth in children with osteogenesis imperfecta: Implications for cell therapy of bone. *Proceedings of the National Academy of Sciences of the United States of America* **99,** 8932–7 (2002).

22. Bifari, F., Pacelli, L. & Krampera, M. Immunological properties of embryonic and adult stem cells. *World journal of stem cells* **2,** 50–60 (2010).

23. Lachmann, P. Stem cell research — why is it regarded as a. **2,** (2001).

24. Yamanaka, S. A fresh look at iPS cells. *Cell* **137,** 13–7 (2009).

25. Maherali, N. *et al.* Directly reprogrammed fibroblasts show global epigenetic remodeling and widespread tissue contribution. *Cell stem cell* **1,** 55–70 (2007).

26. Okita, K., Ichisaka, T. & Yamanaka, S. Generation of germline-competent induced pluripotent stem cells. *Nature* **448,** 313–7 (2007).

27. Stadtfeld, M. & Hochedlinger, K. Induced pluripotency: history, mechanisms, and applications. *Genes & development* **24,** 2239–63 (2010).

28. Yamanaka, S. & Blau, H. M. Nuclear reprogramming to a pluripotent state by three approaches. *Nature* **465,** 704–12 (2010).

29. Yu, J. *et al.* Induced pluripotent stem cell lines derived from human somatic cells. *Science (New York, N.Y.)* **318,** 1917–20 (2007).

30. Stadtfeld, M., Nagaya, M., Utikal, J., Weir, G. & Hochedlinger, K. Induced pluripotent stem cells generated without viral integration. *Science (New York, N.Y.)* **322,** 945–9 (2008).

31. Kaji, K. *et al.* Virus-free induction of pluripotency and subsequent excision of reprogramming factors. *Nature* **458,** 771–5 (2009).

32. Woltjen, K. *et al.* piggyBac transposition reprograms fibroblasts to induced pluripotent stem cells. *Nature* **458,** 766–70 (2009).

33. Wilson, M. H., Coates, C. J. & George, A. L. PiggyBac transposon-mediated gene transfer in human cells. *Molecular therapy : the journal of the American Society of Gene Therapy* **15,** 139–45 (2007).

34. Shi, Y. *et al.* Induction of pluripotent stem cells from mouse embryonic fibroblasts by Oct4 and Klf4 with small-molecule compounds. *Cell stem cell* **3,** 568–74 (2008).

35. Warren, L. *et al.* Highly efficient reprogramming to pluripotency and directed differentiation of human cells with synthetic modified mRNA. *Cell stem cell* **7,** 618–30 (2010).

36. Kim, K. *et al.* Epigenetic memory in induced pluripotent stem cells. *Nature* **467,** 285–90 (2010).

37. Potten, C. S. & Loeffler, M. Stem cells: attributes, cycles, spirals, pitfalls and uncertainties. Lessons for and from the crypt. *Development (Cambridge, England)* **110,** 1001–20 (1990).

38. Herzog, E. L., Chai, L. & Krause, D. S. Plasticity of marrow-derived stem cells. *Blood* **102,** 3483–93 (2003).

39. Robey, P. G. Stem cells near the century mark. *The Journal of clinical investigation* **105,** 1489–91 (2000).

40. Neumüller, R. a & Knoblich, J. a. Dividing cellular asymmetry: asymmetric cell division and its implications for stem cells and cancer. *Genes & development* **23,** 2675–99 (2009).

41. Kørbling, M. & Estrov, Z. Adult stem cells for tissue repair - a new therapeutic concept? *The New England journal of medicine* **349,** 570–82 (2003).

42. Mikkola, H. K. a & Orkin, S. H. The journey of developing hematopoietic stem cells. *Development (Cambridge, England)* **133,** 3733–44 (2006).

43. Friedenstein AJ, Gorskaja JF, Kulagina NN: Fibroblast precursors in normal and irradiated mouse hematopoietic organs. *Exp Hematol* 4:267-274Exp42 (1976).

44. Pittenger, M. F. Multilineage Potential of Adult Human Mesenchymal Stem Cells. *Science* **284,** 143–147 (1999).

45. Muraglia, a, Cancedda, R. & Quarto, R. Clonal mesenchymal progenitors from human bone marrow differentiate in vitro according to a hierarchical model. *Journal of cell science* **113 (Pt 7,** 1161–6 (2000).

46. Caplan, a I. Mesenchymal stem cells. *Journal of orthopaedic research : official publication of the Orthopaedic Research Society* **9,** 641–50 (1991).

47. Mackay, a M. *et al.* Chondrogenic differentiation of cultured human mesenchymal stem cells from marrow. *Tissue engineering* **4,** 415–28 (1998).

48. Xu, W. *et al.* Mesenchymal stem cells from adult human bone marrow differentiate into a cardiomyocyte phenotype in vitro. *Experimental biology and medicine (Maywood, N.J.)* **229,** 623–31 (2004).

49. Woodbury, D., Schwarz, E. J., Prockop, D. J. & Black, I. B. Adult rat and human bone marrow stromal cells differentiate into neurons. *Journal of neuroscience research* **61,** 364–70 (2000).

50. Aggarwal, S. & Pittenger, M. F. Human mesenchymal stem cells modulate allogeneic immune cell responses. *Blood* **105,** 1815–22 (2005).

51. Javazon, E. H., Beggs, K. J. & Flake, A. W. Mesenchymal stem cells: paradoxes of passaging. *Experimental hematology* **32,** 414–25 (2004).

52. Chamberlain, G., Fox, J., Ashton, B. & Middleton, J. Concise review: mesenchymal stem cells: their phenotype, differentiation capacity, immunological features, and potential for homing. *Stem cells (Dayton, Ohio)* **25,** 2739–49 (2007).

53. Galmiche, M. C., Koteliansky, V. E., Brière, J., Hervé, P. & Charbord, P. Stromal cells from human long-term marrow cultures are mesenchymal cells that differentiate following a vascular smooth muscle differentiation pathway. *Blood* **82,** 66–76 (1993).

54. Uccelli,A.,Moretta, L., Pistoia, V. Mesenchymal stem cells in health and disease. *Nature Reviews Immunology* **8**, 726-736 (2008)

55. Ghannam, S., Pène, J., Torcy-Moquet, G., Jorgensen, C. & Yssel, H. Mesenchymal stem cells inhibit human Th17 cell differentiation and function and induce a T regulatory cell phenotype. *Journal of immunology (Baltimore, Md. : 1950)* **185,** 302–12 (2010).

56. Le Blanc, K. & Ringdén, O. Immunobiology of human mesenchymal stem cells and future use in hematopoietic stem cell transplantation. *Biology of blood and marrow transplantation : journal of the American Society for Blood and Marrow Transplantation* **11,** 321–34 (2005).

57. Beyth, S. *et al.* Human mesenchymal stem cells alter antigen-presenting cell maturation and induce T-cell unresponsiveness. *Blood* **105,** 2214–9 (2005).

58. Li, H., Xiao, L., Wang, C., Gao, J. & Zhai, Y. Review: Epigenetic regulation of adipocyte differentiation and adipogenesis. *Journal of Zhejiang University. Science. B* **11,** 784–91 (2010).

59. Noer, A., Sørensen, A. L., Boquest, A. C. & Collas, P. Stable CpG Hypomethylation of Adipogenic Promoters in Freshly Isolated , Cultured , and Differentiated Mesenchymal Stem Cells from Adipose Tissue □. *Molecular Biology of the Cell* **17,** 3543–3556 (2006).

60. Jiang, W.-H. *et al.* Migration of intravenously grafted mesenchymal stem cells to injured heart in rats. *Sheng li xue bao : [Acta physiologica Sinica]* **57,** 566–72 (2005).

61. Li, W.-J., Tuli, R., Huang, X., Laquerriere, P. & Tuan, R. S. Multilineage differentiation of human mesenchymal stem cells in a three-dimensional nanofibrous scaffold. *Biomaterials* **26,** 5158–66 (2005).

62. Tuan, R. S., Boland, G. & Tuli, R. Adult mesenchymal stem cells and cell-based tissue engineering. **5,** (2003).

63. Ifkovits, J. L. *et al.* Biodegradable fibrous scaffolds with tunable properties formed from photo-cross-linkable poly(glycerol sebacate). *ACS applied materials & interfaces* **1,** 1878–86 (2009).

64. Caterson, E. J. *et al.* Three-dimensional cartilage formation by bone marrow-derived cells seeded in polylactide/alginate amalgam. *Journal of biomedical materials research* **57,** 394–403 (2001).

65 Shridharan, I.Adapting collagen/CNT matrix in directing hESC differentiation. Biochemical and biophysical research communications 381,508–512 (2009)

66. Bruder, S. P., Jaiswal, N. & Haynesworth, S. E. Growth kinetics, self-renewal, and the osteogenic potential of purified human mesenchymal stem cells during extensive subcultivation and following cryopreservation. *Journal of cellular biochemistry* **64,** 278–94 (1997).

67. Li, W.-J. W.-J. *et al.* A three-dimensional nanofibrous scaffold for cartilage tissue engineering using human mesenchymal stem cells. *Biomaterials* **26,** 599–609 (2005).

69. Wakitani S, Goto T, Pineda SJ, Young RG, Mansour JM, Caplan AI, Goldberg VM: Mesenchymal cell-based repair of large, full- thickness defects of articular cartilage. J Bone Joint Surg Am. 76:579-592 (1994).

70. Caplan, A. I. Tissue Engineering Designs for the Future: New Logics, Old Molecules.*Tissue engineering* **6,** 1–8 (2000).

71. Ifkovits, J. L. *et al.* Biodegradable Fibrous Scaffolds with Tunable Properties Formed from Photocrosslinkable Poly(glycerol sebacate)*NIH Public Access.* **1,** 1878–1892 (2010).

72. Dalby, M. J. *et al.* The control of human mesenchymal cell differentiation using nanoscale symmetry and disorder. *Nature materials* **6,** 997–1003 (2007).

72. El-Amin, S. F. *et al.* Integrin expression by human osteoblasts cultured on degradable polymeric materials applicable for tissue engineered bone. *Journal of orthopaedic research : official publication of the Orthopaedic Research Society* **20,** 20–8 (2002).

73. Gelain, F. *et al.* Transplantation of Nanostructured Composite Scaffolds Results in the Spinal Cords. **5,** 227–236 (2011).

74. Chen, J.-P. & Chang, Y.-S. Preparation and characterization of composite nanofibers of polycaprolactone and nanohydroxyapatite for osteogenic differentiation of mesenchymal stem cells. *Colloids and surfaces. B, Biointerfaces* **86,** 169–75 (2011).

75. Chen, R. J. *et al.* Noncovalent functionalization of carbon nanotubes for highly specific electronic biosensors. *Proceedings of the National Academy of Sciences of the United States of America* **100,** 4984–9 (2003).

76. Nauta, A. J. & Fibbe, W. E. Immunomodulatory properties of mesenchymal stromal cells. *Blood* **110,** 3499–506 (2007).

77. Zhang, X. *et al.* Guided neurite growth on patterned carbon nanotubes. *Sensors and Actuators B: Chemical* **106,** 843–850 (2005).

78. Mooney, E., Dockery, P., Greiser, U., Murphy, M. & Barron, V. Carbon nanotubes and mesenchymal stem cells: biocompatibility, proliferation and differentiation. *Nano letters* **8,** 2137–43 (2008).

77. Nguyen-Vu, T. D. B. *et al.* Vertically aligned carbon nanofiber architecture as a multifunctional 3-D neural electrical interface. *IEEE transactions on bio-medical engineering* **54,** 1121–8 (2007).

78. Hirata, E. *et al.* Multiwalled carbon nanotube-coating of 3D collagen scaffolds for bone tissue engineering. *Carbon* **49,** 3284–3291 (2011).

79 Ayaloglu-butun, F. & Terzioglu-kara, E. The Effect of Estrogen on Bone Marrow-Derived Rat Mesenchymal Stem Cell Maintenance : Inhibiting Apoptosis Through the Expression of Bcl-x L and Bcl-2. 393–401 (2012). doi:10.1007/s12015-011-9292-0

80. Hong, L., Zhang, G., Sultana, H., Yu, Y. & Wei, Z. The effects of 17-β estradiol on enhancing proliferation of human bone marrow mesenchymal stromal cells in vitro. *Stem cells and development* **20,** 925–31 (2011).

81. Faulds, M. H., Zhao, C., Dahlman-Wright, K. & Gustafsson, J.-Å. Regulation of metabolism by estrogen signaling. *The Journal of endocrinology* 1–23 (2011). doi:10.1530/JOE-11-0044

82. Björnström, L. & Sjöberg, M. Mechanisms of estrogen receptor signaling: convergence of genomic and nongenomic actions on target genes. *Molecular endocrinology (Baltimore, Md.)* **19,** 833–42 (2005).

83. Zhang, Q. *et al.* Estrogen influences the differentiation, maturation and function of dendritic cells in rats with experimental autoimmune encephalomyelitis. *Acta pharmacologica Sinica* **25,** 508–13 (2004).

84. Lonard, D. M., Lanz, R. B. & Malley, B. W. O. Nuclear Receptor Coregulators and Human Disease. **28,** 575–587 (2007).84. Yoshikubo, H. *et al.* Osteoblastic activity and estrogenic response in the regenerating scale of goldfish, a good model of osteogenesis. *Life sciences* **76,** 2699–709 (2005).

85. Klinge, C. M. Estrogen receptor interaction with estrogen response elements. *Nucleic acids research* **29,** 2905–19 (2001).

86. Acconcia, F. & Kumar, R. Signaling regulation of genomic and nongenomic functions of estrogen receptors. *Cancer letters* **238,** 1–14 (2006).

87. Reid, G. *et al.* Cyclic, proteasome-mediated turnover of unliganded and liganded ERalpha on responsive promoters is an integral feature of estrogen signaling. *Molecular cell* **11,** 695–707 (2003).

88. Nilsson, S., Ma, S., Treuter, E., Tujague, M. & Thomsen, J. Mechanisms of Estrogen Action. **81,** (2001).

89. Zubairy, S. & Oesterreich, S. Estrogen-repressed genes key mediators of estrogen action? *Breast cancer research : BCR* **7,** 163–4 (2005).

90. Razandi, M., Pedram, A., Merchenthaler, I., Greene, G. L. & Levin, E. R. Plasma membrane estrogen receptors exist and functions as dimers. *Molecular endocrinology (Baltimore, Md.)* **18,** 2854–65 (2004).

91. Webb, P. *et al.* ERβ Binds N-CoR in the Presence of Estrogens via an LXXLL-like Motif in the N-CoR C-terminus. **15,** 1–15 (2003).

92. Wang, W., Dong, L., Saville, B. & Safe, S. Transcriptional activation of E2F1 gene expression by 17beta-estradiol in MCF-7 cells is regulated by NF-Y-Sp1/estrogen receptor interactions. *Molecular endocrinology (Baltimore, Md.)* **13,** 1373–87 (1999).

93. Feinberg, A. P. Epigenomics reveals a functional genome anatomy and a new approach to common disease. *Nature biotechnology* **28,** 1049–52 (2010).

94. Jaenisch, R. & Bird, A. Epigenetic regulation of gene expression: how the genome integrates intrinsic and environmental signals. *Nature genetics* **33 Suppl,** 245–54 (2003).

95 Martin, C. & Zhang, Y. Mechanisms of epigenetic inheritance. *Current opinion in cell biology* **19,** 266–72 (2007).

96. Tammen, S. a, Friso, S. & Choi, S.-W. Epigenetics: the link between nature and nurture. *Molecular aspects of medicine* **34,** 753–64 (2013).

97. Meissner, A. Epigenetic modifications in pluripotent and differentiated cells. *In Vivo* **28,** 1079–1088 (2010).

98. Teven, C. M. *et al.* Epigenetic regulation of mesenchymal stem cells: a focus on osteogenic and adipogenic differentiation. *Stem cells international* **2011,** 201371 (2011).

99. Fahmi, H., Martel-Pelletier, J., Pelletier, J.-P. & Kapoor, M. Peroxisome proliferator-activated receptor gamma in osteoarthritis. *Modern rheumatology / the Japan Rheumatism Association* **21,** 1–9 (2011).

100. Fouse, S. D. *et al.* Promoter CpG methylation contributes to ES cell gene regulation in parallel with Oct4/Nanog, PcG complex, and histone H3 K4/K27 trimethylation. *Cell stem cell* **2,** 160–9 (2008).

101. Poetsch, A. R. & Plass, C. Transcriptional regulation by DNA methylation. *Cancer treatment reviews* **37 Suppl 1,** S8–12 (2011).

102. Doi, A. *et al.* Differential methylation of tissue- and cancer-specific CpG island shores distinguishes human induced pluripotent stem cells, embryonic stem cells and fibroblasts. *Nature genetics* **41,** 1350–3 (2009).

103. Corfe, B. M., Dive, C., and Hickman, J. A. Cell damage-induced conformational changes of the pro-apoptotic protein Bak in vivo precede the onset of apoptosis, *J Cell Biol 144*, 903-914 (1999)

104. Bock, C., Walter, J., Paulsen, M. & Lengauer, T. CpG island mapping by epigenome prediction. *PLoS computational biology* **3,** e110 (2007).

105. Lander, E. S. *et al.* Initial sequencing and analysis of the human genome. *Nature* **409,** 860–921 (2001).

106. Oswald, J. *et al.* Active demethylation of the paternal genome in the mouse zygote. *Current biology : CB* **10,** 475–8 (2000).

107. Hajkova, P. *et al.* Epigenetic reprogramming in mouse primordial germ cells. *Mechanisms of development* **117,** 15–23 (2002).

108. Liu, L., Wylie, R. C., Andrews, L. G. & Tollefsbol, T. O. Aging, cancer and nutrition: the DNA methylation connection. *Mechanisms of Ageing and Development* **124,** 989–998 (2003).

109. Chen, Z. & Riggs, A. D. DNA methylation and demethylation in mammals. *The Journal of biological chemistry* **286,** 18347–53 (2011).

110. Paulsen, M. & Ferguson-Smith, a C. DNA methylation in genomic imprinting, development, and disease. *The Journal of pathology* **195,** 97–110 (2001).

111. Bird, A. DNA methylation patterns and epigenetic memory. *Genes & development* **16,** 6–21 (2002).

112. Minks, J., Robinson, W. P. & Brown, C. J. A skewed view of X chromosome inactivation. **118,** (2008).

113. Goll, M. G. & Bestor, T. H. Eukaryotic cytosine methyltransferases. *Annual review of biochemistry* **74,** 481–514 (2005).

114. Hendrich, B. & Bird, a. Identification and characterization of a family of mammalian methyl-CpG binding proteins. *Molecular and cellular biology* **18,** 6538–47 (1998).

115. Clouaire, T. & Stancheva, I. Europe PMC Funders Group Methyl-CpG binding proteins : specialized transcriptional repressors or structural components of chromatin ? **65,** 1509–1522 (2010).

116. Jones, P. L. *et al.* Methylated DNA and MeCP2 recruit histone deacetylase to repress transcription. *Nature genetics* **19,** 187–91 (1998).

117. Fujita, N. *et al.* Methyl-CpG binding domain 1 (MBD1) interacts with the Suv39h1-HP1 heterochromatic complex for DNA methylation-based transcriptional repression. *The Journal of biological chemistry* **278,** 24132–8 (2003).

118. Peterson, C. L. & Laniel, M.-A. Histones and histone modifications. *Current biology : CB* **14,** R546–51 (2004).

119. Okano, M., Bell, D. W., Haber, D. a & Li, E. DNA methyltransferases Dnmt3a and Dnmt3b are essential for de novo methylation and mammalian development. *Cell* **99,** 247–57 (1999).

120. Zhang, Y. & Reinberg, D. Transcription regulation by histone methylation: interplay between different covalent modifications of the core histone tails. *Genes & development* **15,** 2343–60 (2001).

121. Henikoff, S. Histone modifications: combinatorial complexity or cumulative simplicity? *Proceedings of the National Academy of Sciences of the United States of America* **102,** 5308–9 (2005).

123. Barth, T. K. & Imhof, A. Fast signals and slow marks: the dynamics of histone modifications. *Trends in biochemical sciences* **35,** 618–26 (2010).

124. Cloos, P. a C., Christensen, J., Agger, K. & Helin, K. Erasing the methyl mark: histone demethylases at the center of cellular differentiation and disease. *Genes & development* **22,** 1115–40 (2008).

125. Kolasinska-Zwierz, P. *et al.* Differential chromatin marking of introns and expressed exons by H3K36me3. *Nature genetics* **41,** 376–81 (2009).

126. Candau, R. *et al.* Identification of human proteins functionally conserved with the yeast putative adaptors ADA2 and GCN5. *Molecular and cellular biology* **16,** 593–602 (1996).

127. Shahbazian, M. D. & Grunstein, M. Functions of site-specific histone acetylation and deacetylation. *Annual review of biochemistry* **76,** 75–100 (2007).

128. Sterner, D. E. & Berger, S. L. Acetylation of histones and transcription-related factors. *Microbiology and molecular biology reviews : MMBR* **64,** 435–59 (2000).

129. Kouzarides, T. Chromatin modifications and their function. *Cell* **128,** 693–705 (2007).

130. Azuara, V. *et al.* Chromatin signatures of pluripotent cell lines. **8,** (2006).

131. Bibikova, M., Laurent, L. C., Ren, B., Loring, J. F. & Fan, J.-B. Unraveling epigenetic regulation in embryonic stem cells. *Cell stem cell* **2,** 123–34 (2008).

132. Boyer, L. a *et al.* Core transcriptional regulatory circuitry in human embryonic stem cells. *Cell* **122,** 947–56 (2005).

133. Bernstein, B. E., Meissner, A. & Lander, E. S. The mammalian epigenome. *Cell* **128,** 669–81 (2007).

134. Meissner, A. *et al.* Genome-scale DNA methylation maps of pluripotent and differentiated cells. *Nature* **454,** 766–70 (2008).

135. Goll, M. G. & Bestor, T. H. Eukaryotic cytosine methyltransferases. *Annual review of biochemistry* **74,** 481–514 (2005).

136. Lupton, S. & Levine, a J. Mapping genetic elements of Epstein-Barr virus that facilitate extrachromosomal persistence of Epstein-Barr virus-

derived plasmids in human cells. *Molecular and cellular biology* **5,** 2533–42 (1985).

137. Hewitt, K. J. & Garlick, J. a. Cellular reprogramming to reset epigenetic signatures. *Molecular aspects of medicine* **34,** 841–8 (2013).

138. Deng, J. *et al.* methylation associated with nuclear reprogramming. **27,** 353–360 (2009).

139. Lister, R. *et al.* Hotspots of aberrant epigenomic reprogramming in human induced pluripotent stem cells. *Nature* **470,** 68–73 (2011).

140. Kim, K. *et al.* Epigenetic memory in induced pluripotent stem cells. *Nature* **467,** 285–90 (2010).

141. Aranda, P. *et al.* Epigenetic signatures associated with different levels of differentiation potential in human stem cells. *PloS one* **4,** e7809 (2009).

142. Yokomori, N., Tawata, M. & Onaya, T. DNA demethylation during the differentiation of 3T3-L1 cells affects the expression of the mouse GLUT4 gene. *Diabetes* **48,** 685–90 (1999).

143. Musri, M. M., Corominola, H., Casamitjana, R., Gomis, R. & Párrizas, M. Histone H3 lysine 4 dimethylation signals the transcriptional competence of the adiponectin promoter in preadipocytes. *The Journal of biological chemistry* **281,** 17180–8 (2006).

144. Shen, J. *et al.* Transcriptional induction of the osteocalcin gene during osteoblast differentiation involves acetylation of histones h3 and h4. *Molecular endocrinology (Baltimore, Md.)* **17,** 743–56 (2003).

145. Takada, I. *et al.* A histone lysine methyltransferase activated by non-canonical Wnt signalling suppresses PPAR-gamma transactivation. *Nature cell biology* **9,** 1273–85 (2007).

146. Ye, L. *et al.* Histone demethylases KDM4B and KDM6B promotes osteogenic differentiation of human MSCs. *Cell stem cell* **11,** 50–61 (2012).

147. Sharma, D. *et al.* Release of methyl CpG binding proteins and histone deacetylase 1 from the Estrogen receptor alpha (ER) promoter upon reactivation in ER-negative human breast cancer cells. *Molecular endocrinology (Baltimore, Md.)* **19,** 1740–51 (2005).

148. Shi, L. *et al.* Histone demethylase JMJD2B coordinates H3K4/H3K9 methylation and promotes hormonally responsive breast carcinogenesis. *Proceedings of the National Academy of Sciences of the United States of America* **108,** 7541–6 (2011).

149. Yang, X. *et al.* Transcriptional Activation of Estrogen Receptor α in Human Breast Cancer Cells by Histone Deacetylase Inhibition Advances in Brief Transcriptional Activation of Estrogen Receptor ⎵ in Human Breast Cancer Cells by Histone Deacetylase Inhibition 1. 6890–6894 (2000).

150. Stossi, F., Likhite, V. S., Katzenellenbogen, J. A. & Katzenellenbogen, B. S. Estrogen-occupied Estrogen Receptor Represses Cyclin G2 Gene Expression and Recruits a Repressor Complex at the. **281,** 16272–16278 (2006).

151. Oesterreich, S. *et al.* Estrogen-mediated Down-Regulation of E-cadherin in Breast Cancer Cells Estrogen-mediated Down-Regulation of E-cadherin in Breast Cancer Cells 1. 5203–5208 (2003).

152. Hsu, P.-Y. *et al.* Estrogen-mediated epigenetic repression of large chromosomal regions through DNA looping. *Genome research* **20,** 733–44 (2010).

153. Stossi, F., Madak-erdogan, Z. & Benita, S. Estrogen Receptor Alpha Represses Transcription of Early Target Genes via Estrogen Receptor Alpha Represses Transcription of Early Target Genes via p300 and CtBP1 .*Molecular and cellular biology* 01476-08 (2009).

154 . Shang, Y. *et al.* Cofactor Dynamics and Sufficiency in Estrogen Receptor – Regulated Transcription. **103,** 843–852 (2000).

155. Carling, T., Kim, K., Yang, X., Gu, J. & Zhang, X. A Histone Methyltransferase Is Required for Maximal Response to Female Sex Hormones A Histone Methyltransferase Is Required for Maximal Response to Female Sex Hormones. *Molecular and cellular biology* 24.16.7032 (2004

156 . Daniel, J. M. Effects of oestrogen on cognition: what have we learned from basic research? *Journal of neuroendocrinology* **18,** 787–95 (2006).

157. Sato, R. Prevention of critical telomere shortening by oestradiol in human normal hepatic cultured cells and carbon tetrachloride induced rat liver fibrosis. *Gut* **53,** 1001–1009 (2004).

158. Lee, D.-C., Im, J.-A., Kim, J.-H., Lee, H.-R. & Shim, J.-Y. Effect of long-term hormone therapy on telomere length in postmenopausal women. *Yonsei medical journal* **46,** 471–9 (2005).

159. Park, H. J. *et al.* Genistein inhibits differentiation of primary human adipocytes. *The Journal of Nutritional Biochemistry* **20,** 140–148 (2009).

160. Bodine, P. V *et al.* Estrogen receptor-alpha is developmentally regulated during osteoblast differentiation and contributes to selective responsiveness of gene expression. *Endocrinology* **139,** 2048–57 (1998).

161. Jenei-Lanzl, Z. *et al.* Estradiol inhibits chondrogenic differentiation of mesenchymal stem cells via nonclassic signaling. *Arthritis and rheumatism* **62,** 1088–96 (2010).

162. Matsumoto, Y. *et al.* Estrogen and glucocorticoid regulate osteoblast differentiation through the interaction of bone morphogenetic protein-2 and tumor necrosis factor-alpha in C2C12 cells. *Molecular and cellular endocrinology* **325,** 118–27 (2010).

163. Evans, R. M., Barish, G. D. & Wang, Y.-X. PPARs and the complex journey to obesity. *Nature medicine* **10,** 355–61 (2004).

164. Cooke, P. S. & Naaz, A. Experimental Biology and Medicine Role of Estrogens in Adipocyte Development and Function. (2004).

165. Jeong, S. & Yoon, M. 17β-Estradiol inhibition of PPARγ-induced adipogenesis and adipocyte-specific gene expression. *Acta pharmacologica Sinica* **32,** 230–8 (2011).

166. Heim, M. *et al.* The phytoestrogen genistein enhances osteogenesis and represses adipogenic differentiation of human primary bone marrow stromal cells. *Endocrinology* **145,** 848–59 (2004).

167. Kim, B. H. *et al.* Signal crosstalk between estrogen and peroxisome proliferator-activated receptor alpha on adiposity. *BMB reports* **42,** 91–5 (2009).

168. Beresford, J. N., Bennett, J. H., Devlin, C., Leboy, P. S. & Owen, M. E. Evidence for an inverse relationship between the differentiation of adipocytic and osteogenic cells in rat marrow stromal cell cultures. *Journal of cell science* **102 (Pt 2,** 341–51 (1992).

169. Jeong, J. & Choi, J. Interrelationship of Runx2 and estrogen pathway in skeletal tissues. 613–618 (2011).

170. Bitirim, V. C., Kucukayan-Dogu, G., Bengu, E. & Akcali, K. C. Patterned carbon nanotubes as a new three-dimensional scaffold for mesenchymal stem cells. *Materials science & engineering. C, Materials for biological applications* **33,** 3054–60 (2013).

171. Bradford, M. M A rapid and sensitive method for the quantitation of microgram quantities of protein utilizing the principle of protein-dye binding, *Anal Biochem 72*, 248-254 (1976).

172. Zama, A. M., & Uzumcu, M. Fetal and neonatal exposure to the endocrine disruptor methoxychlor causes epigenetic alterations in adult ovarian genes. *Endocrinology*, 150(10), 4681–91 (2009)

173. Lee, J.-J. *et al.* Constitution and telomere dynamics of bone marrow stromal cells in patients undergoing allogeneic bone marrow transplantation. *Bone marrow transplantation* **32,** 947–52 (2003).

174. Tokcaer-Keskin, Z. *et al.* The effect of telomerase template antagonist GRN163L on bone-marrow-derived rat mesenchymal stem cells is reversible and associated with altered expression of cyclin d1, cdk4 and cdk6. *Stem cell reviews* **6,** 224–33 (2010).

175. Sitharaman, B. *et al.* In vivo biocompatibility of ultra-short single-walled carbon nanotube/biodegradable polymer nanocomposites for bone tissue engineering. *Bone* **43,** 362–70 (2008).

176. Shi, X. *et al.* Rheological behaviour and mechanical characterization of injectable poly(propylene fumarate)/single-walled carbon nanotube composites for bone tissue engineering. *Nanotechnology* **16,** S531–8 (2005).

177. Tutak, W., Chhowalla, M. & Sesti, F. The chemical and physical characteristics of single-walled carbon nanotube film impact on osteoblastic cell response. *Nanotechnology* **21,** 315102 (2010).

178. Usui, Y. *et al.* Carbon nanotubes with high bone-tissue compatibility and bone-formation acceleration effects. *Small (Weinheim an der Bergstrasse, Germany)* **4,** 240–6 (2008).

179. Zhu, L., Chang, D. W., Dai, L. & Hong, Y. LETTERS DNA Damage Induced by Multiwalled Carbon Nanotubes in Mouse Embryonic Stem Cells. (2007).

180. Lobo, a. O. *et al.* An evaluation of cell proliferation and adhesion on vertically-aligned multi-walled carbon nanotube films. *Carbon* **48,** 245–254 (2010).

181. Kang, Y., Kim, S., Khademhosseini, A. & Yang, Y. Creation of bony microenvironment with CaP and cell-derived ECM to enhance human bone-marrow MSC behavior and delivery of BMP-2. *Biomaterials* **32,** 6119–30 (2011).

182. Sävendahl, L. Hormonal regulation of growth plate cartilage. *Hormone research* **64 Suppl 2,** 94–7 (2005).

183. Zhao, J.-W., Gao, Z.-L., Mei, H., Li, Y.-L. & Wang, Y. Differentiation of human mesenchymal stem cells: the potential mechanism for estrogen-induced preferential osteoblast versus adipocyte differentiation. *The American journal of the medical sciences* **341,** 460–8 (2011).

184. Zhang, M. *et al.* Estrogen and its receptor enhance mechanobiological effects in compressed bone mesenchymal stem cells. *Cells, tissues, organs* **195,** 400–13 (2012).

185. Farmer, S. R. Regulation of PPARgamma activity during adipogenesis. *International journal of obesity (2005)* **29 Suppl 1,** S13–6 (2005).

186. Rosen, E. D. *et al.* C / EBP α induces adipogenesis through PPAR γ : a unified pathway service C / EBP ⌴ induces adipogenesis through PPAR □ : a unified pathway. 22–26 (2002). doi:10.1101/gad.948702

187. MacDougald, O. a & Mandrup, S. Adipogenesis: forces that tip the scales. *Trends in Endocrinology & Metabolism* **13,** 5–11 (2002).

188. Musri, M. M. *et al.* Histone demethylase LSD1 regulates adipogenesis. *The Journal of biological chemistry* **285,** 30034–41 (2010).

189. Wu, Z., Xie, Y., Morrison, R. F., Bucher, N. L. R. & Farmer, S. R. PPAR Induces the Insulin-dependent Glucose Transporter GLUT4 in the Absence of C / EBP ⌴ During the Conversion of 3T3 Fibroblasts Into Adipocytes.

190. Senyuk, V., Sinha, K. K. & Nucifora, G. Corepressor CtBP1 interacts with and specifically inhibits CBP activity. *Archives of biochemistry and biophysics* **441,** 168–73 (2005).

191. Wei, Y. *et al.* CDK1-dependent phosphorylation of EZH2 suppresses methylation of H3K27 and promotes osteogenicosteogenic differentiation of human mesenchymal stem cellsNIH Public Access. **13,** 87–94 (2011).

182. Hwang, C. *et al.* EZH2 regulates the transcription of estrogen-responsive genes through association with REA, an estrogen receptor corepressor. *Breast cancer research and treatment* **107,** 235–42 (2008).

193. Bredfeldt, T. G. *et al.* Xenoestrogen-induced regulation of EZH2 and histone methylation via estrogen receptor signaling to PI3K/AKT. *Molecular endocrinology (Baltimore, Md.)* **24,** 993–1006 (2010).

194. Füllgrabe, J., Hajji, N. & Joseph, B. Cracking the death code: apoptosis-related histone modifications. *Cell death and differentiation* **17,** 1238–43 (2010).

APPENDIX

SOLUTIONS AND BUFFERS

4% Paraformaldehyde (PFA)

4 g PFA

Complete volume to 100 ml with 1XPBS

Dissolve by heating and constant stirring

10% formaldehyde

2 ml Formaldehyde

18 ml ddH_2O

70% Ethanol

70 ml 100% Ethanol

30 ml ddH_2O

10x PBS (pH: 7,2)

80 g NaCl

2 g KCl

8,01 g Na_2HPO_4.2H2O

2 g KH_2PO_4

Complete volume to 1 Lt with ddH_2O

50X TAE Buffer

2M Tris Base (242 g)

57,1 ml Glacial Acetic Acid

50 mM EDTA

Complete volume to 1 Lt with ddH_2O

1M Tris (pH:8)

60.55 g Tris

300 ml ddH2O

21 ml 37% HCl

pH adjusted to 8.0 with HCl, total volume brought to 500ml by adding ddH_2O.

Total Protein Lysis Buffer

2 M NaCl

1 M Tris pH:8.2

0.9% Igepal CA-630 (Sigma, Germany, Germany)

10x Protease Inhibitor Cocktail (Roche, Germany)

778.5 µl ddH_2O

Bradford Reagent

100 mg Coomassie Brilliant Blue G-250

100 ml 85% Phosphoric acid

50 ml 95% EtOH

Complete volume to 1 Lt with ddH_2O

Filtered through Whatman Paper

10%SDS

10 g SDS

Complete volume to 1000 µl with ddH_2O

30% Acrylamide Mix

145 g Acrylamide

5 g Bis-acrylamide

Complete volume to 500 ml with ddH_2O

Filtered, stored in dark at 40C.

SDS-PAGE Running Buffer (5X stock solution)

15 g Tris

73,2 g Glycine

5 g SDS

Complete volume to 1L with ddH_2O

Cracking Buffer (2X Protein Loading Buffer)

50 mM Tris HCl pH: 6,8

2m M EDTA pH: 6,8

1% SDS

20% Glycerol

0,02% BFB

Add 10% ß-mercaptoethanol prior to use

10X TBS (pH:8)

12.19 g Tris

87,76 g NaCl

pH adjusted to 8, Complete volume to 1Lt with ddH_2O

1X TBS-T 0.3%

50 ml 10X TBS

450 ml ddH_2O

1,5 ml Tween-20

1X TBS-T 0.1% (pH: 7.5)

50 ml 10X TBS

450 ml ddH_2O

500 µl Tween-20

pH adjusted to 7.5

Blocking Solution for Western Blot (5% BSA) (Histone protein)

0.5 g BSA

10 mL 1X TBS-T 0.1%

Blocking Solution for Western Blot (4% milk powder)

2 g Milk Powder

50 mL 1X TBS-T 0.3%

Semi-dry Transfer Buffer

2,5 g Glycine

5,8 g Tris base

0,37 g SDS

200 ml Methanol

Complete volume to 1 Lt with ddH_2O

Wet transfer buffer for small proteins

3 g Tris

14.25 g Glycine

200 ml Methanol

Complete volume to 1 Lt with ddH_2O

Coomassie Blue Staining Solution

0,25 g Coomassie brilliant blue

45 ml Mthanol

10 ml Glacial acetic acid

Complete volume to 100 ml with ddH_2O

Destaining Solution

100 ml Methanol

35 ml Acetic acid

365 ml ddH_2O

Blocking Solution for Immunofluorescence (IF) Staining

1 ml 2% BSA

1 ml 1X PBS

5 µl Tween-20

2N HCl solution

16.38 µl ddH_2O

4.3 µl HCl

TEB buffer

0.5% Triton-100

0.02% NaN_3

In 1XPBS

Add 1X protease inhibitor prior to use

LB

10 g Tryptone

10 g NaCl

5 g Yeast extract

Complete volume to 1 Lt with ddH_2O and autoclave

Agar

10 g Tryptone

10 g NaCl

5 g Yeast extract

15 g Bacto agar

Complete volume to 1 Lt with ddH_2O and autoclave

Adipogenic Induction Media (Prepared in DMEM –LG)

1 μM Dexamethasone

0.5 mM IBMX

10 μg/mL Insulin

100 μM Indomethacine

10% FBS

1% penicillin/streptomycin antibiotic solution

Osteogenic Induction Media (Prepared in DMEM –LG)

0.1 μM Dexamethasone

0.2 mM Ascorbic acid ɣ-irradiated

10 mM Glycerol phosphate disodium salt hydrate

10% FBS

1% Penicillin/streptomycin antibiotic solution